Netherlands organization for applied scientific research

FEL

TNO Physics and Electronics Laboratory

P.O. Box 96864
2509 JG The Hague
Oude Waalsdorperweg 63
The Hague, The Netherlands

Fax +31 70 328 09 61
Phone +31 70 326 42 21

TNO-report

report no. FEL-89-B258

copy no. 9

title TD 893875

Electronic scan at millimetre wave frequencies

author(s):

Dr. J. Snieder

classification	
title	: unclassified
abstract	: unclassified
report	: unclassified
no. of copies	: 39
no. of pages	: 126 (incl. titlepage, excl. distr.list + RDP)
appendices	: -
date	: June 1990

All information which is classified according to Dutch regulations shall be treated by the recipient in the same way as classified information of corresponding value in his own country. No part of this information will be disclosed to any party

TNO

report no. : FEL-89-B258
title : Electronic scan at millimetre wave frequencies

author(s) : Dr. J. Snieder
institute : TNO Physics and Electronics Laboratory

date : June 1990
no. in pow '89 : 710.2

ABSTRACT (UNCLASSIFIED)

The possibilities of realizing phased array antennas in the mm-wave region is reviewed in a general way. The use of discrete components and 'bulk' material is discussed.
The MMIC techniques for the realization of phased array components are excluded from this report.
A survey is given of the different electronic scan possibilities. PIN diode phase shifters and different types of ferrite phase shifters are discussed, including the principle functioning of these components as well as the advantages and disadvantages.
The availability of various ferrite materials for phase shifters is discussed.
The requirements for phased array antennas and its phase shifters are given. This includes a discussion on array element spacing, side-lobe level and related power levels, effect of pulse repetition frequency and mutual coupling.
An attempt is made to correlate all the available information at cm-wavelength (3-18 GHz) and to extrapolate it to mm-wavelength. All the detailed properties of the phase shifters are included.
The experimental results of mm-wave phase shifters are given and compared with the extrapolated results given.

The design and the experimental results of three millimetric phased array antenna systems are discussed.
Some eleven conclusions and recommendations are given.

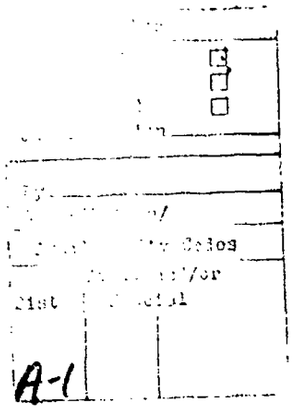

rapport no. : FEL-89-B258
titel : Electronische bundelsturing voor mm-golf radar

auteur(s) : Dr. J. Snieder
instituut : Fysisch en Elektronisch Laboratorium TNO

datum : juni 1990
no. in iwp '89 : 710.2

SAMENVATTING (ONGERUBRICEERD)

De realisatiemogelijkheden van array antennes in het millimeter golflengtegebied met electronisch gestuurde bundels worden besproken.
Het gebruik van losse componenten en van "bulk" materiaal is beschouwd.
De realisatiemogelijkheden met behulp va. monolytische microgolf geïntegreerde circuits (MMIC) zijn niet behandeld in dit rapport omdat momenteel nog te weinig hierover bekend is.
In de toekomst zal deze mogelijkheid in een separaat rapport worden behandeld.
Phased array antennes worden veelvuldig gebruikt in het cm/dm-golflengtegebied. In het mm-golflengtegebied zijn nu enkele systemen in ontwikkeling en in de toekomst zullen er vele volgen. Het gebruik van elektronische scan kan de eigenschappen van deze systemen verbeteren.
Verschillende typen fasedraaiers die gerealiseerd zijn worden besproken.
De beschikbaarheid van de materialen hiervoor vormen een punt van discussie.
Een uitvoerig overzicht is gegeven van de eigenschappen van een geproduceerde serie fasedraaiers met de resulterende eigenschappen van een lineaire phased array antenne waarin deze elementen zijn geplaatst.

1. INTRODUCTION

The possibilities of realizing phased array antennas in the mm-wave region is reviewed in a general way. The use of discrete components and bulk material is discussed.

The MMIC technique for the realization of phased array components are excluded from this report. This topic might be presented in the future in a separate report after that this technique has matured.
Phased array antennas are widely used in the cm/dm wavelength region in a large variety of military systems during the last two decennia. During the last decennium a large activity has taken place in the mm-wave region and a few military systems have been fielded and many others are under development. The need for electronic scanning has become clear. It reduces systems complexity and replaces mechanical gimbals which are expensive and have too slow a scanning rate for many applications. In certain applications the components and devices must endure high acceleration (g's).
In this report;

1) A survey is given of the different electronic scan possibilities and of the available phase shifter types and of those aspects and properties which might be critical in the mm-wave region.
2) The requirements for phase shifters to be used in a phased array antenna are discussed.
3) A survey of achieved phase shifter properties at cm wavelength is given with an extrapolation to the mm-wave region.
4) The availability of suitable ferrite materials for phase shifters in the mm-wave region is reviewed.
5) The experimental results of phase shifters with these ferrites in the mm-wave region is presented.
6) An electronic scan technique at mm-wavelength using 'bulk material' is discussed.

7) The results of a linear phased array antenna at 35 GHz with broad bandwidth and low side lobes which has been designed and manufactured in the Netherlands is given.

8) The possibility to realize a planar phased array antenna with 2N master drivers instead of N^2 standard ferrite drivers is reviewed.

2. SURVEY OF ELECTRONIC SCAN POSSIBILITIES

2.1 Frequency scan in a linear phased array antenna

This method uses a frequency change to scan the beam in one plane as shown in figure 2.1. The drawing at the top is a waveguide with radiating slots in one wall. The wavelength λg inside this waveguide is frequency dependent and so is also the freespace wavelength λ. However, the frequency dependence of λg is different from that of λ.
A certain phase difference will exist between the radiator A and B. The result will be the equal phase plane BC and the radar wave will propagate perpendicular to it. A change in frequency will result in a change of phase between A and B resulting in a change of the equal phase front BC. The direction of the propagation is therefore related to the frequency. A ten percent frequency change will result in only a beam direction (scan angle) change of about 8°. In order to obtain more scan angle change, a serpentine like waveguide structure is used as indicated at the bottom curve of figure 2.1. In this construction many λg's are present between the radiating apertures A and B resulting in an increased scan angle variation with frequency. The fact that the scan direction is frequency dependent is not so ideal regarding ECM.

2.2 Phase scan in a linear phased array antenna

This method uses a phase change to scan the beam in one plane. The structure with which this can be achieved is given in figure 2.2 and consists of a row of parallel phase shifters placed at a short distance ($\approx\lambda/2$) from each other. Each phase shifter can change the phase by 360°. In the example given in figure 2.2 the required beam direction is given by the arrow and an equal phase front has to be realized perpendicular to it. The shortest distance of each phase shifter to this plane can be calculated and expressed in wavelengths. Each wavelength equals 360° (2π radian) of phase. In this way, the phase value $n.360° + \varphi$ will be known.

The phase shifter in question needs to be set at this φ deg of phase shift. ($n.360°$ can be omitted at a fixed frequency). In setting all the phase shifters at the required phase value, the equal phase front will be formed. It is assumed that all phase shifters are fed in phase at the other end (input).
When this is not the case, the known phase differences can be incorporated in the phase settings.
For each frequency these phase settings can easily be calculated for the same antenna beam direction. Therefore all frequency values can be used for each direction which is a good ECCM feature. In case the frequency is changed during transmission (at fixed phase settings), it can be shown that an equal phase front remains but that its position is changed slightly. This change is scan angle Θ dependent and the change is largest at the largest Θ value (largest number of wavelengths between antenna front and equal phase plane). The frequency bandwidth which can be accepted regarding angle accuracy is called instantaneous bandwidth.
From transmitted pulse to pulse the beam direction can be changed arbitrarily within the designed scan sector (within for example +60° and -60°).
The energy is distributed over the phase shifters and depending on this distribution (side-lobe level requirement) the percentage of each phase shifter is known.
Another less attractive way of phase scanning in one plane is to place the phase shifters in serier instead of parallel. This case is given in figure 2.3 by the left hand part. The disadvantage of this solution is that the first phase shifter has to support the total power and that the losses of the phase shifters will be added cumulatively. The amplitude distribution for the required side-lobe level is more difficult to realize. The phase setting is identical for all the phase shifters.

2.3 Phase-phase scan in a planar phased array antenna

For a planar phased array antenna with n x m phase shifters the beam can be scanned in all directions within a solid angle in space (for instance ±60° from the perpendicular of the antenna surface (broadside)). The situation is presented in figure 2.4. In a similar way as explained section 2.2 the distance from each phase shifter to the equal phase plane can be calculated resulting in the required phase setting each element.
At each frequency the same beam direction can be obtained which is again a good ECCM feature. The total radiated power will be distributed over a much larger amount of phase shifters then for the linear phased array antenna resulting in a much lower required power handling capability.

Also the dissipation in each array elemsnt (phase shifter) is reduced.

2.4 Phase-frequency scan in a planar phased array antenna

The beam direction can also be directed in a solid angle in space with the aid of a combination of frequency scan and phase scan. (section 2.1 and 2.2). The antenna structure is presented in figure 2.5. With the phase scan the beam direction can be altered in the vertical plane of figure 2.5 and with the frequency scan in the horizontal plane. The phase and frequency scan planes are of course interchangeable.
Less phase shifters are needed than for the phase-phase scan case but instead n serpentine waveguides are needed and the required power handling capability of the phase shifter is larger again.
The direction is frequency dependent which is not ideal from an ECM point of view
An alternative construction is given in figure 2.3 However, the disadvantages associated with this construction have been mentioned in section 2.2.

3. SURVEY OF DIFFERENT TYPES OF PHASE SHIFTERS

The phase shifters to be used in a phased array antenna can in the first instance be split into two groups, the PIN diode phase shifter and the ferrite phase shifter. The PIN diode phase shifter can be split into two groups and the ferrite phase shifter into three groups. Each of them will have different properties, advantages and disadvantages as discussed below.
In practice the exact required phase shift for each phase shifter will not be utilised. The phase is set in a "digital" way as for example in values of 180°, 90°, 45°, 22.5°, 11.25° etc. With a combination of these values, the required one is approached as closely as possible.
The smaller the number of digital values which are available, the larger will be the resulting error. A 4 bit phase shifter is one where the values 180°, 90°, 45° and 22.5° are available. The maximum error is then ±11.25°. For a 3 bit phase shifter the maximum error is 22.5° etc.

3.1 PIN diode phase shifter

3.1.1 PIN diode phase shifter on substrate

The PIN-diode phase shifter is usually realized on a substrate of which Al_2O_3 (alumina) substrate is the most common one. With the aid of PIN diodes different stripline lengths are switched in each representing a certain corresponding phase shift. The h.f. wave will enter this length section and after reflection this wave will propagate backwards to the entrance. For instance, a quarter wavelength section will correspond to 180°. For each bit, two PIN diodes are needed and a 4 bit phase shifter needs therefore, 8 PIN diodes.
With an increase in number of bits more diodes, a larger total path length and inherently higher cost and losses are the result. Since the employed path length is a reciprocal component, the phase setting will be independent of the h.f. propagation direction which means the same on transmit and receive. The PIN diode can be switched very fast.

The power handling capability can be adapted within limits, by the choice of the PIN diodes. The higher the power level, the higher the loss in the phase shifter. As will be shown later in this report (section 7.1), the insertion loss of this type of phase shifter increases significantly with increasing frequency in the mm-wave region. A photo of a 4 bit PIN diode phase shifter at 10 GHz is given in figure 3.1.

3.1.2 PIN diode phase shifter mounted on dielectric waveguide

3.1.2.1 Introduction

Dielectric waveguide integrated circuits have been introduced at millimetre wave frequencies for circumventing the difficulties the conventional rectangular waveguide and microwave integrated circuits technology is expected to encounter at millimetre wave frequencies. Above 60 GHz metal rectangular waveguide becomes progressively more expensive and lossy with increasing frequency, and the use of high purity semiconducting materials as low-loss dielectric waveguide becomes particularly important since active devices, such as oscillators, Gunn or IMPATT diodes, mixers, detectors, and modulators can all be monolithically fabricated into the semi-conducting waveguide. Furthermore, the dielectric wave-guide can serve also as a conventional radiating element and it is easy to fabricate.

The cross-sectional dimensions of a single mode dielectric waveguide are typically of the order of one wavelength. The wave propagating mechanism in dielectric waveguide does not depend on the existence of metallic boundaries, but rather on the total internal reflections at the dielectric boundaries. Instead of conductor losses, the main contribution to the wave attenuation comes from the dielectric material loss and radiation loss caused mainly by bends and junctions.

Therefore, at the junction of a solid state device and a dielectric waveguide, quite complicated wave interactions take place. The success of dielectric waveguide techniques largely depends on the correct understanding of such phenomena and subsequent suppression or prevention of them.

Several types of dielectric waveguides have been investigated for millimetre wave integrated circuit applications. The most frequently used one is the rectangular rod waveguide placed in free space.

3.1.2.2 Principle of operation of phase shifter

One important aspect of millimetre wave devices is the control of phase and amplitude of a wave propagating through the dielectric waveguide.

A well-known method of altering the dispersion of millimetre waves in the dielectric waveguide is to change the boundary conditions of the semiconductor waveguide through conductivity modulation of the PIN diode mounted on the sidewall of the waveguide. Confined propagation in the low-loss silicon waveguide is due to total internal reflection. An exponentially decaying evanescent field exists external to the guide. Confinement imposes either decreasing the wavelength, increasing the guide dimensions or increasing the dielectric constant of the dielectric waveguide.

In the limit of large conductivity in the PIN diode intrinsic region, the diode effectively appears as a metal plane. For the large conductivity condition, conduction current is much greater than the displacement current in the intrinsic region of the PIN diode. A quantitative measure of this ratio is given by

$$\frac{\sigma}{\omega\epsilon}$$

where σ = conductivity, ω = frequency, and ϵ = permittivity. A critical conductivity value, $\sigma_c = \omega\epsilon$, can be used to define a crossover point of conductivity required to yield a phase shift condition characteristic of metal boundary. This is a qualitative measure, yet it provides an insight to the phase shifter that is consistent with experimental results. The incorporation of this type of phase shifter in an electronic scan technique will be discussed in chapter 8.

3.1.2.3 PIN diode phase shifter design

When a PIN diode is operated under forward bias in the state of the high carrier concentration, the average conductivity of the intrinsic region is given by $\sigma = (1630\tau I)/(WA)$. In order to minimize the required current I for a given conductivity σ it is required that the PIN diode be designed with a minimum of depletion region W, large excess carrier lifetime τ, and small cross-section area, A.

A variety of geometrical PIN diode designs have been explored. The structure utilized to measure phase shift consisted of rectangular semiconductor waveguide with tapered ends to allow efficient transition of millimetre wave energy both to and from a conventional metal waveguide. The width a and height b of the guide are selected such that it supports the E^y_{11} mode. The PIN diodes either of rectangular or trapezoidal shape have been metallized on two opposite sides and positioned either symmetrically or asymmetrically on the silicon wave guiding structure in such a way that the E field is normal to the metallic surfaces. In figure 3.2 is a schematic of the electronically controllable PIN phase shifter.

The phase shift, $\Delta\phi$, for given section of waveguide of length l is determined by computing the propagation constant in the direction of wave propagation first in the unbiased state of the PIN diode K_z and then with the biased state of the PIN diode K'_z as follows:

$$\Delta\phi = (K'_z - K_z)l$$

Equations for the propagation constants K_z and K_z' can be derived [1].

An example of phase shifter test fixture is given in figure 3.2. Shown are the two transitions from the metal waveguide to the silicon dielectric waveguide with a cross-section of 0.04 x 0.04 inch. A PIN diode is placed against one side of the silicon waveguide and bias wires are attached to this diode.
An example of the generated phase shift with the bias current is given in figure 3.3. The results are preliminary results at about 73 GHz. Much improvement is still foreseen as will be discussed in section 7.4.

3.2 Ferrite phase shifters

3.2.1 Reggia-Spencer type of reciprocal ferrite phase shifter

The first type of developed ferrite phase shifter was the so called Reggia-Spencer phase shifter [2]. A rod of ferrite is placed around the centre of a waveguide and matched to the empty waveguide in front and behind, with the aid of quarter wavelength transformers.
A large amount of windings in the form of a solenoid are wrapped around the waveguide. With the aid of a d-c current through this solenoid, an axial magnetic field is produced it in which magnetizes the ferrite rod.
A sketch of the phase shifter is given in figure 3.4.
The guide wav. length of the section with the ferrite is a function of the magnetization of this rod and due to a change in magnetization a phase change will result. The phase change as a function of d.c current is given in figure 3.5. With the choice of the ferrite material and the optimum cross-section and length of the rod, a 360° phase change can be realized with a minimum loss. The quality of a phase shifter is given by the so called figure of merit, which is the ratio of saturated differential phase shift with insertion loss (deg/dB). The component is reciprocal which means that the phase change is the same for both propagation directions through this phase shifter.

The d.c current must be maintained in order to preserve the phase setting (hold current). For "fast" switching the standard waveguide wall is replaced by a very thin one, but nevertheless the switching time remains large due to the self induction of the many hundred turns in the solenoid.
This type of phase shifter is frequency dependent which means that for each frequency a separate phase-current curve must be used. Moreover the temperature dependence is not always ideal.
This type of phase shifter is used in the first operational phased array radar in the years sixties [3]. Later more suitable phase shifter types have been designed which will be discussed in the following sections.

3.2.2 Non-reciprocal latched ferrite phase shifter

3.2.2.1 Principle of operation

Theoretically it can be shown [4] that two narrow ferrite slabs placed close together in the centre part of a waveguide with the slab plane parallel to the narrow wall and magnetized in an opposite direction perpendicular to the broad wall of the waveguide can produce a phase shift. The situation is sketched in figure 3.6.
Magnetizing the two slabs in the opposite direction will result in a change in phase shift.
This theoretical situation can be adapted to a practical one by using a toroidal ferrite rod as sketched in figure 3.7. In this way a closed magnetic loop in the transverse direction is obtained and the magnetization in the two opposite directions can be realized with a axial switching wire through the hole in the toroid.
The advantage of this construction is that the ferrite remains magnetized because of the closed loop (no hold current). The solenoid of figure 3.4 (section 3.2.2) is replaced by one wire (loop) and a fast switching time is the result.
Toroids with a circular cross-section and a concentric axial hole are used frequently. A wave propagating through this phase shifter with the direction of the d.c. current, will see a clockwise magnetized ferrite.

For the same situation a wave propagating in the opposite direction will see a counter clockwise magnetization. The phase shift is therefore not the same for both directions and the phase shifter is therefore a non-reciprocal component.

After the transmission of the radar energy through a phased array antenna with these type of phase shifters, the antenna phase setting must be adapted in order to receive the reflected energy from targets in the transmit direction. The phase setting does not have to be recalculated. Only the same d.c current pulse must be sent through the switching wire but in the opposite direction.

In order to make sure that the starting point before each required phase setting is identical, a very large saturation pulse is sent through the switching wire which magnetizes the ferrite toroid into saturation. The saturation point is called remanent point and depending on the magneza-tion direction and h.f. wave propagation direction this point is called +remanent point or -remanent point.

The saturation pulse followed by the phase setting pulse will cost some time (≈20 μs) and during this time the antenna has no receiving beam in the direction of the transmission. The equivalent range involved where the radar cannot detect targets in an appropriate way is called the dead-zone. For 20 μsec this will be 3000 m. Because the received reflection of close-in targets is very large, a signal will always be received via "mainbeam"/ sidelobes, but the direction of the target cannot be established. For long range systems this disadvantage is not a problem. For short range systems generally much higher frequencies are used and the amount of ferrite to be magnetized is then also much smaller and a faster switching time can be realized with practical switch circuit voltages (30 Volt). Special switching techniques can also avoid the large dead-zone problem.

The required phase setting can be achieved with two different methods. In the first one, a 180°, 90°, 45°, 22.5° bit etc. can be realized, each bit with its own driver, where a saturation pulse is used to magnetize each ferrite toroid. The second one uses one large toroid which can deliver at least 360° phase shift in saturation. By partly magnetizing

this large ferrite toroid any required phase setting below 360° can be achieved. In this case only one driver is needed. This driver must magnetize the large ferrite rod and must be therefore more powerful. In practice a constant voltage is employed and the duration of the magnetizing pulse is used to obtain the required phase shift value.
After this magnetizing pulse, the maximum achieved magnetization during the pulse will be reduced slightly. The situation is given in figure 3.8.
The frequency bandwidth for which the differential phase shift (phase setting) is independent of frequency can be achieved with the proper cross-section of the phase shifter, namely the ferrite cross-section and the optimized waveguide width.
The width of the ferrite loaded waveguide can therefore not freely be chosen, and is a dependent quantity. Examples will be given in chapter 6 and 7.

3.2.2.2 Temperature dependence

In order to understand the temperature dependence of this type of ferrite phase shifter (and also of the dual-mode one to be discussed in section 3.2.4) the reaction of an isotropic ferromagnetic material such as the employed ferrite, to a high frequency magnetic field, when also a static magnetic field is applied, will be given. The relation of the magnetic induction B to the h.f.magnetic field H is as follows.

$B = \|\mu\| H$. The $\|\mu\|$ tensor has the form

$$\|\mu\| = \begin{Vmatrix} \mu 1 & -j\mu 2 & 0 \\ j\mu 2 & \mu 1 & 0 \\ 0 & 0 & \mu 3 \end{Vmatrix}$$

in which μ_1, μ_2 and μ_3 are in general complex quantities and are all proportional to the saturation magnetization $4\pi M_s$.

This magnetization is temperature dependent. In remanent point B of figure 3.8 the phase shift value is proportional to $\mu_1 - \mu_2$ and in remanent point F proportional to $\mu_1 + \mu_2$. Point B is called +remanent point and F -remanent point. Since the phase shift is proportional to the magnetization it follows that the temperature dependence at +remanent (point B) is lower than at -remanent (point F).
In between +remanent and -remanent the temperature dependence of the differential phase shift is lower than in point F. This is the reason why the +remanent is always taken as the starting point for the phase setting and further that, the phase shifter is designed to be able to produce more than 360° phase shift. This last point means that the worst temperature dependent situation of -remanent will never be used.
It now also becomes clear that the phase shifter with separate bits obtained via a saturation pulse for each bit will have a worse temperature dependency than the other method with one large toroid partially magnetized.
It also becomes clear from figure 3.8 that after the phase settings for transmit and receive in a phased array system the full curve of this figure will be followed. As a result the area of this curve will be proportional to the required switching energy and to the transfer of switching energy into heat.
In a phased array radar several hundreds to a few thousand of pulses will be transmitted per second with the consequent dissipation. To obtain a small switching time and to minimize this dissipation, a ferrite material will be preferred with a narrow hysteresis loop as given in figure 3.8 and with as square a hysteresis loop as possible to obtain the largest remanent phase shift in F(D) after the magnetizing pulse E(C).

3.2.2.3 Power handling

Regarding the power handling capability of the phase shifter we have to consider in the first place the average power which is limited by the dissipation due to the losses and the temperature dependence of the phase shifter.

In a linear phased array antenna with n elements appropriate cooling must be applied since the power rating per phase shifter is high namely about 1/n of the total power.
In a planar phased array antenna with n x m element this average power is generally of lesser concern.
In the second place we have to consider the peak power handling capability of the phase shifter. In this case the limitation is not due to sparking or burning out the ferrite, but due to the fact that above a certain critical peak power level ($P_{crit.}$) the so called spin waves are in resonance and will absorb a part of the high frequency energy, resulting in high losses. A typical curve of insertion loss as a function of peak power is given in figure 3.9. From this curve we see that the increase of loss is very drastic above the critical peak power level. The critical peak power is slightly different in + and -remanent point. In between these two points an in between critical value is observed. The peak power handling capability can be improved with the use of certain ferrite compositions, but in general a higher peak power handling capability will go hand in hand with a higher insertion loss of the phase shifter. Examples of peak power values will be given in chapter 7.

3.2.2.4 Pressure dependence

At last it must be mentioned that most ferromagnetic ferrites are magnetostrictive, which means that some of the ferrite properties are pressure dependent. For the phase shifter this means that the phase shift will change as a function of the applied pressure, both in the transverse direction (see figure 3.10) as well as in the longitudinal direction of the toroid (see figure 3.11).
A good contact between the ferrite toroid and the waveguide wall is needed to avoid high absorption peaks and to ensure proper heat transport for cooling purposes. This can result in an applied transverse pressure on the ferrite. By addition of small amounts of other materials in the ferrite composition this pressure dependency can be reduced.

An example is given in figure 3.12, for a 3 GHz phase shifter using a garnet material and in figure 3.13 for a 5.6 GHz phase shifter. The magnesium-manganese ferrite is considered to be non-magnetostrictive. An example of such a ferrite is R5 and the experimental result for it is also given in figure 3.13.
From these results we see that the pressure dependence for z=0.15 is nearly the same as for R5.
The fixation of the ferrite toroid in the waveguide housing will result in an axial longitudinal pressure on the ferrite when temperature changes occur, due to the different thermal expension coefficients of the ferrite and of the metal of the waveguide wall.
The addition of small amounts of other materials in the ferrite composition to avoid this longitudinal pressure dependence is generally not the same as the addition needed for the transverse pressure.
An example for compensation for longitudinal pressure is given in figure 3.14. A comparison between figure 3.12 and 3.14 shows that a value z=0.18 is optimum for longitudinal pressure compensation but that a value of z =0.13 must be preferred for the tranverse pressure case. Nevertheless a very good compromise is possible (see also [5]). At last it must be mentioned that in case the ferrite toroid is not ideally straight a pressure will be applied on the ferrite in the waveguide. An easy way of testing the magnetostrictive properties is by measuring the change of B-H loop outside a waveguide as a function of pressure. This method is moreover frequency independent.
An example for tranverse pressure is given in figure 3.15 for the original garnet (z=0.0) and for a compensation z=0.12 and z = 0.18.
The longitudinal case is given in figure 3.16 for z = 0, 0.12 and 0.18.
The percentage change in differential phase shift and in B-value are put together in figure 3.17 for the transverse pressure case and in figure 3.18 for the longitudinal case. Good agreement has been found here and also for the 5.6 GHz case not presented here.

With these results it is shown that a measurement of the B-H loop as a function of pressure gives a fair indication of the magnetostrictive properties of the ferrite and is a much simpler measurement method than the phase shift measurements.
The B-H loop approach is employed at mm-wave frequencies and examples are given in section 7.3.

3.2.3 Reciprocal dual-mode ferrite phase shifter

The research with the dual-mode type of phase shifter was started at a later date than the non-reciprocal one described in section 3.2.3 . The dual-mode phase shifter makes use of a metallized circular or square rod (without concentric hole or gap) and is comparable with a waveguide completely filled with ferrite. Matching transformers are used at both ends of the phase shifter. The match can be to empty waveguide for design, development and test purposes or to free space in an array environment.
A linearly polarized wave entering the phase shifter is transformed into a circularly polarized wave with the aid of a quarter wave polarizer as can be seen in figure 3.19. At the other end of the phase shifter a quarter wave polarizer transforms the circularly polarized wave into a linearly polarized one. A cross-section of it is also given in figure 3.19. In between these quarter wave transformers a magnetic return path is realized with the aid of the U-shaped ferrite blocks. Only the thin evaporated metal waveguide wall is in the magnetic "closed" path, which only slightly degrades the remanent magnetization.
Around the metalized ferrite inside the magnetic closed loop a solenoid of 10 to 20 turns is applied. In this way the ferrite rod can be partly magnetized in its length direction in a similar way to that described in section 3.2.1 for the Reggia-Spencer type of reciprocal ferrite phase shifter.
The length of the ferrite rod is chosen in such a way that again at least 360° saturated differential phase shift is available. In reality each of the three parts of this phase shifter (2 quarter wave transformers and central part) is non-reciprocal but it can be proved that the complete phase shifter is a reciprocal component.

The metallized ferrite rod is capable of supporting two orthogonal - "dominant" modes, e.g. right-hand and left-hand circularly polarized quasi-TE_{11} modes for a round rod. When a longitudinal magnetic bias field exists in the variable-phase section of the rod, the insertion phase increases for one sense of circular polarization and decreases for the other. The insertion phase through the rod is antisymmetric with respect to the bias field direction and the sense of polarization; i.e., the same insertion phase is obtained if the direction of the bias field and the sense of polarization are both reversed. The non-reciprocal quarter-wave plates produce opposite senses of polarization in the two directions of propagation and the bias field direction is intrinsically opposite, hence the insertion phases for an ideal dual-mode phase shifter are equal for all settings of the longitudinal bias field level. In actual devices, small errors in the quarter-wave plates, in the structure symmetry, and in material homogeneity will cause minor deviations from absolute reciprocity.

All the properties of the non-reciprocal phase shifter as discussed in section 3.2 , are also relevant for this type of phase shifter with the exception of reset of the phase shifter after transmit since this one is a reciprocal component.

4. AVAILABILITY OF FERRITE MATERIALS FOR PHASE SHIFTERS

Ferrite material must be selected in such a way that no high insertion loss values occur when the ferrite is unmagnetized or weakly magnetized (ferrite becomes in resonance due to certain internal magnetic fields which can be as high as the $4\pi M_s$ value). A criterium is that $\gamma\, 4\pi M_s/\omega_o < 1$, with γ the gyromagnetic ratio, $4\pi M_s$ the saturation magnetization and ω_o the angular frequency.

It is generally agreed that a value of $\frac{\gamma\, 4\pi M_s}{\omega_o} \approx 0.6$

gives a good result for most applications.
Since γ is in general close to 2.8, in particular for ferrites and garnets with low porosity, a value of

$$4\pi M_s = \frac{0.6\,\omega_o}{2.8} \approx 0.214\,\omega_o \text{ is needed}$$

This means that for 10 GHz a $4\pi M_s$ value of 2140 Gauss* is required, at 16.5 GHz a value of 3510 Gauss, at 35 GHz a value of about 7500 Gauss and at 94 GHz a value of about 20100 Gauss.

Ferrites have been derived principally from two basic metal-oxide families, the ferrimagnetic spinels and the garnets. A typical spinel ferrite is $NiFe_2O_4$. In addition nickel, cospositions of magnesium-manganese and lithium have been used.

---

* 1 Gauss = 10^{-4} Wb/m^2

The following ferrites/garnets are available

garnets	$4\pi M_s \leq 1800$ Gauss
MgMn ferrites	$4\pi M_s \leq 2400$ "
NiZn ferrites	$4\pi M_s \leq 5500$ "
Lithium ferrites	$4\pi M_s \leq 5500$ "

We see therefore that the required value of 7500 Gauss is not available and that the maximum frequency with optimum choice of $4\pi M_s$ value is 26 GHz.

The maximum $4\pi M_s$ values for these type of ferrites are also from a fundamental point of view the highest values and no higher values for these types can therefore be expected in the future.

Another ferrimagnetic material is the hexagonal ferrimagnetic oxide. This semiconducting material, $BaFe^{3+}_{12}O_{19}$ ($BaO \cdot 6Fe_2O_3$), which is very similar to the ferrites, is of considerable practical importance because it exhibits high resistivity, is ferrimagnetic, has an internal anisotropy field of 17,000 oersteds*, and is a permanent magnet with a coercive force of 3000 oersteds. The crystal, which has a hexagonal, magnetoplumbite structure, exhibits its high magnetic anisotropy along only one axis of easy magnetization, resulting in the large coercive force. All of these properties make this compound uniquely valuable for the construction of waveguide resonance isolators in the millimetre-wave range, since a portion of the large d-c magnetic field required for ferromagnetic resonance at high frequencies is already built into the material in the form of anisotropy field. The commercial polycrystalline forms of the substance are usually fabricated in the presence of a magnetic field to align the crystallites permanently.

---

* 1 oersted = $10^3/4\pi$ A/m

There is an additional group of ferrimagnetic hexagonal compounds, very similar to $BaFe^{3+}_{12}O_{19}$, which can be formed from combinations of BaO, Fe_2O_3 and MeO^{2+}, where Me^{2+} denotes the usual divalent transition metals Co, Ni, Mg, and so on. One of these, Me_2Y, has been given the trade name *Ferroxplana* because, instead of uniaxial anisotropy, it has an easy *plane* of magnetization.

Similary, there exist Me_2Y and Me_2Z. A very large magnetic field is required to turn the magnetization out of the easy plane or direction of magnetization. The magnetic anisotropy field depends upon the particular formulation and is usually of the order of 10,000 oersteds up to 28,000 oersteds.
These materials are very suitable for certain applications in the mm-wave region where very high magnetic field strengths are needed and where the internal magnetic field can contribute to it in a considerable way.
Thompson and Rodrigue [6] have shown that hexagonal ferrites with planar anisotropy could be used in a remanent type of ferrite phase shift and could even produce a larger differential phase shifter per unit length than the sofar used materials with spinel and garnet structures.
No indication has been given regarding the losses to be expected. The article ends with the following sentences: "These results offer some promise to meet the needs of millimetre-wave phase shifters where maximum realizable magnetization currently limits performance. However, at this time (November 1985), the planar hexagonal materials are not available on the open market".
At millimetre wave frequencies the $\gamma 4\pi M_s/\omega_0$ of 0.6 cannot be obtained with the available ferrites and garnets. Therefore a lower value than 0.6 has to be accepted. However, it will be be shown in chapter 7 that a phase shifter with over 400° differential phase shift can be realized up to 66 GHz with a loss of maximal 1 dB.
Values close to these can be expected at 94 GHz.

The possibilities with new magnetic materials including hexagonal ferrites are not clear at this moment but might be promising in the near future.

5. REQUIREMENTS FOR PHASED ARRAY ANTENNAS AND ITS PHASE SHIFTERS

5.1 Array element spacing and cross-section

In a fully filled phased array antenna the phase shifters are in general placed in a regular pattern. An example for a linear phased array antenna is given in figure 5.1. The distance d between the elements cannot be chosen arbitrary. For a distance d larger than a free space wavelength it can be shown that more than one equal phase front will be formed at the same time. The direction of received echo's from a target can therefore not be determined unambiguously.

For exactly a wavelength (λ) spacing and for all phase shifters with identical phase shift setting three beam directions are present, namely perpendicular to the antenna and at +90° and -90° from broadside.

For a scan angle $+\Theta$, the +90° direction disappears (>90°) and the -90° value is going towards broadside.

For a half wavelength ($\lambda/2$) spacing only one beam exists in front of the antenna. Only when the beam is at +90° another one appears at -90°. For in between spacing values ($1/2 \leq d \leq \lambda$), the broadside beam can be scanned over a certain angle without the occurance of the second beam. For a scan angle interval of +60° to -60° a spacing of 0.53λ is required. For +45° to -45° a spacing of 0.56λ.

From these values it follows that a scan angle area reduction will only result in a small decrease of required elements. Generally speaking we can say that a $\lambda/2$ spacing is required. This sets the limit to one dimension of the cross-section of the phase shifter. In a linear array the other dimension of the cross-section is not restricted.

In a planar phased array antenna the limitation found for one dimension is also valid for the other dimension. It can be shown that two lattices can be used for which the second main beam (grating lobe) is not present in front of the antenna surface (half hemisphere). The two possibilities are given in figure 5.2. The rectangular lattice with an element cross-section of about $\lambda/2 \times \lambda/2$ and the triangular lattice with an element

cross-section of about λ x 0.28λ. A cross-section of 1/2 x 0.56λ is also possible.
For the case of λ x 0.28λ we see that one dimension can be λ which means that a standard waveguide width can be used in the radiating end of the phase shifter. We further see that the area of the phase shifter is slightly larger than 1/4 λ^2 which will result in a reduction in number of elements with about 10-13% depending on the largest required scan angle.
In this cross-section the fixation in the array antenna, the wiring, the driver (phase shifter power supply etc.) and cooling must be incorporated.

5.2 Antenna side-lobe level and related power level in the phase shifter

The information presented in section 5.2 is valid for all frequencies.
For an antenna with uniform illumination the first side-lobe level of a linear array antenna and of a rectangular shaped planar array antenna will be -13.2 dB which is very high. The next side lobes will be reduced gradually until a level is reached which is caused by the various errors of the antenna.
For a circular shaped antenna this first side-lobe level is -17.6 dB.
The power requirement of the phase shifter can easily be calculated and amounts to P_{total}/N with P_{total} the total average or peak power of the antenna and N the number of phase shifters. A lower side-lobe level can be obtained by using a tapered illumination which means a larger power value in the centre of the antenna and a lower one at the edge (periphery) of the antenna.
The result is an increase of required power handling capability for the phased shifters in the centre. For a circular shaped planar phased array antenna with a half-power antenna beamwidth of 2° for uniform illumination, the power increase factor is 2.6 for a first side-lobe level of -25dB, 3.3 for -30dB, 3.9 for -35dB and 4.5 for -40dB.

At the same time the half-power beamwidth is increasing and a larger antenna with more phase shifters is needed to maintain the 2° value. The numbers for a 2° beamwidth are N=2690 for uniform illumination (-17.6 dB), N=3157 for -25 dB, N=3718 for -30dB, 4162 for -35 dB amd 4632 for -40 dB first side-lobe level.
From these examples it follows that a lower required side-lobe level will result in an increased beamwidth or an increased amount of phase shifters. Also the required level of the averar and peak power handling capability of the phase shifter increases with decreasing side-lobe level. With increasing beamwidth at fixed side-lobe level the number of phase shifters decreases and for a fixed total power level the power handling capability of the phase shifter increases.

5.3 Pulse repetition frequency

The time between the transmission of energy pulses is dependent on the required maximum range of the radar system. The next transmission must wait till the reflection from targets from the previous transmission is received (waves travelling with speed of light = $3 \cdot 10^8$ m/s). The amount of pulses (transmissions) per second is called the pulse repetition frequency (p.r.f.). For a long range system this p.r.f is of the order of 500-1000 Hz.
For a short range system such as a mm-wave system the required p.r.f is much higher. For a maximum range of 10 km a p.r.f of 15 KHz is a good choice. Airborne radars (at cm wavelength) have in general three p.r.f values, a low one of 500 Hz-1KHz, a medium one of 10-15KHz and a high one of 200KHz. This last one is to obtain doppler information but no range information can be obtained.
In case phased arrays are used for these applications the impact of a medium/high p.r.f on the choice of phase shifter type and on the cooling must be examined. For a non-reciprocal phase shifter the hysteresis loop area times the p.r.f -value and the insertion loss will be transferred into heat. For a reciprocal phase shifter with the same phase setting (same beam direction) only the insertion loss will contribute to the dissipation (fixed scan direction is assumed).

For non-reciprocal phase shifters with special driver technique, the dissipation can be reduced.

5.4 Mutual coupling

In a phased array antenna each radiating element is transmitting its energy into free space with the intention to contribute in a optimum way to the antenne main beam and to a known way to the side lobes. However, in an array environment with the closely packed radiators also energy is coupled into the neighbour elements. The total amount coupled into one element by all the surrounding elements is called mutual coupling. This amount is not to be neglected and will vary with frequency and with scan angle due to the change in phase between adjacent elements.
A compensation for this mutual coupling has to be incorporated in each phase shifter element. However, a complete compensation for a frequency bandwidth of say 10% and a maximum scan angle of say 60° in all directions from broadside is not possible. The remaining coupled energy will interact with the transmitted energy and a standing wave pattern will be the result. In the maxima of this pattern the energy density is increased. This means that the phase shifter must have a peak power handling capability ($P_{crit.}$ value) which corresponds with it. An increase in required peak power handling capability of 25% is quite normal for a well designed antenna. In case reflections of nearby objects are received during transmission a factor four higher capability is needed. This is not a must for ferrite phase shifters but it is for a PIN diode phase shifter in order to avoid the burn out of the diodes.
The presented information in section 5.4 is valid for all frequencies.

5.5 Reproducibility and cost

In a phased array antenna many phase shifters are needed. For a required maximum side-lobe level a related illumination is applied. Large phase and amplitude errors will increase the side-lobe level in particular the phase errors. For that reason a sufficient number of bits must be used in the phase shifter in order to reduce the remaining round off error (see chapter 3).

The spread in insertion loss, insertion phase (about 3000° for a ferrite phase shifter) and differential phase shift must be kept within tight known limits.

In case a large number of bits is used large phase errors can be corrected with the phase setting. Precaution must then be taken in the driver to incorporate this method on an individual element basis. The system has become more complex, but a better yield in phase shifter production will be the possitive side of it. Amplitude errors cannot be compensated in an easy way.

The lower the required side-lobe level the higher are the production requirements and therefore the cost per element. The cost of the thousands of phase shifters in a planar phased array antenna and the fact that four to five antennas are needed to cover half the hemisphere has been of concern over the years. A very large production has never taken place so far so that companies were never in a position to introduce large scale production methods economically.

6. EXPERIMENTAL PHASE SHIFTER RESULTS AT CM WAVELENGTH AND EXTRAPOLATION TO MM-WAVELENGTH

The results presented [7] are mainly associated with a large experimental program undertaken by the Physics and Electronics Laboratory TNO, The Netherlands over a period of greater than ten years. The aim of this program was to examine the usefulness of three particular ferrite materials, the magnesium-manganese ferrite (M), the lithium ferrite (L) and the (mixed) garnet (G), for various phased array antenna designs. This program has been carried out over the frequency range 3-18 GHz and extrapolated to 94 GHz.

6.1 Non-reciprocal latched ferrite phase shifter

6.1.1 Phase shifter configuration

The shape of the ferrite is for all examined cases a cylinder with axial concentric hole for the switching wire. The flux drive principle (partly magnetization) is used for the driver. Two narrow flat strips are ground on the cylinder in order to achieve good contact with both broad walls of the rectangular waveguide in which the ferrite toroid is placed. The width of the waveguide over the length of the toroid is adjusted is such a way that the differential phase shift is independent of frequency over a bandwidth of at least 20%. In general this width is smaller than the standard waveguide width. The height of this waveguide part is identical to the height between the two ground narrow flat strips and therefore just a little smaller than the diameter of the toroid. With the aid of matching transformers, the cross-section of the ferrite loaded waveguide is matched to that of the standard waveguide (radiating aperture). With this set-up, the phase shift, the insertion loss, the temperature dependence of the phase shift and the peak power capability of the phase shifter is measured.

6.1.2 Differential phase shift and insertion loss

The quality of a phase shifter is given by the Figure Of Merit (FOM), the differential phase shift-insertion loss ratio. The saturated phase shift value is used and the loss value is determined for a real phase shifter to be used in a phased array antenna. The result is given in figure 6.1. From this figure and following figures the diameter of the rods with optimum properties can be reduced.These values are presented in figure 6.2, where the free space wavelength is given as a function of rod diameter. For a frequency of about 35 GHz, the required rod diameter will be of the order of 2 mm. If the correct ferrite is available (see chapter 4), an insertion loss of 0.5-0.6 dB can be achieved for all frequency bands for the required 450° saturated differential phase shift. Even a tendency for lower loss at 35 GHz is present.

6.1.3 Dimensions of the phase shifter

The length required for 450° saturated differential phase shift follows from figure 6.3, where the phase shift per cm length is given as a function of diameter for all four frequency bands. The complete phase shifter length is formed by the ferrite length plus about one guide wavelength (λg) for both the two matching transformers and some length for the two apertures. This last contribution is essential in order to attenuate the higher order modes, so that they cannot reach the matching transformer. The average curve drawn through all the data of figure 6.3 is given by the equation $\Delta\varphi/cm \cdot \lambda \approx 150$.

At 35 GHz we expect therefore a $\Delta\varphi/cm$ value of 175°/cm (at diameter ≈ 2 mm).

The volume of the ferrite follows from figure 6.4, where the saturated differential phase shift per cm^3 is given as a function of diameter. It is clear that the smaller the waveguide the less ferrite is required. As a consequence the driver power and therefore the size of the driver can also be made smaller for the higher frequencies. The average curve drawn through all the data of figure 6.4 is now given by the equation $\Delta\varphi/cm \cdot \lambda^2 \approx 2000$. At 35 GHz we expect therefore a $\Delta\varphi/cm^3$ value of about $2700°/cm^3$.

The required waveguide width follows from figure 6.5. There is no restriction in this width value for a linear array with E-plane scan. For use in a planar array antenna the cross-section of the phase shifter must be smaller than or equal about λ x 0.28λ or about 1/2λ x 1/2λ for wide angle scan in all directions (λ = wavelength). The average curve through the data is a straight line going through (0,0). The waveguide width for frequency independent differential phase shift at 35 GHz (2 mm ferrite rod diameter) is about 5.7 mm.

6.1.4 Peak power capability

The peak power capability (in kW) is given in figure 6.6. The critical peak power value $P_{crit.}$ is the minimum of all phase settings of the phase shifter from +remanent to -remanent. The values given here are measured with r.f. pulse length of 0.5 μs
Measurements have been made also with longer pulse lengths, but not the same one for all ferrite materials. For some ferrites, the $P_{crit.}$ value is a little lower for a longer pulse length than 0.5 μs
This is due to the fact that the spin waves need some time to come into resonance. The average curve through the data going through (0,0) is given in figure 5.6 and at 35 GHz (2 mm diameter) a peak power capability is expected of 0.5 kW.

6.1.5 Temperature dependence

In order to have a fixed level as a starting point for the phase setting of the phase shifter, the toroid is magnetized into "saturation" with a magnetic field strength of about five times the coercive force.
The resulting remanent state is used. Two remanent states can be distinguished, namely +rem and -rem. As explained already in section 3.2.2, the +rem is used as the starting point for the differential phase shift setting since it has the lowest temperature dependence. The loading of the wave-guide with the ferrite toroid increases the insertion phase with about 2500°-3000° and from this level a differential phase shift of maximum 360° is installed with the driver. Starting in +rem, this means a reduction of the insertion phase with maximum 360° and this differential phase shift is therefore negative. The temperature dependence of

the insertion phase of +rem is given in figure 6.7 and that of -rem in figure 6.8. The values are valid for a saturated differential phase shift $\Delta\varphi = 450°$. The definition of $\delta\varphi_{+rem}/\delta T$ is given in figure 6.7 and that of $\delta\varphi_{-rem}/\delta T$ in figure 6.8. The temperature dependence of the differential phase shift $\Delta\varphi$ is given in figure 6.9 and is negative. The definition of $\delta\Delta\varphi/\delta T$ is given in figure 6.9. A comparison of the results given in figure 6.7 with that of figure 6.8 clearly shows that the temperature dependence of +rem is smaller than that of -rem. It must be mentioned that the -remanent state with $\Delta\varphi = 450°$ will never be used since a maximum of 360° is sufficient. In this way a much smaller temperature dependence will result than that of -rem and this is the reason why a saturated differential phase shift of 450° is used.
The maximum temperature dependence of all phase shift values between 0° and 360° is given in figure 6.10. These values are equal to or greater than the ones of figure 6.7. In case +rem is the worst case, the 450° of $\Delta\varphi$ can be decreased until another value is equal to that of the now also reduced +rem value. The disadvantage of a large reduction in saturated differential phase shift will be an increased switching time and/or less straight phase-switching time curve.
From figure 6.7, 6.8, 6.9 and 6.10 it follows that the temperature dependency does not vary a lot with diameter. For that reason similar values can be expected at 35 GHz (2 mm diameter) unless the properties of the most suitable ferrites at 35 GHz deviate a lot from those at the lower frequencies (see chapter 4).

6.1.6 Discussion and conclusion of non-reciprocal latched ferrite phase shifter

It is impossible to mention here all conclusions that can be drawn from the given data in chapter 6, particularly because it depends on the application in mind. In general, however, one can conclude from figure 5.1 that the same Figure Of Merit (FOM) can be obtained with all three examined ferrite types (G, L, M).

At Ku-band two types of material have been studied, a MnMg ferrite M1 with a $4\pi M_s$ value of about 2400 Gauss and a lithium ferrite L1 with a $4\pi M_s$ value of about 3200 Gauss. From figure 6.1 we can see that the lithium ferrite L1 gives the highest FOM-value and from figure 6.3 that the phase shift per unit length is also higher for L1 than for M1. This last factor is in accordance with theory.
At 35 GHz we expect therefore a little lower FOM-value than follows from the average curve through the given data of figure 6.1 and moreover a little smaller $\Delta\varphi$/cm value than the one of the average curve of figure 6.3. This, however, will not be a limiting factor for the realization of this type of phase shifter at 35 GHz and higher frequencies.
In the beginning it has been difficult to manufacture the ferrite rods for Ku-band with a diameter of about 3.5 mm and with an axial hole concentric in it. After having obtained experiences, a reproducable serie of ferrite rods have been manufactured successfully with a diameter of 2.2 mm. (see also chapter 7 and 9).
For other non r.f. applications very cheap toroids with a diameter of about 1 mm have been produced in large quantities, where another ferrite type and another production technique has been applied.
A survey of the insertion loss of ferrite phase shifters as a function of frequency is given in figure 6.11 (indicated by crosses).

6.2 Reciprocal dual-mode ferrite phase shifter

The work on this type of phase shifter has started at a later date than the non-reciprocal one mentioned in section 6.1. The amount of available data is therefore smaller.
From the limited information in literature and from our own results we have composed the curve in figure 6.12 of the wavelength as function of ferrite rod diameter.
From figure 7.1 it follows that at 35 GHz a rod diameter of about 2.2 mm is required, however, this time without a concentric hole in it.
A rod of this dimension can be reproduced in manufacture. In practice it must be proved that the quarter wave polarizer can be built and will function.

At 94 GHz, the rods with a diameter of about 0.8 mm can just be manufactured, but we believe the quarter wave polarizer might cause some difficulties. Insertion loss values between 0.5 dB and 1.0 dB have been observed. No extrapolation regarding insertion loss (figure of merit) can be made for the mm-wave region. Actual data will be given in chapter 7.

6.3 PIN Diode phase shifter on substrate

The theoretical loss of a PIN diode phase shifter is increasing with increasing frequency. The loss of a ferrite phase shifter, however, is decreasing with increasing frequency. For that reason we have to accept a high loss value with PIN diode phase shifters at millimetre wavelength. A survey of some cases from literature and from our own work shows this tendency clearly in figure 6.11 for the PIN diode phase shifter. Above a frequency of 10 GHz only one case at 16 GHz and one at 35 GHz is available. The oldest data of 16 GHz, where a loss of 3.2 dB has been reported, is incorporated in figure 6.11. The 35 GHz result will be discussed in chapter 7.

6.4 Reggia-Spencer type of reciprocal ferrite phase shifter

This type of phase shifter has been studied a lot before the non-reciprocal latched ferrite phase shifter has been invented. The Reggie-Spencer phase shifter is reciprocal but not latched and no use is made of its remanent state (see section 3.2.2 for more details) The cross-section of the rods or slabs are in general of the order of 8-20% of that of the empty waveguide. At 35 GHz the size of the wave-guide cross-section is 3.6 x 7.1 mm^2 and at 94 GHz 1.3 x 2.5 mm^2. The cross-sections of the ferrite rods and slabs are therefore of such a magnitude that they can be manufactured at 35 GHz (2-5 mm^2) and at 94 GHz (0.26-0.65 mm^2).

7. EXPERIMENTAL PHASE SHIFTER RESULTS AT MM WAVELENGTH

In the mm-wave region three types of phase shifters have been realized, a 35 GHz PIN-diode phase shifter, dual-mode ferrite phase shifters at 35 and 60 GHz and non-reciprocal latched ferrite phase shifters at 35, 47, 52 and 66 GHz. The results obtained will be described in the following three sections 7.1-7.3.

7.1 PIN diode phase shifter on substrate at 35 GHz

At the 1987 IEEE MTT conference Lang and Edward [8] have reported their experimental results of a 4 bit PIN diode phase shifter at 35 GHz. An insertion loss of 3.9 dB has been obtained for a realization on 0.01 inch thick alumina. They predicted a theoretical insertion loss of 2.3 dB. The 3.9 dB point fits nicely on the extention of the minimum curve of realized diode phase shifters of figure 6.11 as is shown in figure 7.1. Also the predicted theoretical value of 2.3 dB is given in between brackets.

7.2 Dual-mode reciprocal ferrite phase shifters

In 1971 the first results of a dual-mode ferrite phase shifter was reported by Whicker and Boyd [9]. Later Boyd has improved the design at Microwave Application Group and has extended the frequency range to 63 GHz [10]. Use is made of a Mg-Mn ferrite with a $4\pi M_s$ value of 3000 Gauss. This lower $4\pi M_s$ value is chosen because it will result in a larger rod diameter than for the Li and NiZn ferrites with a $4\pi M_s$ of 5500 Gauss and for Li also with its higher dielectric constant. Boyd also expects the insertion loss to be lower for the Mg-Mn ferrite. However, less phase shift per unit length must be expected for this lower $4\pi M_s$ value and therefore more ferrite (longer length) has to be used with its inherent increase of insertion loss.

For comparison purposes, it would be nice to see therefore the realized loss of a phase shifter using Li ferrite, since low losses have been realized with Li ferrite in the non-reciprocal latched ferrite phase shifter (see section 7.3).
In a brochure of Boyd's company Microwave Applications Group he has mentioned the obtained properties of a 35 GHz dual-mode phase shifters with characteristics suitable for system applications. The supplied information can be seen in table 1 and in figure 7.2.

Frequency Range	34.0 to 36.0 GHz
Insertion Loss	0.8 dB minimum 1.0 dB typical
Return Loss	20 dB typical
Latching Phase Shift Range	
20°C	430° typical
50°C	400° typical
RMS Phase Error, (Optimum Drive)	
20°C	2.3° typical
50°C	2.5° typical
Switching Time, (Reset-Set Cycle)	55 μs maximum

Table 1 Summary of 35GHz phase shifter performance

In figure 7.3 he has presented the minimum insertion loss (base loss) as a function of frequency for the dual-mode ferrite phase shifter and also the predicted values for a non-reciprocal version. This last curve will be compared in section 7.3 with actual obtained results.
The base loss values are still lower than the published experimental data of 1 dB at 35 GHz and 1.5 dB for 60 GHz [10]. Nevertheless, all these values are acceptable and much lower than those of the PIN diode phase shifter.

For use in phased array antennas, where the beam direction has to be changed continuously, the switching time of 55 μs (see table 1) might have to be decreased despite the fact that the phase shifter is reciprocal.
The survey curve of rod diameter as a function of free space wavelength given in figure 6.12 includes the 60 GHz case. The final cross-section of the dual-mode phase shifter is larger than these values because of quadrupole magnets and of the magnetic return path (yoke).

7.3 Non-reciprocal latched ferrite phase shifters

At the Physics and Electronics Laboratory TNO, the Hague, The Netherlands, non-reciprocal ferrite phase shifters have been examined at 35 GHz since 1979. The first results were presented at the Orlando MTT conference [11] without being published in the proceedings.
Lithium and nickel zinc ferrite have been employed with a $4\pi Ms$ value of respectively 4810 and 5103 Gauss. Circular toroids were used with a length of 35 mm, a diameter of 2.2 mm and a concentric hole of 0.35 mm diameter. The initial internal waveguide width was 7.1 mm. At room temperature a saturated differential phase shifter of 433° has been measured for the lithium ferrite and 425° for the nickel ferrite. The losses were respectively 0.55 and 0.7 dB. The differential phase shift was nearly frequency independent and the match (VSWR) was better than 1.5 over a frequency band of 6 GHz around 34 GHz as can be seen in figure 7.4 for lithium ferrite on top and for nickel ferrite at the bottom. A very shallow cylindrical gap was machined in the two walls of the phase shifter to hold the ferrite rod and also to make good contact with this rod. The height of the waveguide was therefore 2.1 mm.
The width of the waveguide has been further reduced to 5.14 mm and the diameter of the ferrite rods to 2.17 mm.
For 4 rods of Li ferrite the saturated differential phase shift varied between 430° and 454°, the minimum insertion loss between 0.5 and 0.6 dB. The temperature dependence in the +remanent point was 0.8°/°C and in -remanent point 1.6°/°C.

The critical peak power P_{crit}= 1.8 kW at -remanent and 2.5 kW at +remanent for a pulse length of 0.2 μs The measured curves with these results are given in figure 7.5. Also the case for 0.1 μs pulse length is given and the P_{crit} values are slightly higher than for 0.2 μs pulse length as expected (see section 6.1.4). The remanent (squareness) ratio of the Li ferrite is 0.9. The magnetostriction will be discussed separately at the end of this section. For two nickel-zinc ferrite rods the following result has been measured. Saturated differential phase shift 400°-425°, minimum insertion loss 0.7-0.8 dB, temperature dependence 1.04°/°C at +remanent and 1.95°/°C at -remanent, P_{crit} = 15 kW at +remanent and 17 kW at -remanent for a pulse length of 0.2 μs For a pulse length of 0.1 μs these values, are respectively 15 and 20 KW. The curves are given in figure 7.6. The points at which the losses start to increase are more sharply defined in figure 7.6 than in figure 7.5. The intersection of the two lines is used for the P_{crit} value. This is perhaps the reason that the P_{crit} value for Li ferrite is lowest at -remanent and for Ni ferrite at +remanent.

The insertion loss values for low power are arbitrary and not real calibrated values. The loss of 0.3 dB of the two employed waveguide tapers are also included in these values. It must be mentioned that these first rods were not perfectly manufactured. Some of them were slightly conical or not perfect straight. Also the hole was not always perfect concentric. All these factors gave rise to some fluctuating properties as a function of frequency and from rod to rod. The best loss values have been taken here. An example of the experimental results is given in figure 7.7. Later a production series has been made with better rods. The result of it is given in chapter 9 and compares very well with the quoted numbers here. For a reduced waveguide width of 5.14 mm the measurements were repeated and similar properties were obtained as can be seen in table 2. In order to take away the conical shape of some of the NiZn rods, these rods were ground to a uniform diameter of 2.17 mm and measured again at 35 GHz for a waveguide width of 5.14 mm.

The most promising is the Li ferrite when the extreme large peak power capability of NiZn ferrite is not required. As will follow later, from a point a view of magnetostriction, the Li ferrite is preferred.
Some of the Li ferrite rods have been ground to 2.0 mm diameter and tested by us at FGAN, Werthhoven, Germany with their microwave equipment at 47 GHz [12]. The result is given in table 2. A VSWR at this fixed frequency between 1.1 and 1.3 has been measured for a matching 3/4 wavelength transformer of 1.9 x 0.8 x 3.07 mm made from a dielectric material with $\epsilon_r = 6$. A switching time of 25 μs was needed for reset and set for a driver voltage of 30V.
After these measurements the rod diameter has been decreased further till 1.7 mm and measured at 52 and 66 GHz again at FGAN and also at 47 GHz [13]. The results are given in table 2. At 52 GHz the available transformer of 0.7 mm was too large and a 3/4 wavelength transformer has been used of 1.6 x 0.57 x 1.7 mm ($\epsilon_r = 6$) resulting in a VSWR between 1.1 and 1.43. The 1/4 wavelength transformer will be about 0.6 mm long (1.6 x 0.57 x 0.6 mm). At 66 GHz the matching transformer with a length of 0.7 mm gave good results. The VSWR was for all cases below 1.5. At last the measurements were also made at 47 GHz with the 0.7 mm long transformer. The VSWR was larger than 3 and for that reason the insertion loss has not been measured. A very large differential phase shift has been measured (see table 2). A photo of the measurement set-up and of the opened phase shifter is shown in figure 7.8.

Frequency (GHz)	35	35	47	47	52	66
Ferrite type	Li	Ni	Li	Li	Li	Li
4πMs (Gauss)	4810	5103	4810	4810	4810	4810
diameter (mm)	2.2	2.17	2.0	1.7	1.7	1.7
length (mm)	35	35	35	35	35	35
$\Delta\varphi$ at 20°C (deg)	433	400	430	520	340	385
ins.loss (dB)	0.55	0.8	1		1	1
$P_{crit.}$ (kW)	1.9	14.2	-	-	-	-
rem.ratio	0.9	0.85	0.9	0.9	0.9	0.9
$\frac{\delta\Delta\varphi}{\delta\Delta T}$ (°/°C) (+rem)	0.8	1.04	-	-	-	-
$\frac{\delta\Delta\varphi}{\delta\Delta T}$ (°/°C) (-rem)	1.60	1.95	-	-	-	-
waveguide width (mm)	5.14	5.14	4.7	2.3	2.3	2.3
waveguide height (mm)	2.1	2.1	1.9	1.6	1.6	1.6
magnetostriction	low	high	low	low	low	low
FOM	780	500	430	520	340	385
$\Delta\varphi$/cm	123	114	123	148	97	110
$\Delta\varphi/cm^3$	3250	3090	3910	6540	4280	4840
$\Delta\varphi/cm\cdot\lambda$*	105	97	79	94	56	50
$\Delta\varphi/cm^3\cdot\lambda^2$*	2350	2230	1590	2660	1420	1000

* For lower frequencies } $\Delta\varphi/cm\cdot\lambda = 150$; $\Delta\varphi/cm^3\cdot\lambda^2 = 2000$

Table 2 Experimental results of mm-wave non-reciprocal ferrite phase shifters

The magnetostrictive properties of the employed NiZn and Li ferrites have been obtained with the aid of the measurement of the B-H loop as a function of pressure as described in section 3.2.3. The original B-H loop and those as a function of transverse and as a function of longitudinal pressure are given in figure 7.9. The percentage change in B value as a function of pressure, which follows from figure 7.9, is presented in figure 7.10. Simular results for the lithium ferrite are given in figure 7.11 and figure 7.12. A comparison of figure 7.10 with figure 7.12 shows that the pressure dependence of the lithium ferrite is very small and that of the nickel ferrite much higher. Up to now we have not examined whether a compensation is possible via a small change in the chemical composition of these ferrites.
A large series of 900 phase shifters have been built and tested at 5.6 GHz with the use of z = 0.15 of figure 3.11 and the spread in properties were within acceptable limits. Up to now only the absolute pressure has been considered but in an antenna the difference in pressure between the elements does count. The pressure dependence of the lithium ferrite is of the same order of magnitude as that of the 900 phase shifters with z = 0.15 and quite likely this lithium ferrite can be used as it is.

A survey of the insertion loss of a complete ferrite phase shifter (>360° saturation differential phase shift) as a function of frequency is given in figure 7.13. The boundary for P_{crit} = 0.5-12 kW from figure 5.11 is indicated by the dashed line. Probably due to the fact that an optimum $4\pi M_s$-value is not available above 26 GHz, the losses are slightly higher at 50-60 GHz than at lower frequencies. The value at 50-60 GHz are minimum measured values for the first constructed phase shifter. After optimization it will become clear whether the loss will remain at this level under all circumstances (e.g. as a function of frequency over a 10% bandwidth etc.). However, the loss values presented here are lower than the predicted one presented in figure 7.3 despite the fact that no dielectric loading of a larger ferrite hole in the toroid has been applied. It might be possible that the assumed high losses in the walls,

due to concentrated r.f. field near the area of contact with the ferrite, is lower in our case since a circular toroid is used with very little contact area (much smaller than for a rectangular cross-section of the toroid). We have further employed a ferrite with a higher $4\pi Ms$ value than used by Boyd.

7.4 PIN diode phase shifter mounted on dielectric waveguide

Results in the 60-80 GHz band will be discussed
The principle of this type of phase shift has been described in section 3.1.2. Since the phase shift is proportional to the length l of the PIN diode section, a diode as long as possible is preferred. Also the possibility of using two diodes placed on opposite walls is examined. In figure 7.14, an example is given of two symmetrically mounted PIN diodes and in figure 7.15, of an offset mounted diode pair. The resulting phase shift for a single diode and for the symmetrically mounted pair of diodes is given in figure 7.16 for a frequency of 76 GHz.
A considerable increase in phase shift can be observed for the two diode case in comparison with the one diode case. However, also the loss is increased for the two diodes case. An example for the offset mounted diode pair is given in figure 7.17. These results must be considered as preliminary ones and improvement in phase shift and reduction in attenuation are possible. Horn et all. [14] came to the following conclusions in 1983.
Quote: "An electronic distributed PIN diode phase shifter design technique compatible with the dielectric waveguide antenna has been developed. The performance of the semiconductor phase shifter using this technique has been investigated and described in the 60-80 GHz frequency region. Exceedingly low power drain electronically modulated PIN diodes have been utilized as the phase shifting elements placed on the sidewall of the dielectric waveguide. The guide wavelength in the dielectric waveguide is changed by the electronic modulation of the diode conductivity from the nonconducting state into a high conductivity state, resulting in phase shifts of 15 degrees per wavelength, with a loss of approximately 1.0 dB per wavelength.

The present characteristics of the phase shifter can be improved, particularly its loss, through the utilization of technologies, such as conventional epitaxial deposition, molecular beam epitaxial deposition, and monolithic metallization techniques, in design and fabrication of the PIN diodes. It is felt that with these processing technologies the present barrier problem of a rather high absorption loss in the phase shifter basically created by the PIN diodes, particularly in their biased state, can be overcome. Furthermore, utilization of these techniques at 100 GHz and above would not only provide an excellent flexibility in handling the small physical size of the phase shifter in maintaining its required dimensional tolerances, but would also provide ruggedness, better reliability and reproducibility of the millimetre wave phase shifting devices to be used in phased arrays conformal with the surfaces of missiles and projectiles in the 100-300 GHz frequency region. In light of the fact that there are no better phase shifter designs in existence today in the frequency region from 60-80 GHz and due to the ever increasing requirements for millimetre wave phase shifting devices above 100 GHz, further investigation and development of semiconductor millimetre and submillimetre wave compact, light weight, and cost-effective phase shifter design is recommended." Unquote.
The incorporation of this type of phase shifter in an electronic scan technique will be discussed in chapter 8.

8. AN ELECTRONIC SCAN TECHNIQUE AT MM WAVELENGTH USING BULK PIN DIODES

8.1 Introduction

Since 1978 US Army Electronics Research and Development Command, Fort Monmouth, New Jersey has been experimenting with a new method of scanning a linear array antenna. For this study dielectric waveguide is employed which approach is very applicable at mm-wavelength. They have confined their investigation to the frequency range of 55-100 GHz. In the beginning, the optimum dielectric waveguide dimensions were selected for which only one mode can propagate in this waveguide with minimum loss. Silicon is used as dielectric material.

8.2 Frequency scan

With the silicon dielectric rod an antenna has been realized and consists of the rod with period metallic stripe perturbation on one side. A sketch of the test set-up with this antenna is given in figure 8.1.
With this set-up the feasibility of electronically scanning through a range of angles has been shown by varying the frequency fed into the silicon rod. This antenna has been optimized theoretically and experimentally aiming at a large frequency scan for a single fundamental waveguide mode of operation [15].
In table 3 the minimum and maximum waveguide sizes for the fundamental propagation mode are given.

Mode E_{11}^{y}

FREQUENCY (GHz)	GUIDE SIZE (mm)			
	MIN	$\lambda_1/2$	MAX	λ_1
60	0.775	0.772	1.4	1.443
70	0.67	0.619	1.2	1.237
94	0.50	0.416	0.9	0.921

Table 3 Minimum and Maximum Waveguide Sizes for Fundamental

In figure 8.2 an example is given of the change of guide wavelength λg as a function of frequency. The dimension of the silicon guide of 0.9 x 0.9 mm cross-section is the maximum size for single mode operation at 94 GHz. For frequencies below the design frequency λg increases rapidly. In figure 8.3 an example is given of the radiation angle as a function of frequency. For frequencies between 57 and 65 GHz, the centre of the radiated beam (Θmax) varied from -68° to -7°, a change of 7.5°/GHz. The fact that these radiated beam angles are negative agrees with theory. With this simple and light construction a large frequency scan has been realized, which result can be compared to that of the serpentine waveguide construction discussed in section 2.1 at lower frequencies.

For various applications, the power handling capability and loss must also be considered. For applications in missiles and smart munition these two items will not be a problem for this technique and the large radiation angle from the antenna normal, is an advantage when the antenna has to be placed on the surface of the missile around the nose. The entire angular scan range can be shifted by changing the spacing of the perturbation as is shown in figure 8.4 and also by altering the silicon rod dimensions. The total length of the perturbation for the case given in figure 8.3 with 22 strips is only 4 cm.

8.3 Electronic scan with PIN diodes

The silicon dielectric waveguide with perturbations described in section 8.2 has been extended with PIN diodes. These diodes are placed at the side wall making a 90° angle with the wall with the perturbations on it. A sketch of this line scanning antenna is given in figure 8.5. With a change of bias current of the three employed PIN diodes the guide wavelength in the silicon rod can be varied.

In section 3.1.2 this principle is described and has resulted there in a change of phase shift. Here it will result in a change of scan angle as -has been demonstrated in section 8.2. The electronic scan capability of this set-up has also been studied at the US Army Electronics Research & Development Command at Fort Monmouth since about 1980 [16], [17].

The frequency for this study was about 60 GHz. For the situation presented in figure 8.5 a shift in scan angle of about 10° was easily obtained, corresponding to approximately a 6.7 percent change in guide wavelength or a phase shift of 24.3° per wavelength as can be seen in figure 8.6. The expected 3 dB antenna beamwidth of this set-up with 16 strips at 63 GHz will be about 10° for a moderate tapered illumination. An experimental value of about 8° has been measured as can be seen in figure 8.6 for curve A with zero bias current and for curve D for large bias current (300 mA).

For bias current values in between these two extremes, the gain of the radiated beam is reduced (curve B and C for respectively 10 and 18 mA bias current).

The result shown in figure 8.6 at 60 GHz can also be achieved at other frequencies as can be seen in figure 8.7 where the scan angle for 0 mA and 300 mA bias current is given as a function of frequency from 61 to 66 GHz.

An explanation for the gain reduction presented in figure 8.6 was found and was published in 1982 [18]. As the energy propagates down the dielectric runner, an evanescent portion of the wave is in the air space surrounding the dielectric (figure 8.8) both in the vertical and hori-

zontal directions. In the unbiased state the PIN diode behaves like an insulator and in the biased state as a conductor.

When the bias current is in between these two extremes, energy will be absorbed by the PIN diode modulation since the conductivity of the intrinsic (I) region is intermediate between an insulator and a metal-like conductor.

In the intermediate conductivity state, the energy is not only being absorbed but is refracting into the lossy intrinsic medium. The fields in the runner and PIN modulator are envisaged as shown in figure 8.8. In figure 8.8(a), (b), and (c), a metal wall is brought in from infinity to a fixed position h_3, determined by a low permittivity spacer which will later also serve as a decoupling device to prevent the wave from diffracting entirely into the modulators.

The presence of the metal wall has been found to increase λ_z thus making the radiation angle Θ shift to a more negative value. In figure 8.8(d), (e), and (f), it was theorized that by changing the excess carrier density in the PIN diode i-region, a moving conduction wall will have a similar effect to a moving metal wall.

In an attempt to minimize the absorption-refraction losses it was found necessary to use an optimum thickness (h_3) of low dielectric constant insulating layer between the silicon runner and the PIN diode modulators. The insulator serves as a space which provides less coupling from the runner to the long PIN diodes (total length is 2.4 cm) and hence little refraction into the diodes where losses occur due to absorption and re-radiation. If the insulating layer is too thick there is less modulation, with the evanescent portion of the wave traveling down the runner undisturbed and little or no scan angle changes observed.

The optimum thickness of the insulation layer (h_3) shown in figure 8.9 has been determined for which the line scanning antenna provides an as nearly as possible continuous analog scan.

For the set-up shown in figure 8.9 an optimum result has been obtained which is given in figure 8.10 and amounts a scan of about 5° with nearly uniform radiated power as a function of radiation angle. The lowest radiated power is observed for a total bias current of about 3 mA (1 mA per diode).
The maximum scan angle has been reduced due to the h_3 layer from 8° to 5°. A theoretical calculation (with metal walls) resulted in a scan angle of about 3.5° which is reasonably close to the experimental value of about 5°.
A continuous variable bias current is needed for analog scanning. With the two extreme bias states a digital scan can be realized. When small scan angle changes are required the corresponding change in guide wavelength must be realized with sufficient small diodes which must fit in the available space between each radiator of the linear array antenna. This situation is comparable with that presented in figure 2.3 where each phase shifter has all the phase setting possibilities with the aid of 2 PIN diodes per bit.
However, this is no longer a cheap and simple approach. At industry (see section 8.4) a combination of digital and analog scanning with the aid of more PIN diodes on top of each other has been examined.

8.4 Continued research at industry

A study contract has been placed at industry from July 1981-January 1982 to explore the realizability of a antenna with a few linear arrays in parallel with prescribed properties. The result has been presented in two reports [19],[20]. A more detailed understanding of various topics of the set-up has been gathered. In order to reduce the losses for bias currents between the two extremes (0 and about 100 mA per PIN diode). It was found that the resistivity ρ of the diode should be as large as possible. Values of $\geq 10^4$ ohm-cm were found resulting in a low loss ($\tan\delta \leq 1.6 \cdot 10^{-4}$). For a large resistivity, the conductivity σ is small ($\sigma = 1/\rho$)

On the other hand a large conductivity is required to achieve a large carrier lifetime of the PIN diodes. A carrier lifetime of 10-20 μs has been obtained for the size of PIN diode needed in this linear array set-up. With a larger diode a larger carrier lifetime can be obtained. Values of 80 μ-sec have been found.

The general conclusion of this study was that most requirements of the antenna construction could be met and that theoretical and experimental results are in good agreement with each other, but that the carrier lifetime for this type of application is unsatisfactorily small.

9. RESULTS OF A 35 GHZ LINEAR PHASE ARRAY ANTENNA WITH 40 NON-RECIPROCAL FERRITE PHASE SHIFTERS

9.1 Introduction

At the Physics and Electronics Laboratory TNO, a linear phased array antenna with 40 non-reciprocal ferrite phase shifter has been designed, developed and tested. Use is made of the Lithium ferrite and the geometry mentioned in section 7.3. Some of the production results will be mentioned in section 9.2. A constrained feed antenna distribution network is used and the design is aimed at an antenna with low side lobes and broad bandwidth. Some results will be given in paragraph 9.3.
A beam steering computer is used as interface between the drivers of the phase shifters and the unit deciding upon the beam direction and frequency to be employed. This interface will not be discussed further. To avoid the large dead-zone of the radar of about 3 km due to the reset time of the phase shifters of about 20 μsec for receive after the radar pulse has been transmitted, a special driver technique is developed resulting in a dead-zone of only about 250 m. At the end of the receive time (just before the transmission of the following radar pulse) a time of 6 μs is needed with this special driver technique to set the phase shifters for the next transmission.
The maximum p.r.f. for a 10 km range is 15 KHz but only 4.5 KHz is used in this array. This is due to the fact that the phase shifters are stabilized in an easy way at 45°C without any extra cooling. For a larger p.r.f than 4.5 KHz forced cooling will be needed or stabilization at a higher temperature which will amongst others has the disadvantage of a reduced differential phase shift with the need of longer ferrite rods.

9.2 Phase shifter production results

After the initial measurement on ferrite rods with the tolerance specification presented in section 7.3, the phase shifter with Lithium ferrite has been further optimized [20]. A two step matching transformer is used resulting in a good match over a much larger bandwidth than presented in figure 7.4. The result can be seen in figure 9.1 for the phase shifter with two waveguide tapers and load for test purposes and also for the tapers and load separately. The result of the phase shifter alone, as used in an array, will be lower than the top curve.

A series of 150 rods now with size tolerances has been purchased. Unfortunately the manufacturing has taken place in two batches which resulted in slightly different average properties of each batch. On the other hand information has been obtained regarding the spread between two production runs.

The first batch contains 87 rods and the second one 63 rods. The size of the diameter, the concentricity error (diameter variation over the length), the length and the concentricity of the hole with its tolerances could be specified. The physical properties of the ferrite are not easy to specify. Still more difficult is the specification of the phase shift, in particular if one reminds that the insertion phase shift is about 3000° and that from that level as starting point the differential phase shift (0-360°) is set (see section 6.1.5)

The best one can do is to require that one batch of raw material is used for the total production and that the rods are all produced in an identical way The waveguide width employed for the ferrite selection has been 5.14 mm (up to figure 9.17). The conical error distribution for the first batch is given in figure 9.2 and in figure 9.3 for the second batch.

The spread in diameter is given in figure 9.4 for the first batch and in figure 9.5 for the second batch. The spread in length for the 150 rods is presented in figure 9.6. The differential phase shift distribution for the first batch is given in figure 9.7 and for the second batch in figure 9.8.

The concentricity error distribution of the hole in the toroid is shown in figure 9.9 for the first batch. There were no errors in the second batch. The result for the total of 150 rods is given in figure 9.10. The relation between differential phase shift and concentricity error is shown in figure 9.11.

After these measurements 50 rods have been selected to be used for the linear phased array antenna (40 + 10 spare ones). The insertion loss has been measured at various frequencies and the result is given in figure 9.12 for 31.5 GHz, in figure 9.13 for 34 GHz, in figure 9.14 for 35 GHz, in figure 9.15 for 36 GHz and in figure 9.16 for 38.5 GHz. The differential phase shift distribution for these 50 rods is presented in figure 9.17. The results on the right of the dashed line are obtained by using one driver for the 50 rods. The waveguide width is still 5.14 mm.

Because an antenna constrained feed was used with a standard waveguide width of 7.14 mm and since a waveguide taper between this feed and the phase shifters was undesirable, the 50 selected rods were all tested with a waveguide width of 7.14 mm and each phase shifter with its own not selected driver. This result is presented in figure 9.17 at the left of the dashed line.

When the rods are used with a selected driver the result presented in figure 9.18 is obtained (waveguide width 7.14 mm). The insertion loss distribution for the final selected 40 phase shifters for all phase shift settings is given in figure 9.19 for a bandwidth of 2 GHz around 35 GHz . In these insertion loss values the loss of 0.2 dB of the two waveguide tapers needed for the measurements is included. The average value of 0.7 dB mentioned in figure 9.20 for instance will be 0.5 dB when the single phase shifters are used in the phased array antenna. An example of an insertion loss measurement for one phase shifter as a function of frequency for various phase shift settings is given in figure 9.21.

The work presented in figure 9.2 till figure 9.21 was performed by F.A. Nennie of the research group Radar of the Physics and Electronics Laboratory TNO, The Netherlands.

9.3 Constrained feed of 35 GHz linear phased array antenna

The constrained feed with an amplitude distribution for low side lobes and broad bandwidth has been designed and constructed at the Physics and Electronics Laboratory TNO. No large effort was made in minimizing the size of it. A sketch of the feed is given in figure 9.22 where we see three units, the antenna feed ending in a linear array of waveguides at an mutual distance larger than the required half wavelength ($\lambda/2$), a tapering section towards a half wavelength spacing and the row of phase shifters. The first and second part are both composed of two halfs, a top and a bottom one (as can be seen in figure 9.22) which are fixed together. In figure 9.23, a photo is shown of one half of the feed construction. The couplers to achieve the required amplitude distribution and the tapering part can be seen. Efforts have been made to reduce the number of different couplers to a minimum, slighty at the expense of the amplitude distribution.

In the first constructed feed small coupling errors are still present but nevertheless an acceptable side-lobe level has been achieved over 25-30% frequency band as can be seen in figure 9.24. Improvements are therefore still possible.

10. A PLANAR PHASED ARRAY ANTENNA WITH 2N MASTER DRIVERS INSTEAD OF N^2 DRIVERS

A rectangular phased array antenna can be considered to be built up of N rows and N columns. The required phase shift for an arbitrary scan direction is for each array element a combination of a contribution of its row and of its column.

With low loss phase shifters and a small amount of ferrite, as is the case at mm wavelength, each array element could be realized by two phase shifters in series [21]. One of them will be used for the row phase setting and the other one for the column one. All phase shifters in a row have the same phase setting and can therefore be driven by a master driver, placed at the periphery of the array antenna. The same situation exists for the columns.

In this way 2N master drivers are needed, N for the rows and N for the columns. Moreover, no space is needed in the array for the drivers. At 35 GHz for example the average insertion loss is 0.5 dB (see figure 9.21) and the total loss for this situation will therefore be 1.0 dB which is still an acceptable value. The size of the ferrite rod for a 3 GHz non-reciprocal ferrite phase shifter follows from figure 6.4. For the garnet G2, the diameter is 13 mm and the length for 425° saturated differential phase shift is 17 cm, resulting in a volume of 22.5 cm^3. The volume of a 35 GHz ferrite rod is $\pi/4\ (0.22)^2\ 3.5\ cm^3 \approx 0.13\ cm^3$. The volume of the 3 GHz rod is therefore a factor 170 larger than the 35 GHz one.

An antenna with a 2° half power beamwidth will have about 64 phase shifters in the row and in the column (rectangular lattice). The amount of ferrite to be magnetized by the 35 GHz master driver of 8.5 cm^3 is therefore less than half the amount of the 3 GHz rod and slightly more than a 5.6 GHz rod of 5.6 cm^3. The dissipation in this array will be about 700 Watt based upon a p.r.f. of 4.5 kHz, a driver voltage of 100V and a saturation pulse duration of 2 μsec with an average current of 2 Ampere. The antenna cross-section is 30 x 30 cm^2 and the depth is about 8 cm, resulting in a dissipation of 0.1 W/cm^3.

The antenna amplitude distribution network must be realized in such a way that equal path length is present or a path length difference that can be compensated per row and/or per column. For a space fed (optical feed) configuration the spherical-planar phase front correction must be approached by that of two cylinders, resulting in phase errors in the four corners of the array at the periphery. For an array with a focal length of the order of the diameter of the antenna, the side-lobe degradation due to these phase errors are for many cases acceptable, but not when low side-lobes are required.

11. CONCLUSIONS AND RECOMMENDATIONS

- The advantages of electronic scan have been demonstrated during the last two decennia in many fielded phased array radars operating in the cm/dm wavelength region.
- The components and devices for electronic scan in the millimetre wave region can be realized with good properties and have been demonstrated in the laboratory up to 66 GHz. It is expected that a 95 GHz phase shifter can be developed.
- The extrapolation of phase shifter properties from the cm wave region to the mm wave region has been demonstrated.
  So far no real large production of phase shifters has taken place and the related expected cost reduction has never been demonstrated therefore.
  In addition, there are aspects of mm-wave antenna/phase shifter design, for example masterdrivers, which might lead to cost reduction.
- The use of 'bulk' PIN diodes for electronic scan has shown not to be feasible due to two contradictory requirements.
- The PIN diode phase shifter has too high an insertion loss at mm wave frequencies and must be disregarded for practical use.
- An optimum choice of ferrite material is possible up to 26 GHz. Experimental results obtained above this frequency up to 66 GHz are found to be acceptable.
  Hexagonal ferrites are being examined for use in phase shifters and this development has to be followed carefully, particularly with regard to all essential phase shifter properties and the availability of this ferrite material.
- With the realization of a linear phased array antenna at 35 GHz, it has been demonstrated that a series production of ferrite phase shifters with tight requirements is possible.

- The minimum dead-zone of about 3 km due to the employement of non-reciprocal ferrite phase shifter has been reduced to 250 m in this phased array antenna with the aid of a special driver technique.
- The non-reciprocal latched ferrite phase shifter and the reciprocal dual-mode ferrite phase shifter can both be considered for phased array antennas.
- For low loss phase shifters the use of 2N master drivers at the periphery of a planar phased array antenna can considerably reduce the number of drivers (from N^2 to 2N) but at the expense of an increase of phase shifters without drivers (from N^2 to $2N^2$).
- The use of the MMIC and MIC technique for the realization of phased array components at mm-wave frequencies is being explored at a few centres.
  It is recommended that this development be followed carefully since it might in the long end result in the required breakthrough.

Ir. G.A. v.d. Spek (Groupleader)

Dr. J. Snieder (Author)

12. REFERENCES

1. Freibergs, E., H. Jacobs, R.E. Horn, Millimeter-Wave P-I-N Diode phase shifter, Research and Development Technical Report DELET-TR-83-5, ERADCOM, Fort Monmouth, N.J., pp. 1-24, December 1983 (US Government agencies only).

2. Reggia, F. and E.G. Spencer: A new technique in ferrite phase shifting for beam scanning of microwave antennas, Proc. IRE, vol. 45, pp. 1510, 1957

3. AN/SPS-33
Frequency-phase scanned radar developed by Hughes Aircraft compagny and installed on US Naval ships.
Enterprise and Longbeach, (1963)

4. Treuhaft, M.A., and L.M. Silber: Use of Microwave ferrite toroids to eliminate External Magnets and Reduce Switching Power, Proc. IRE, Vol. 46, pp. 1538, August, 1958

5. Hudson, A.S., J. Snieder, J.W.F. Dorleyn, Manganese Substition in Garnets for Remanent Phase Shifters, IEEE Trans.MTT. Vol. MTT-19, pp. 119-120, Jan. 1971.

6. Thompson, S.B., G.P. Rodrigue, The application of planar anisotropy to millimeter-wave ferrite phase shifters, IEEE Trans. MTT, Vol. MTT-33, No.11, pp. 1204-1209, Nov. 1985.

7. Snieder, J., Ability of ferrite and diode phase shifters at millimetre wavelength, Proceedings of NATO Symposium on Microwave Components for the frequency range above 6 GHz, pp. 410-429, 23-24 January 1978.

8. Lang, R.J., B.J. Edward, A 35 GHz electronically steered line array, IEEE MTT-S Digest, pp. 937-940, 1987.

9. Whicker, L.R., C.R. Boyd, A new reciprocal phaser for use at millimeter wavelengths, 1971 IEEE-MIT Symposium Digest, pp. 102-103, May 1971
Or: Boyd, C.R., A dual-mode latching reciprocal ferrite phase shifter, IEEE Trans. MTT, Vol. MTT-18, pp. 1119-1124, Dec. 1970

10. Boyd, C.R., A 60 GHz dual-mode ferrite phase shifter, 1982 IEEE MIT-S Digest, p.p. 257-259, 1982

11. Rodrigue, G.P., MTT-S. International Microwave Symposium Highlights, Ferrite Session & Magnetostatic Waves, Microwave Journal, pp. 28, June 1979.

12. Snieder, J., F.A. Nennie, Feasibility study of a 47 GHz non-reciprocal latched ferrite phase shifter, Physics Laboratory TNO Report, PHL 1983-06, February 1983

13. Snieder, J., F.A. Nennie, Feasibility study of a non-reciprocal latched ferrite phase shifter in the 52-66 GHz frequency band, Physics Laboratory TNO Report, PHL 1983-08, March 1983

14. Horn, R.E., H. Jacobs, K.L. Klohn, E. Freibergs, Single-Frequency Electronic-Modulated Analog Line Scanning Using a Dielectric Antenna, IEEE-Trans. MTT., Vol. MTT-30, No. 5, pp. 816-820, May 1982.

15. Klohn, K.L., R.E. Horn, H. Jacobs, E. Freiberg, Silicon Waveguide Frequency Scanning Linear Array Antenna, IEEE. Trans. MTT, Vol. MTT-26, No. 10, pp. 764-773, October 1978.

16. Horn, R.E., H. Jacobs, E. Freibergs, K.L. Klohn, Electronic Modulated Beam-Steerable Silicon Waveguide Array Antenna, IEEE. Trans. MTT, Vol. MTT-28, No. 6, pp. 647-653, June 1980.

17. Hindin, H.J., P-I-N diodes steer silicon antenna, Electronics Review, Electronics, pp. 42 and 44, September 11, 1980.

18. Bales, G.W. of Martin Mariëtta Corp., Electronic Phased Array Scanner, Research and Development Technical Report, DELET-TR-81-0401-1, prepared for ERADCOM, Fort Monmouth, N.J., pp. 1-74, June 1982.

19. Bales, G.W. of Martin Mariëtta Corp., Electronic Phased Array Scanner, Research and Development Technical Report, DELET-TR-81-0401-2, prepared for ERADCOM, Fort Monmouth, N.J., pp. 1-64, December 1982.

20. Nennie, F.J., Internal results at Physics and Electronics Laboratory TNO, The Netherlands

21. Cheston, T.C . J. Frank, private communication at Applied Physics Laboratory of The Johns Hopkins University, USA, about 1968.

13. ACKNOWLEDGEMENT

The author likes to thank Dr. M. Downey of RSRE, Great Malvern, U.K. for his comments and suggestions and his help with the English language, and the employees of the Physics and Electronics Laboratory TNO for typing the report and realizing the figures.

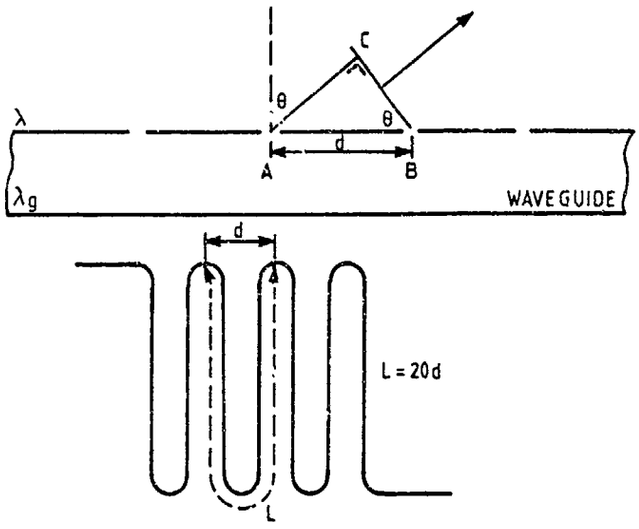

Figure 2.1

Frequency scan in a linear phased array antenna

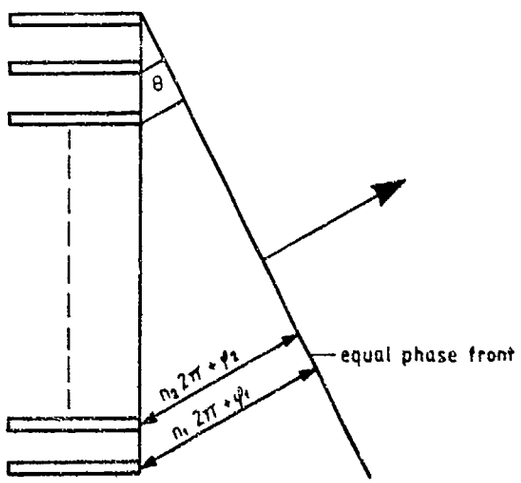

Figure 2.2

Phase scan in a linear phased array antenna. Phase shifter parallel to each other

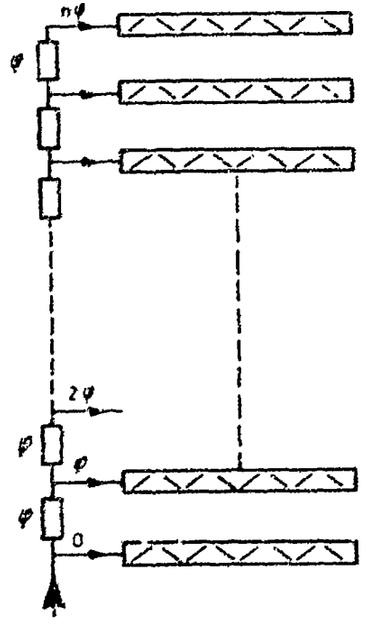

Figure 2.3

Phase-frequency scan in planar phased array antenna. Phase shifters in series

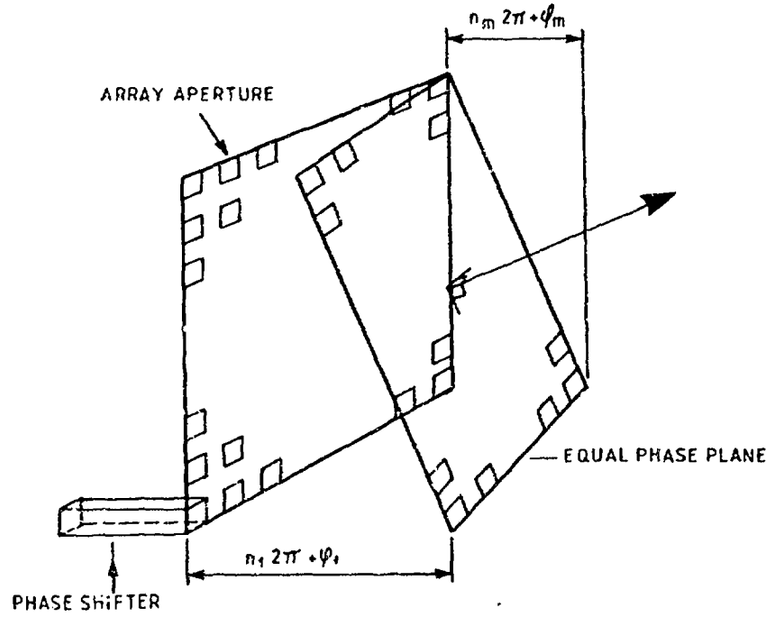

Figure 2.4

Phase-phase scan in planar phased array antenna

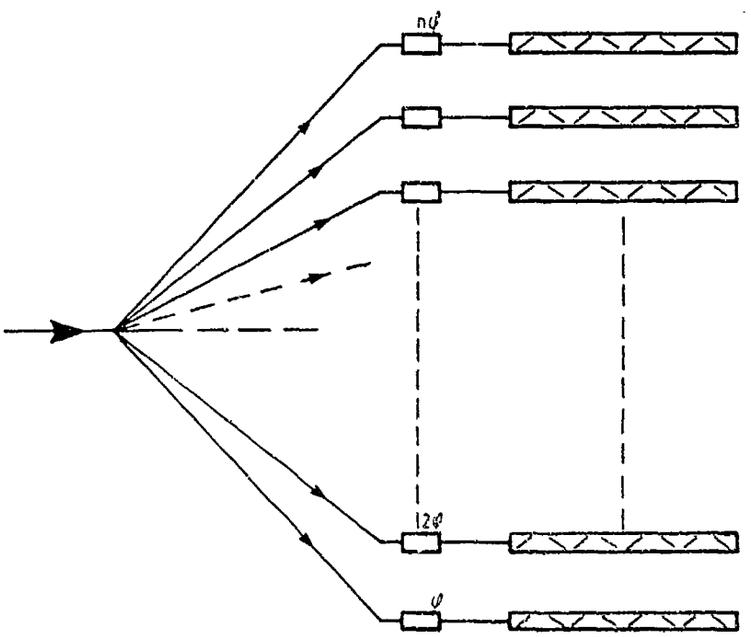

Figure 2.5

Phase-frequency scan in planar phased array antenna.
Phase shifter parallel to each other

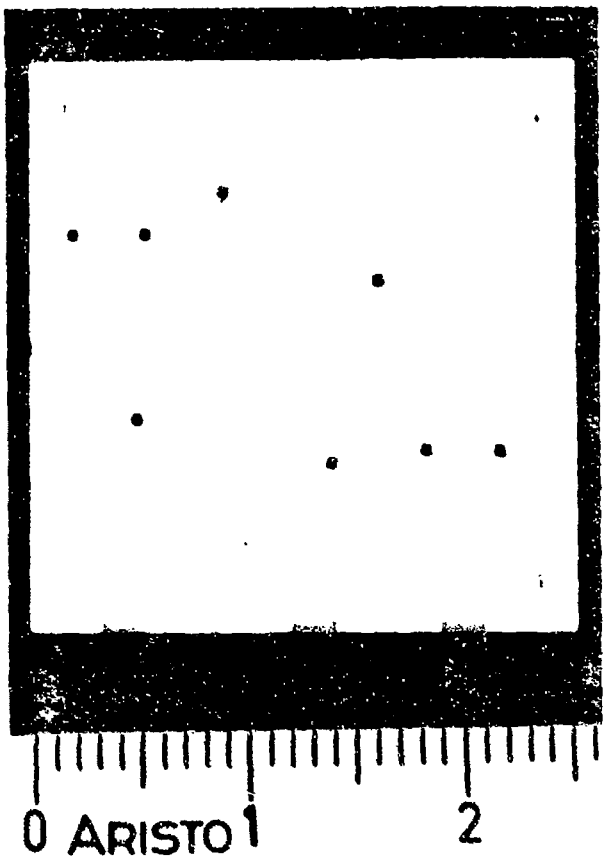

Figure 3.1

X-band 4 bit PIN diode phase shifter

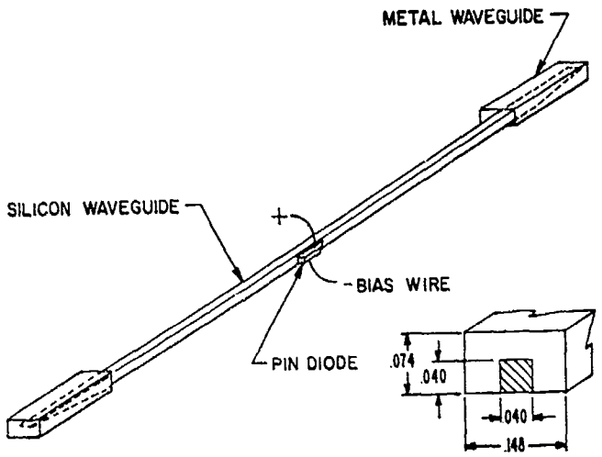

Figure 3.2

Phase shifter test fixture

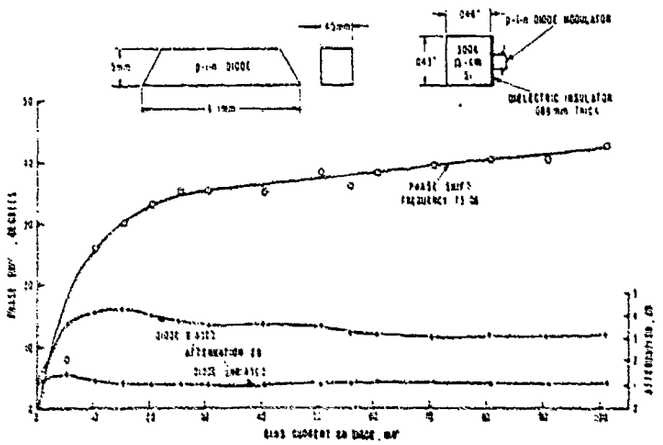

Figure 3.3

Phase shift as a function of bias current on p.i.n diode

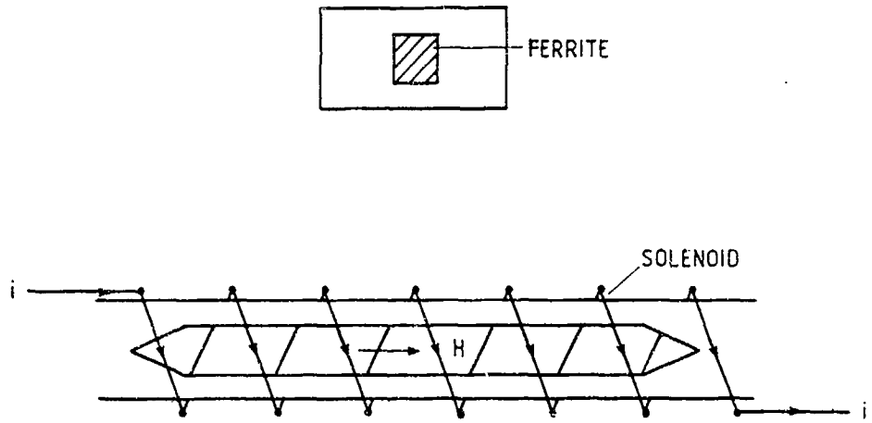

Figure 3.4

Reggia-Spencer type phase shifter

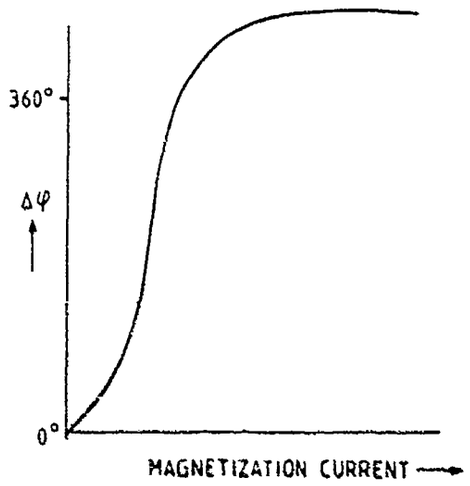

Figure 3.5

Differential phase shift as a function of magnetization current

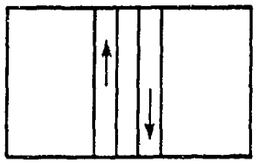

Figure 3.6

Twin slab ferrite phase shifter

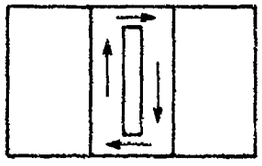

Figure 3.7

Ferrite phase shifter using rectangular toroid

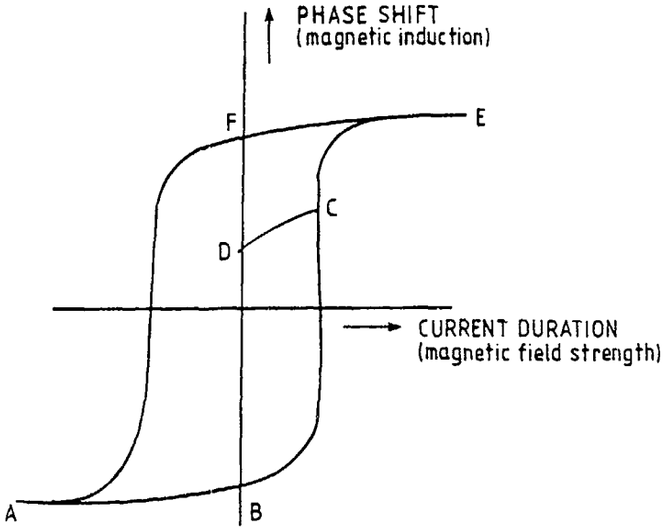

Figure 3.8 Phase shift (magnetic induction) as a function of dc current pulse duration (magnetic field strength) of ferrite phase shifter

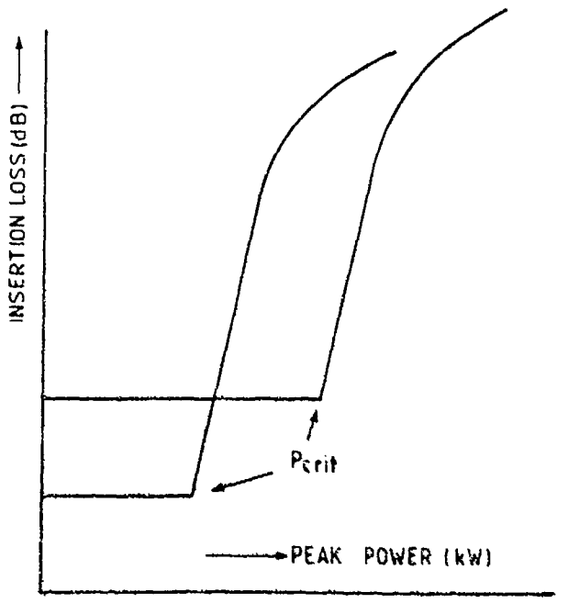

Figure 3.9 Insertion loss as a function of applied peak power for two different types of ferrite phase shifters

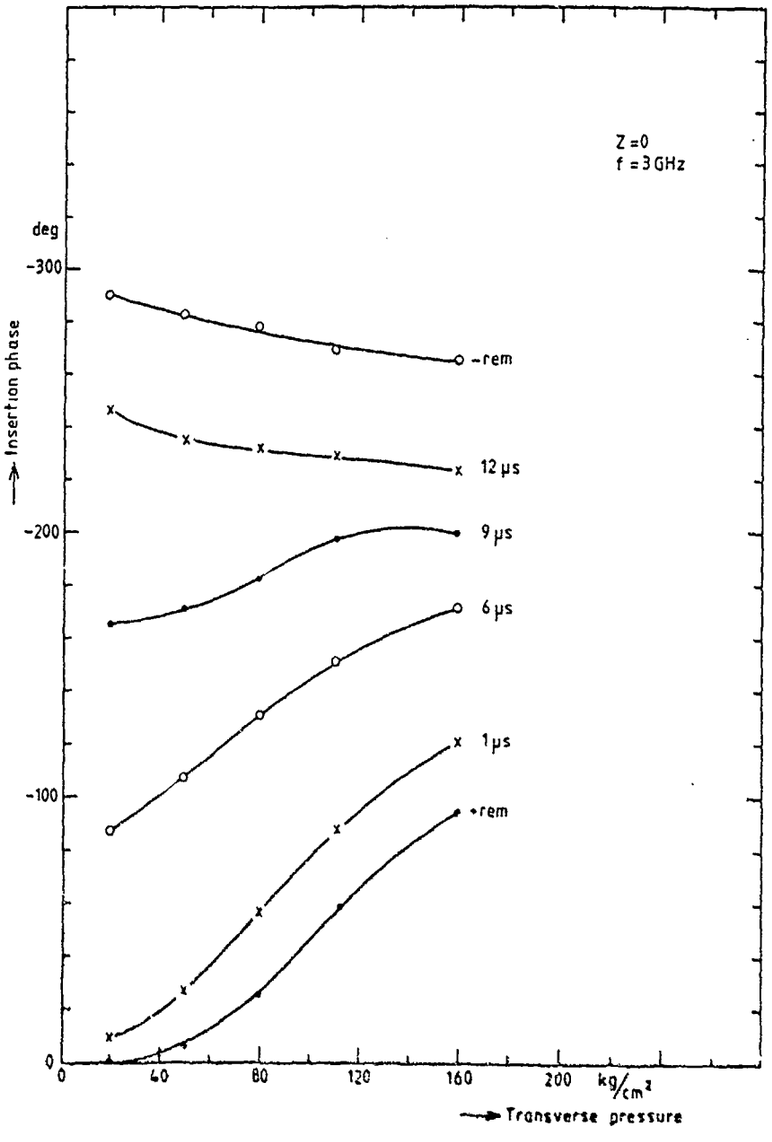

Figure 3.10

Insertion phase as a function of transverse pressure for different magnetization states from +rem to -rem
Frequency 3 GHz; Z = 0

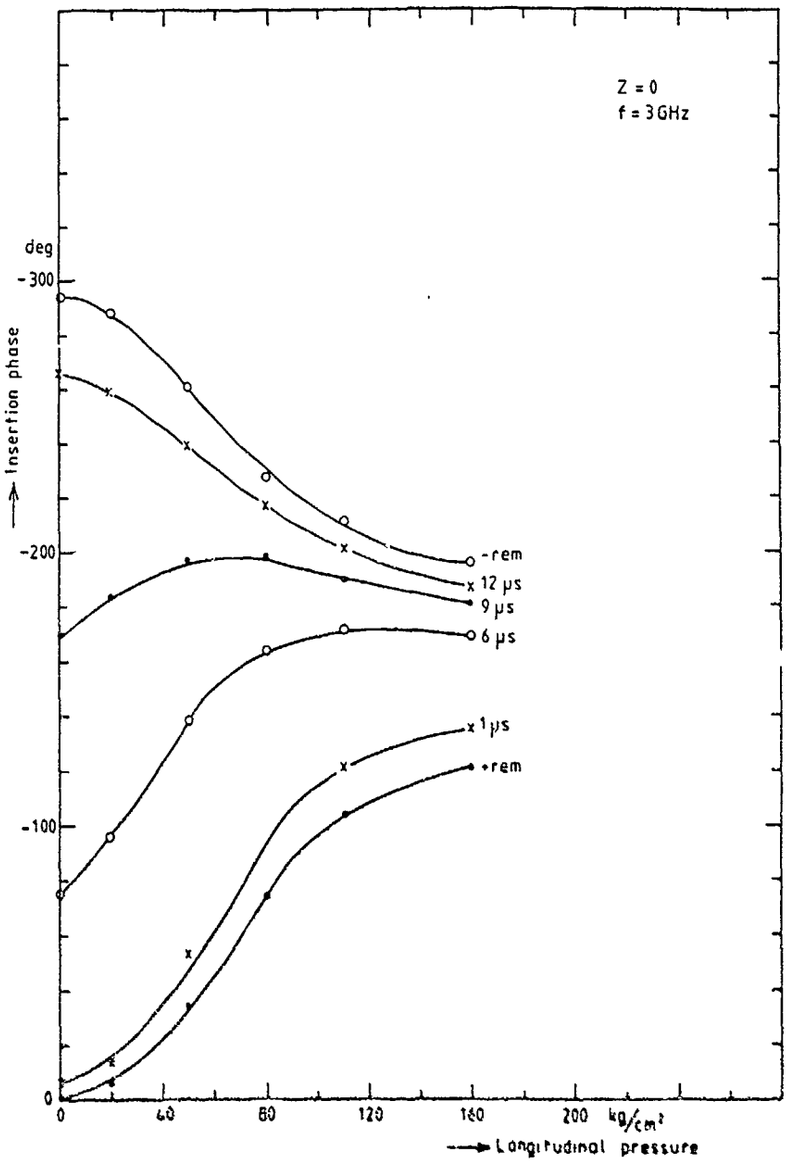

Figure 3.11

Insertion phase as a function of longitudinal pressure for different magnetization states from +rem to -rem
Frequency 3 GHz; Z = 0%

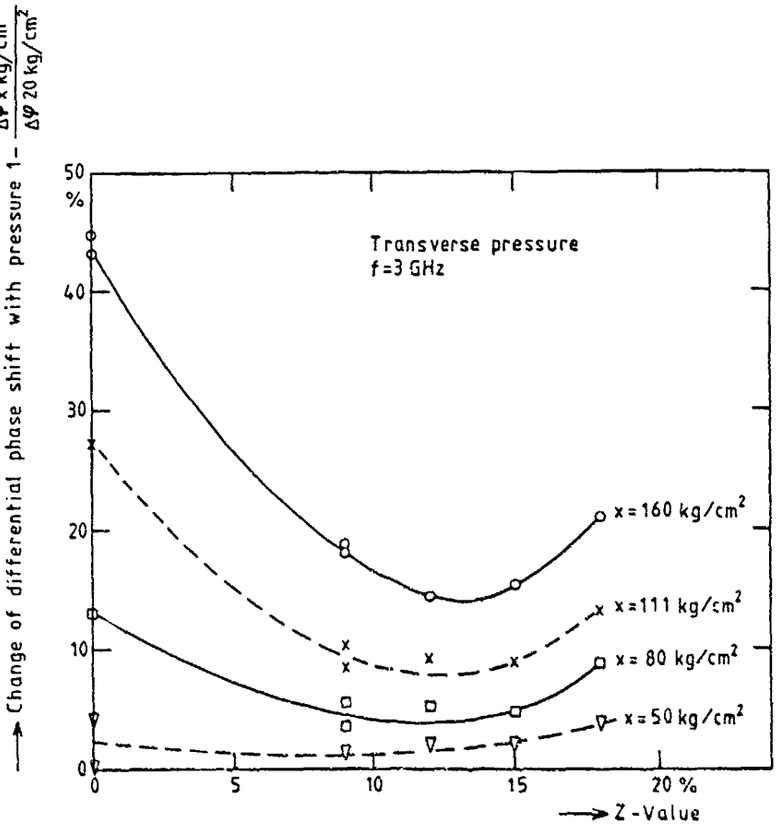

Figure 3.12

Change of differential phase shift with pressure in percentage for applied transverse pressures of 50, 80, 111 and 160 kg/cm² as a function of Z-value for a frequency of 3 GHz. The reference pressure is 20 kg/cm²

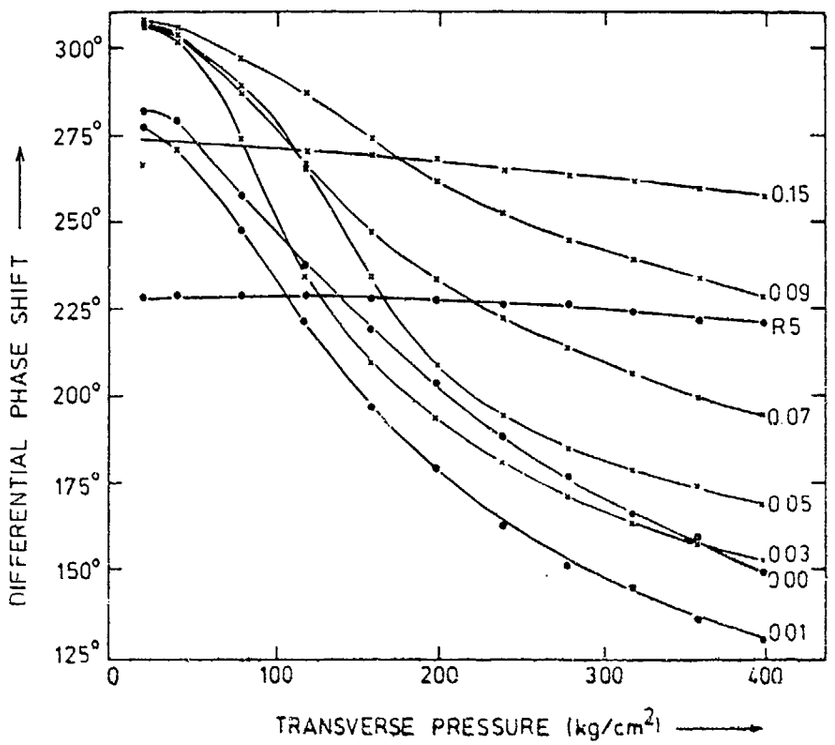

Figure 3.13

Differential phase shift as a function of applied transverse pressure for various Mn substitution in garnet (x-value) and for a magnesium-manganese ferrite R5 (f = 5.6 GHz)

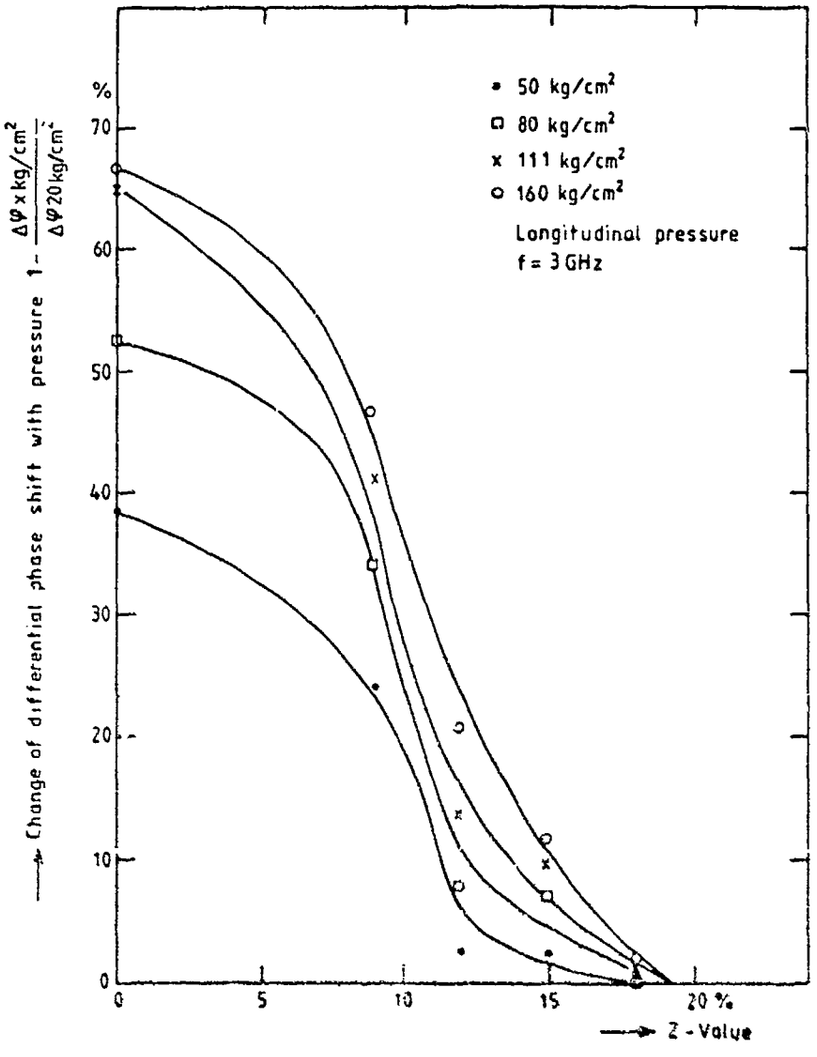

Figure 3.14

Change of differential phase shift with pressure in percentage for applied longitudinal pressures of 20, 50, 80, 111 and 160 kg/cm² as a function of Z-value for a frequency of 3 GHz. The value of one rod is used for each point and 20 kg/cm² is the reference

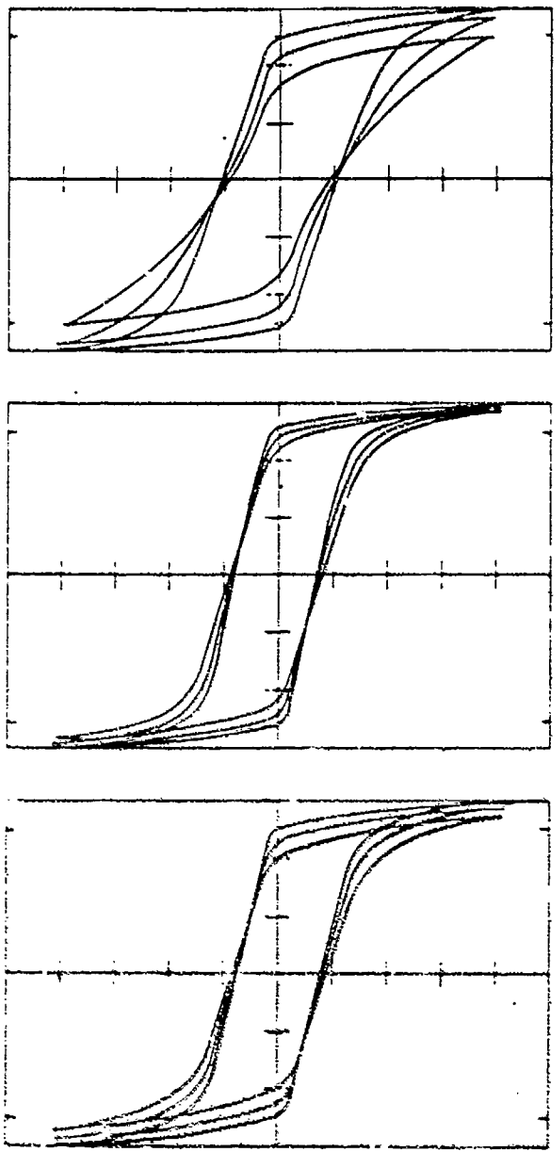

Figure 3.15

B-H loops for transverse pressures of 20, 80 and 160 kg/cm² and Z = 0, 12 and 18%

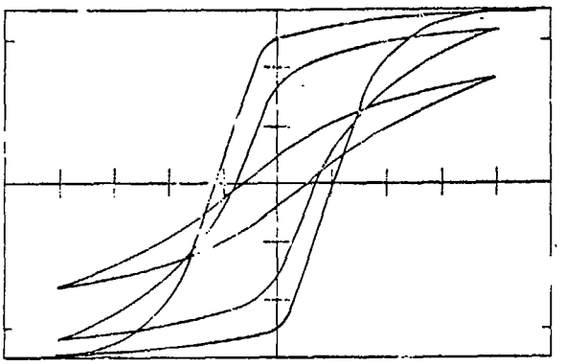

Z = 0%

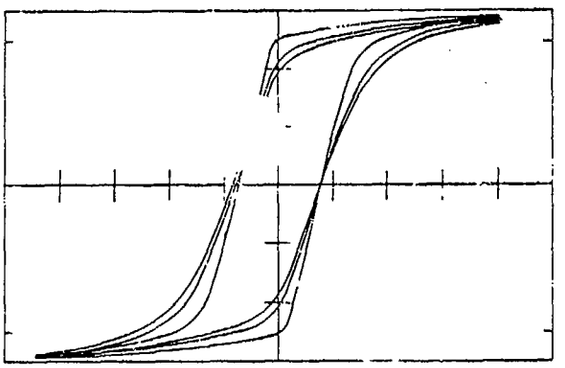

Z = 12%

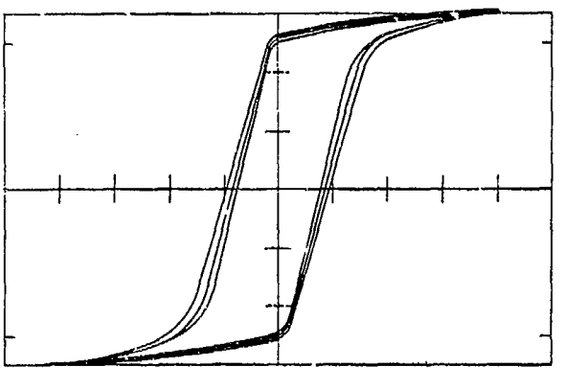

Z = 18%

Figure 3.16

B-H loops for longitudinal pressures of 20, 80 and 160 kg/cm² and Z = 0, 12 and 18%

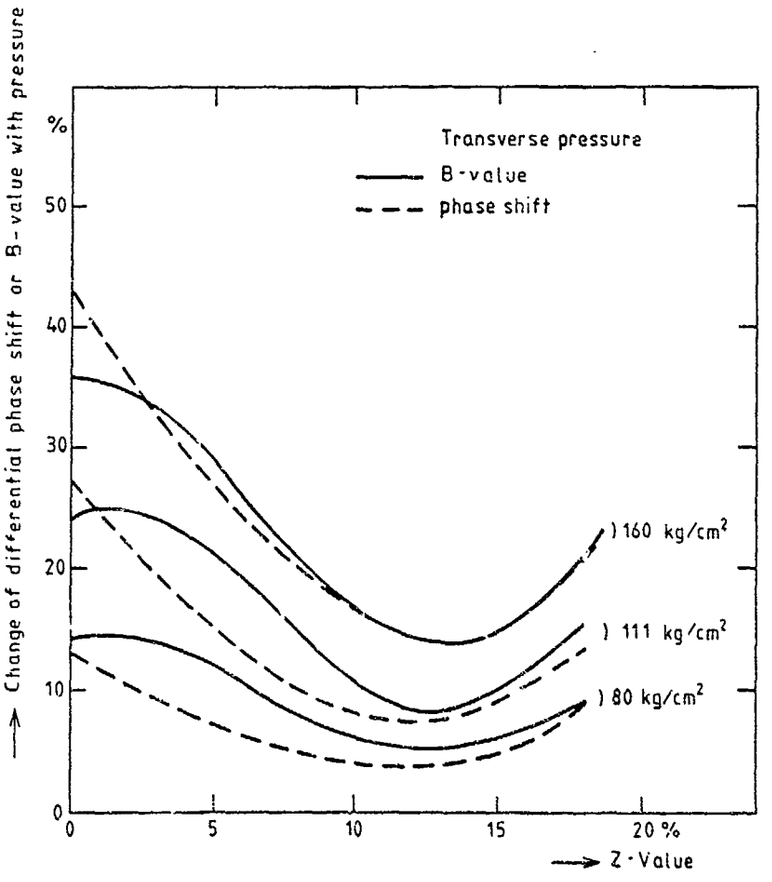

Figure 3.17

Comparison of change of B value with pressure with that of change of differential phase shift with pressure (in percentage) as a function of Z-value for transverse pressures of 80, 111 and 160 kg/cm² with 20 kg/cm² as a reference (B-value solid lines, phase value dashed lines)

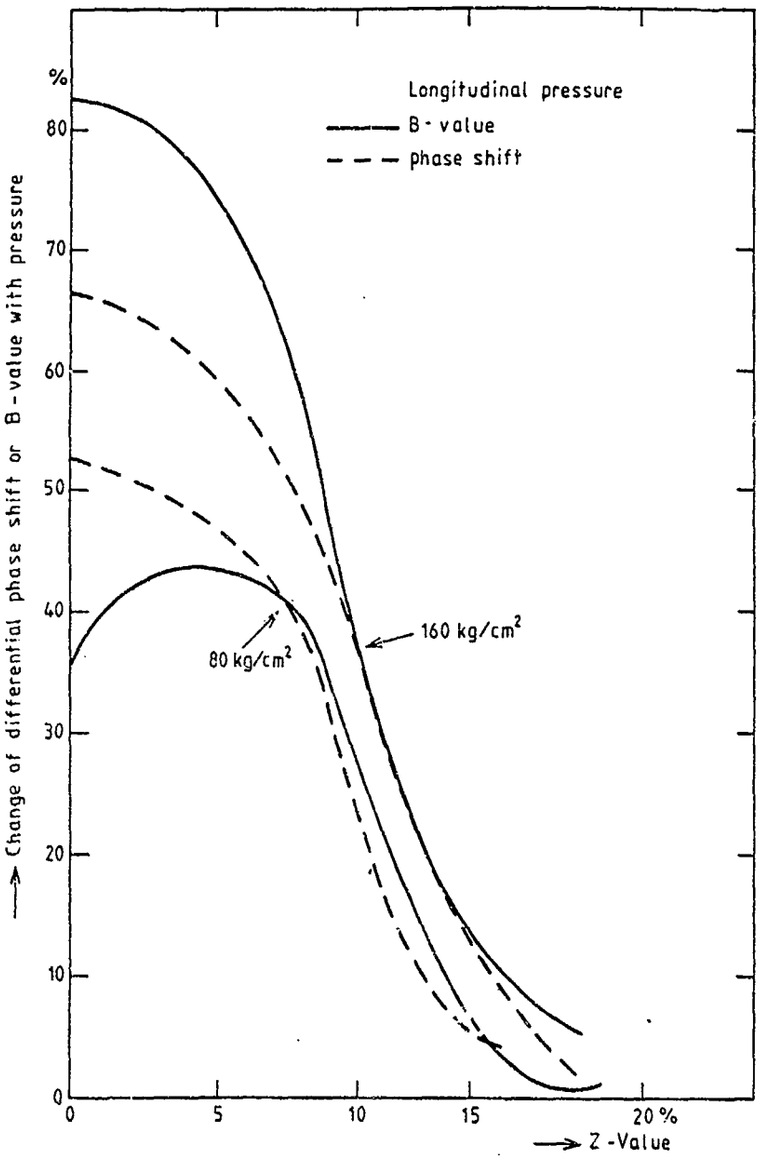

Figure 3.18

Comparison of change of B-value with pressure with that of change of differential phase shift with pressure (in percentage) as a function of Z-value for longitudinal pressures of 80 and 160 kg/cm² with 20 kg/cm² as a reference (B-value solid lines, phase value dashed lines)

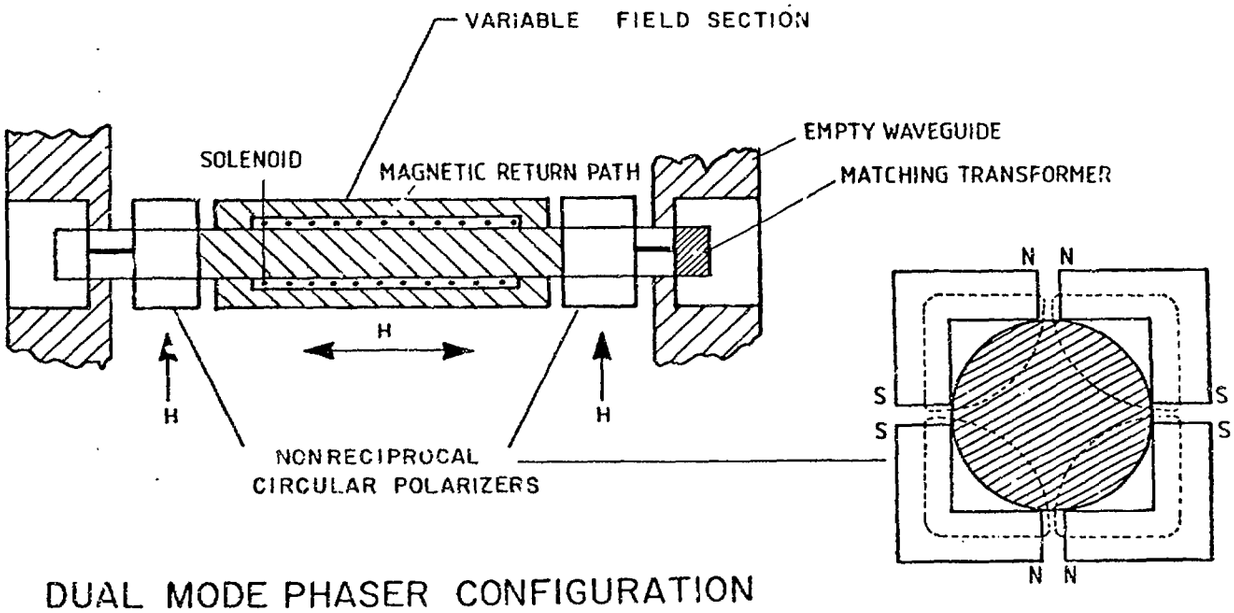

Figure 3.19

Schematic drawing of dual-mode phase shifter

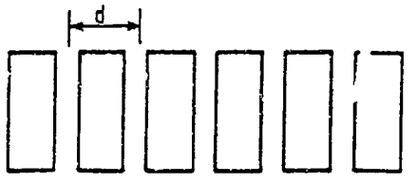

Figure 5.1

Front view of linear phased array antenna with waveguide apertures as radiators

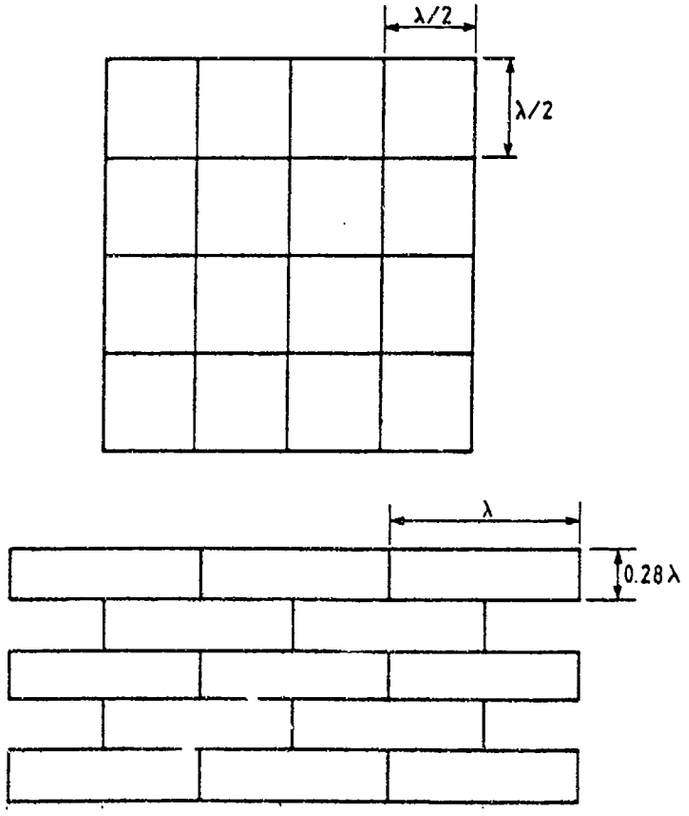

Figure 5.2

Rectangular array lattice (λ/2 * λ/2) and trianguiar lattice (λ x 0.28 λ) of planar array antenna

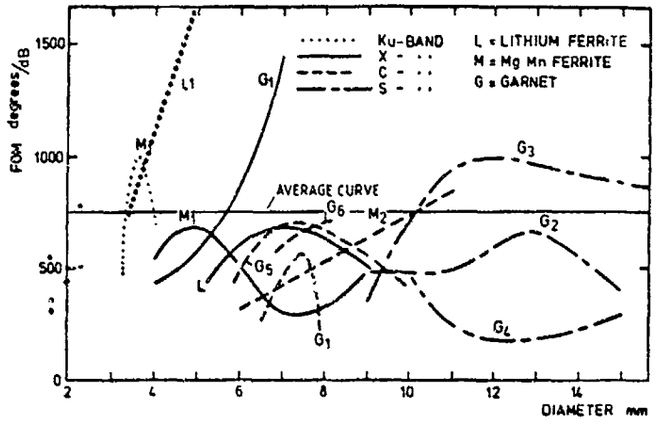

Figure 6.1

Figure of merit as a function of rod diameter

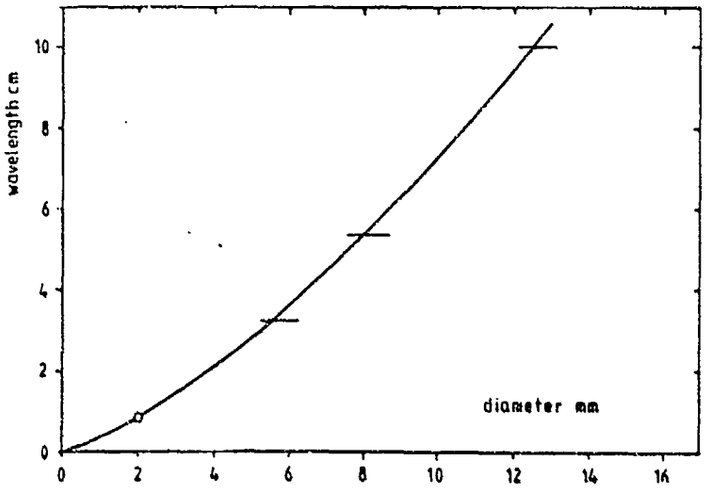

Figure 6.2

Free space wavelength as a function of diameter of ferrite rod

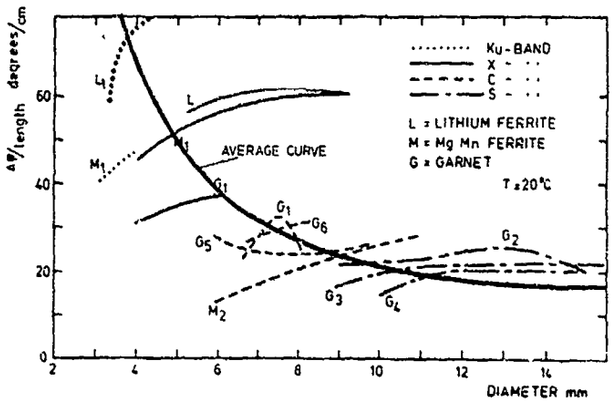

Figure 6.3

Differential phase shift per cm length as a function or rod diameter

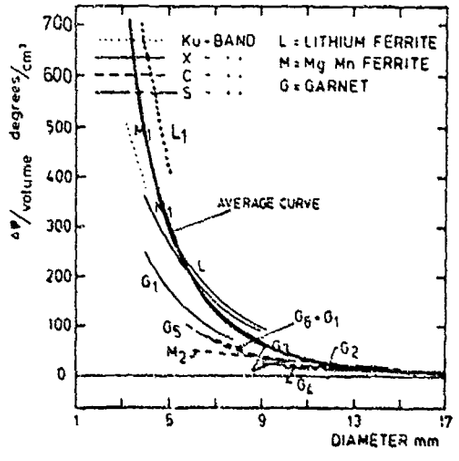

Figure 6.4

Differential phase shift per cm^3 as a function of rod diameter

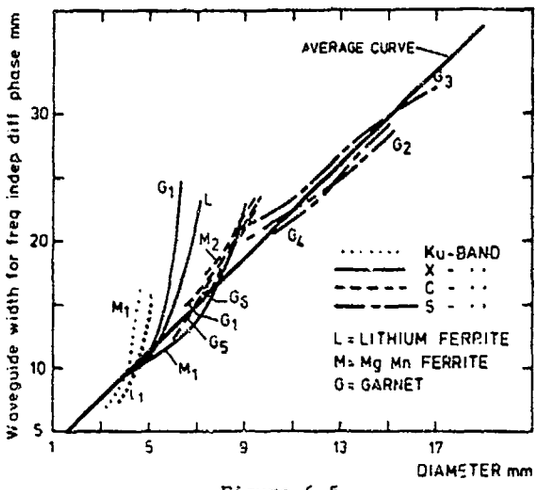

Figure 6.5

Waveguide width at frequency independent differential phase shift as a function of rod diameter

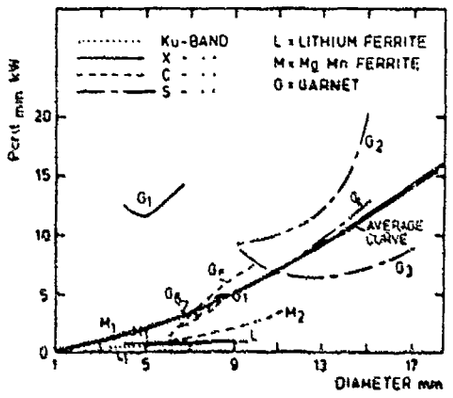

Figure 6.6

Peak power $P_{crit.}$ as a function of rod diameter

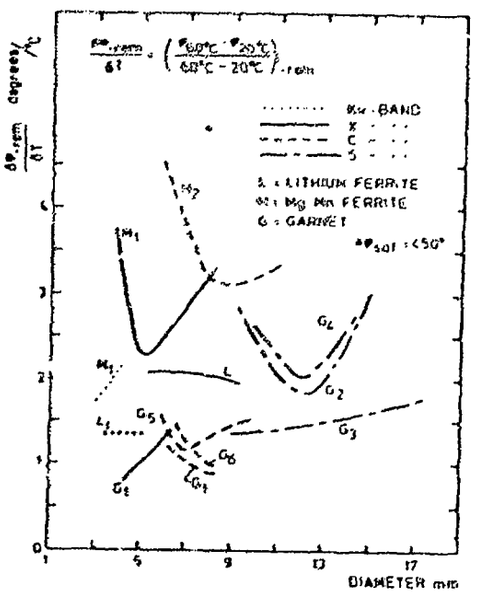

Figure 6.7

Temperature dependence of phase shift in +remanent as a function of rod diameter

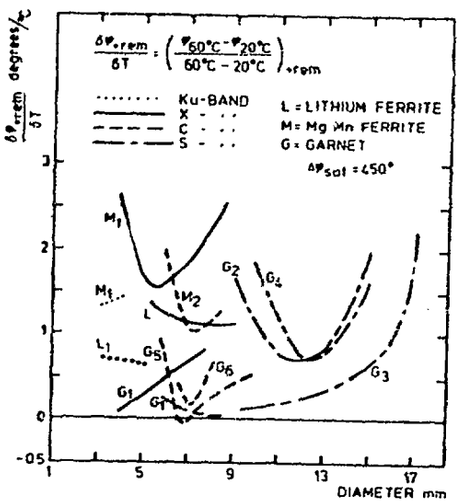

Figure 6.8

Temperature dependence of phase shift in -remanent as a function of rod diameter

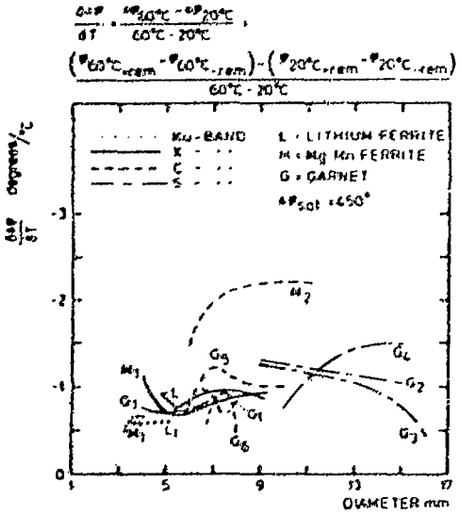

Figure 6.9

Temperature dependence of differential phase shift as a function of rod diameter

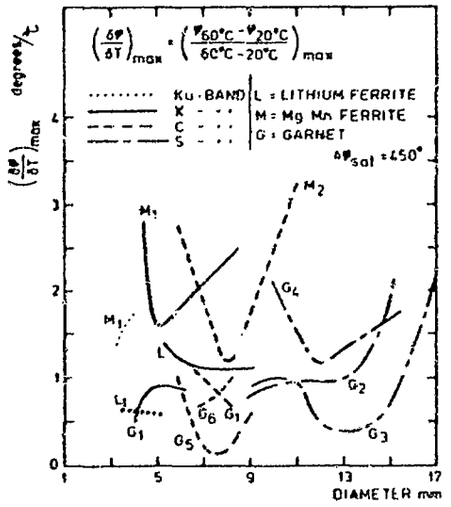

Figure 6.10

Maximum temperature dependence of phase shift as a function of rod diameter

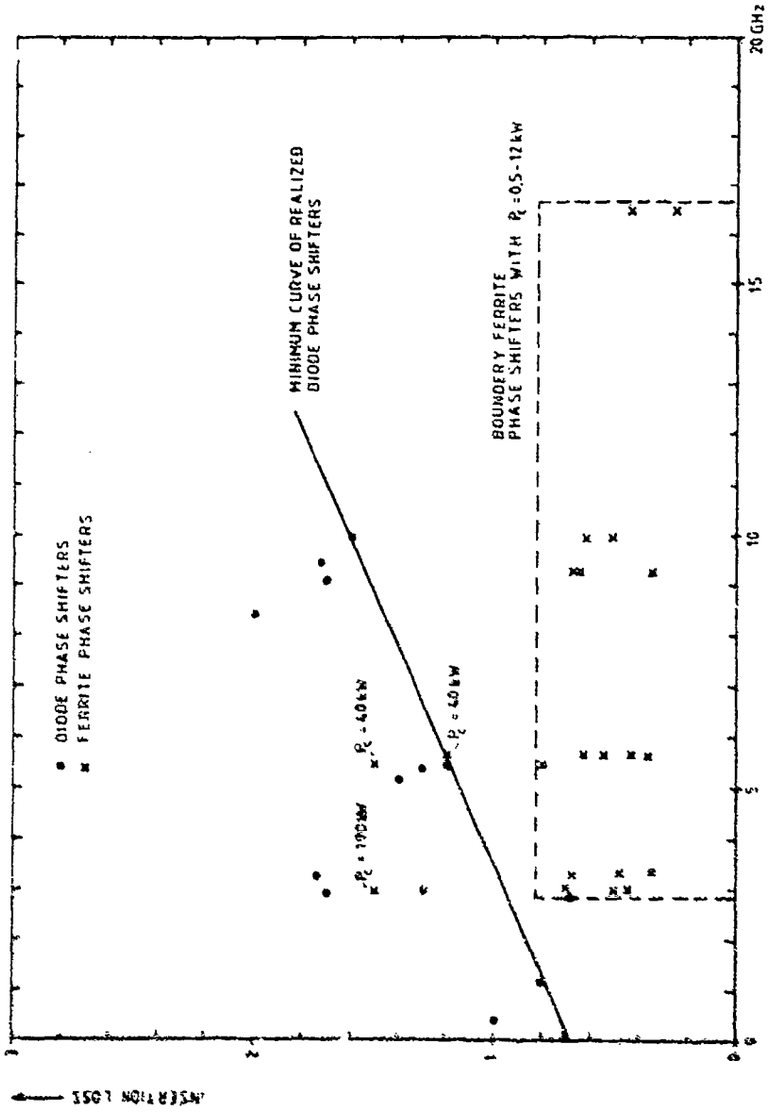

Figure 6.11 Insertion loss of ferrite- and diode phase shifters as a function of frequency

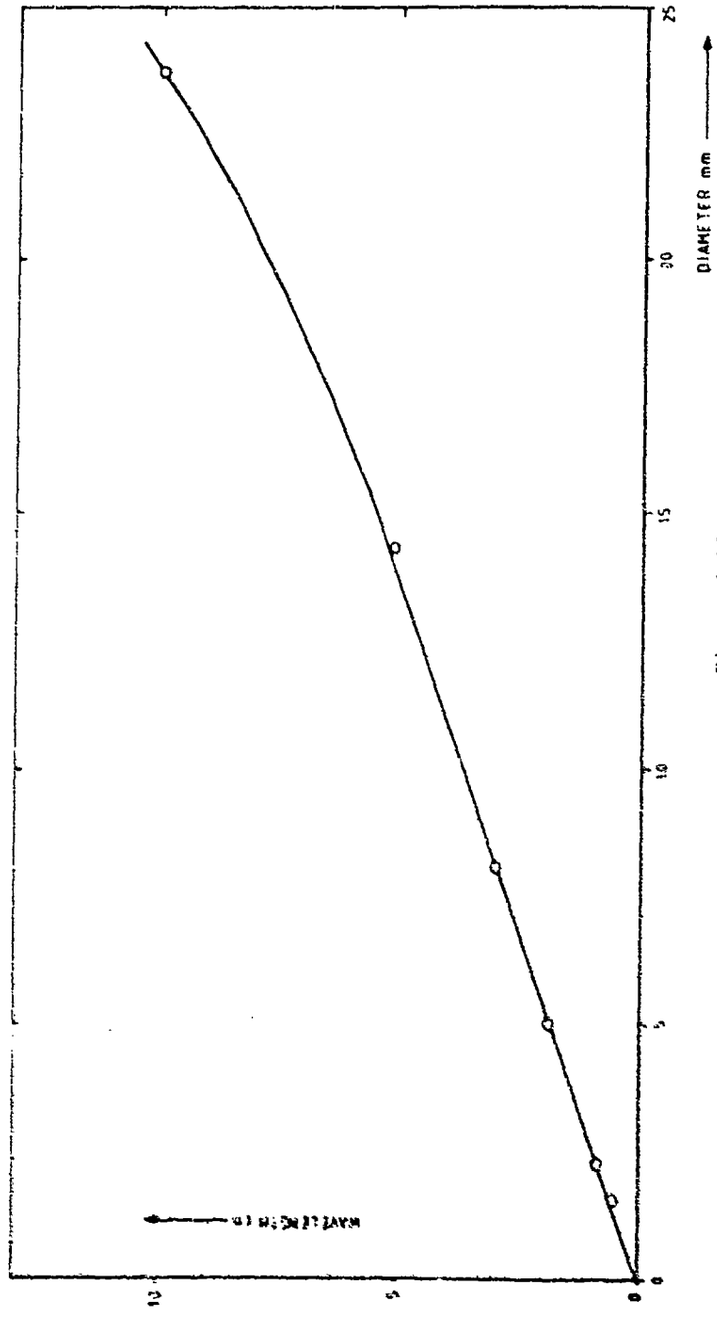

Figure 6.12

Wavelength as a function of rod diameter of a dual-mode phase shifter

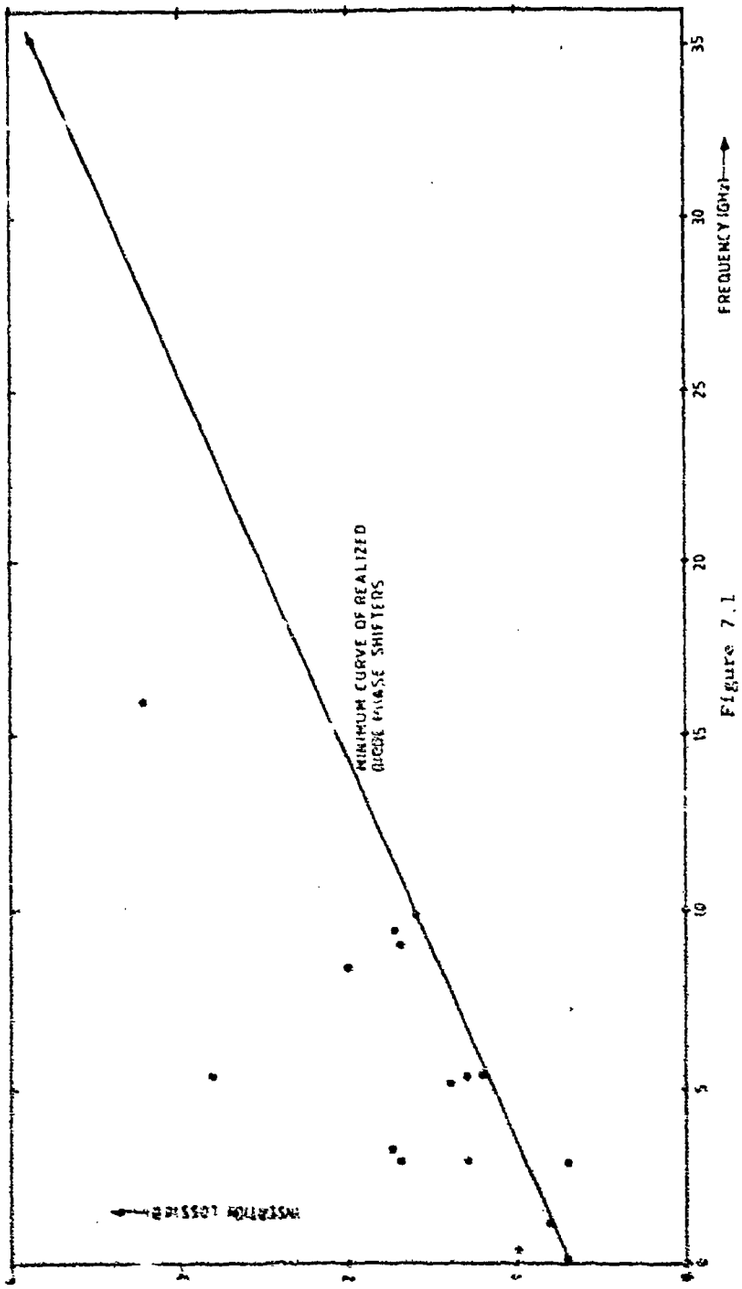

Figure 7.1 Insertion loss of diode phase shifters as a function of frequency

TABLE 1

SUMMARY OF 35 GHz PHASE SHIFTER PERFORMANCE

Frequency Range	34.0 to 36.0 GHz
Insertion Loss	6.8 dB minimum 1.0 dB typical
Return Loss	20 dB typical
Latching Phase Shift Range	
25°C	430° typical
50°C	400° typical
RMS Phase Error, (Optimum Drive)	
25°C	2.3° typical
50°C	2.5° typical
Switching Time, (Reset-Set Cycle)	55 μs maximum

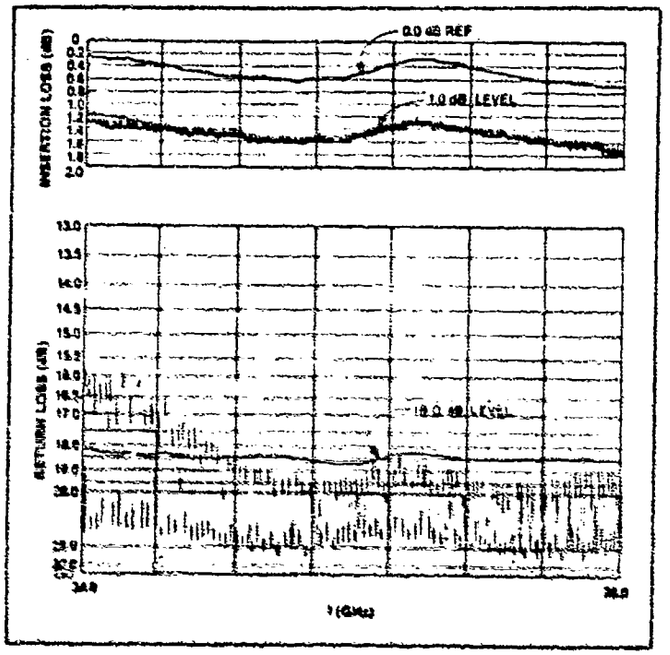

Figure 7.2

Typical plot of insertion loss and return loss data

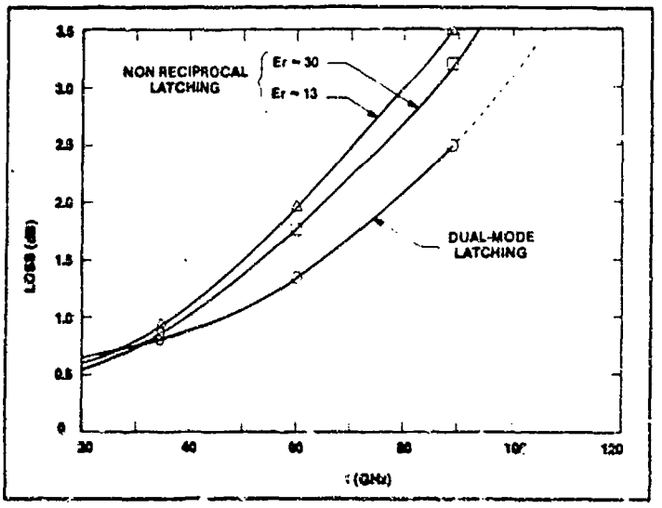

Figure 7.3

Comparison of base loss levels for latching ferrite phase shifters

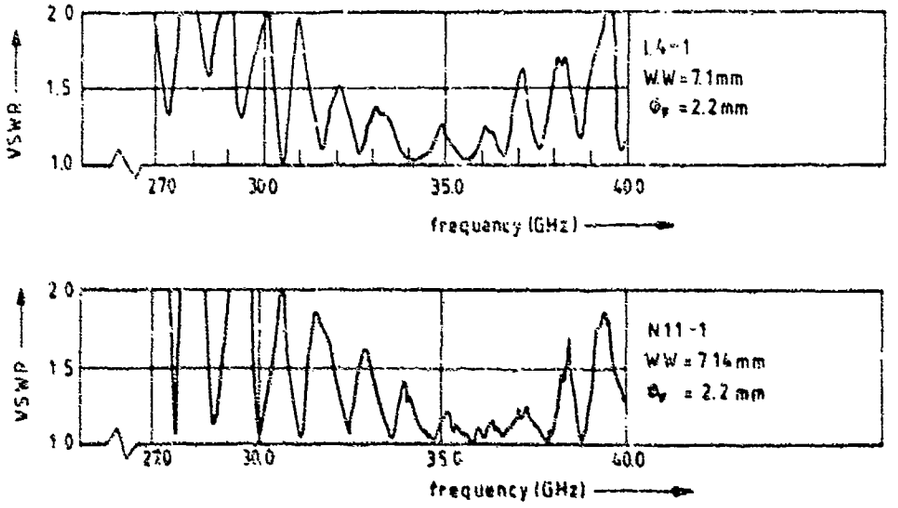

Figure 7.4

Voltage Standing Wave Ratio as a function of frequency

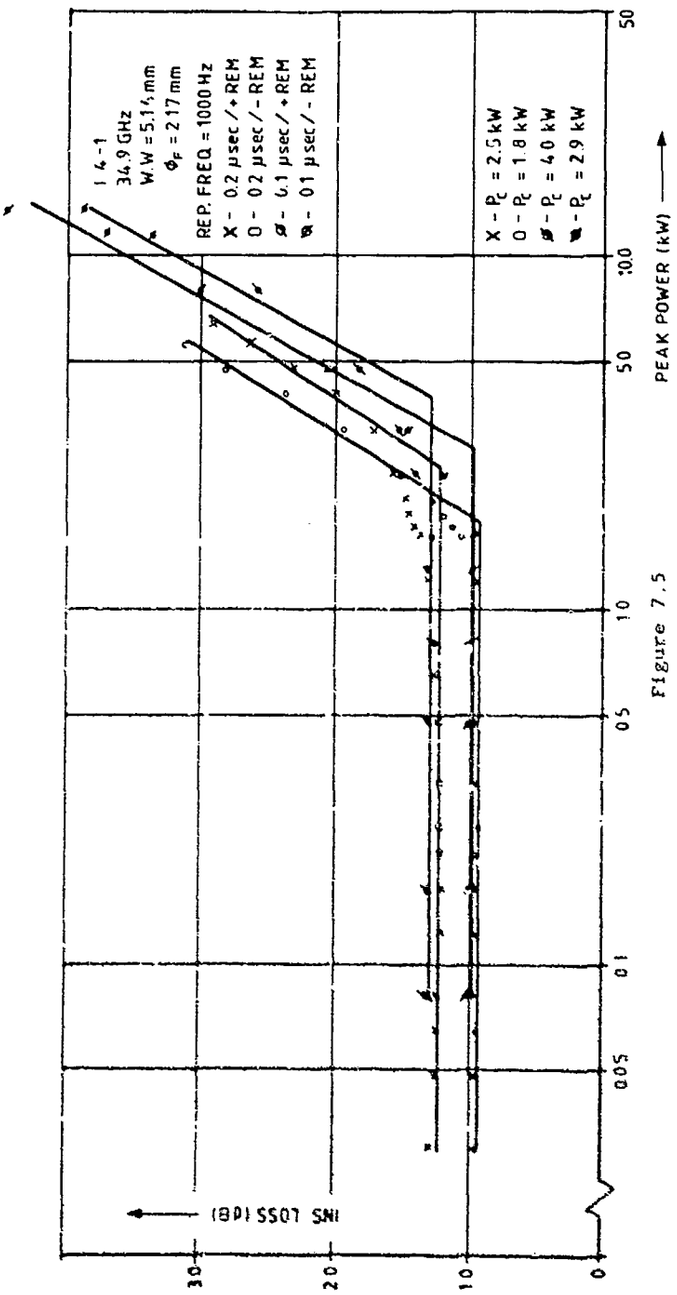

Figure 7.5 Insertion loss as a function of peak power for lithium ferrite

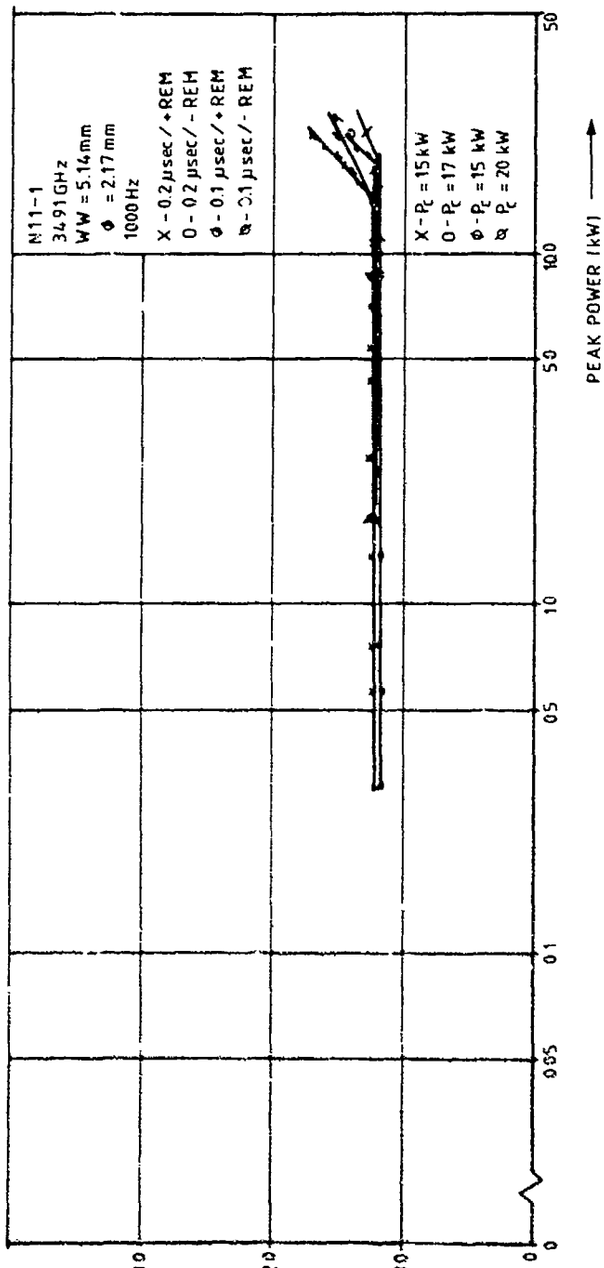

Figure 7.6

Insertion loss as a function of peak power for nickel ferrite

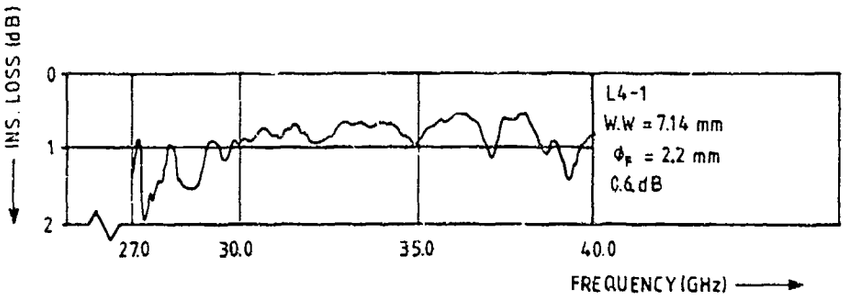

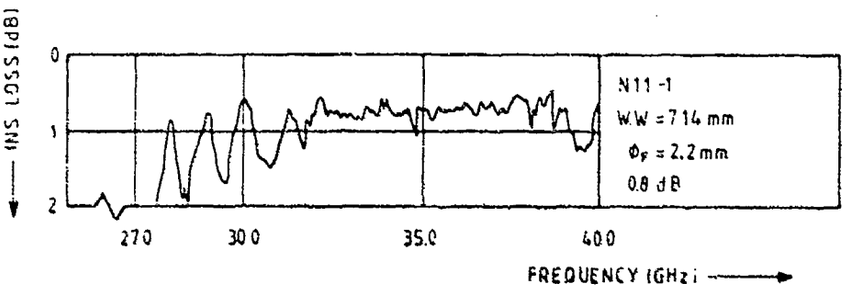

Figure 7.7

Insertion loss as a function of frequency for lithium (top curve) and nickel (bottom curve) ferrite

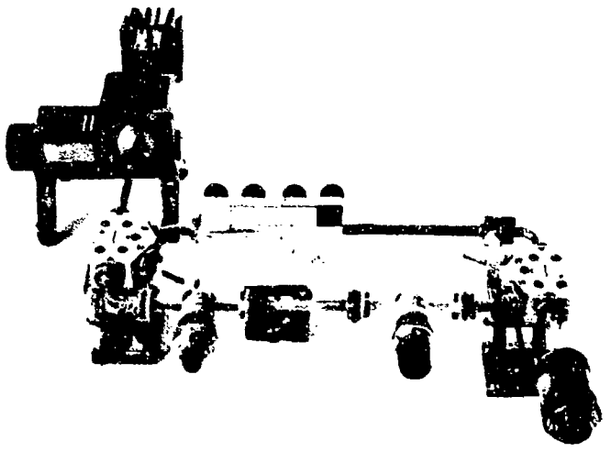

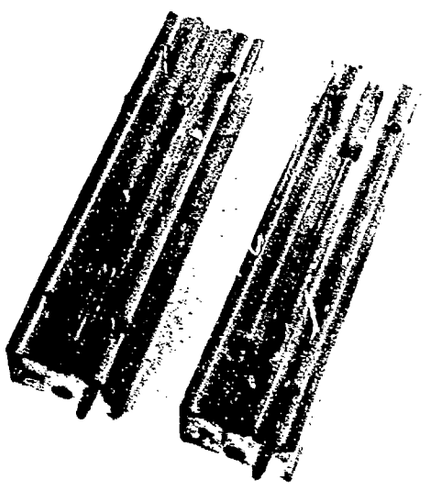

Figure 7.8

Photo of phase bridge used at 66 GHz and of the open measuring section

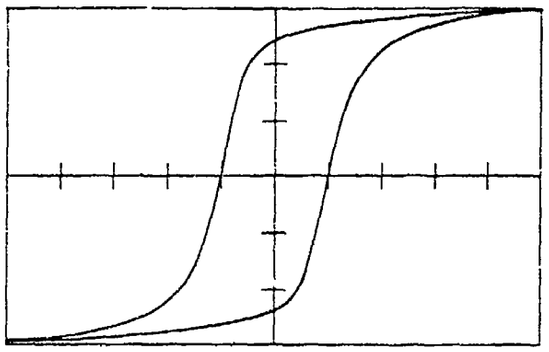

Nickel ferrite

B-H loop

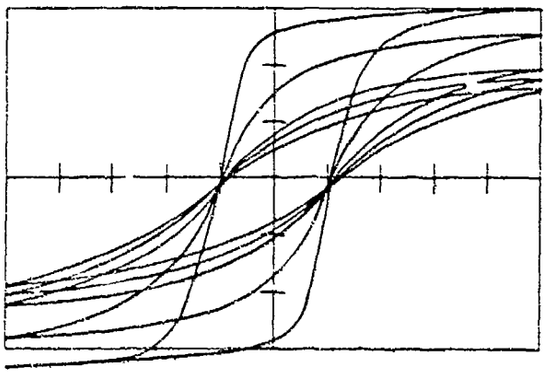

Transverse pressure

0 kg/cm²
56.2
112.4
168.5
196.6

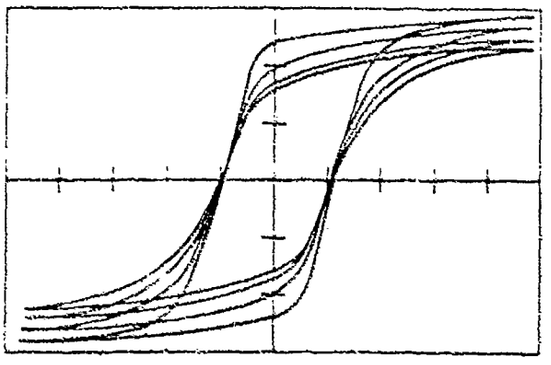

Longitudinal pressure

0 kg/cm²
56.2
112.4
168.5
196.6

Figure 7.9

B-H loop as a function of transverse and longitudinal pressure for nickel ferrite

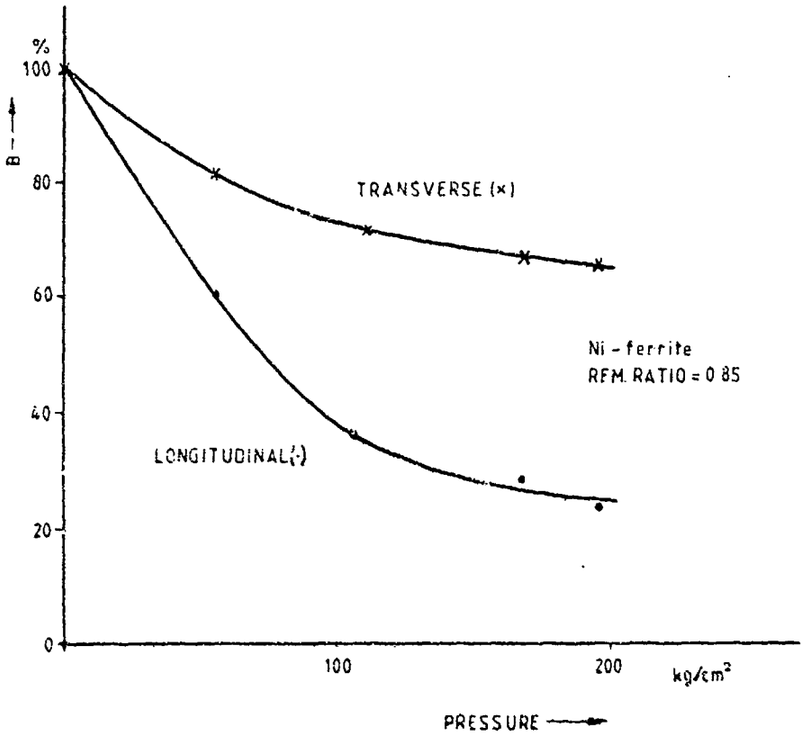

Figure 7.10

Magnetic induction B as a function of transverse and longitudinal pressure for nickel ferrite

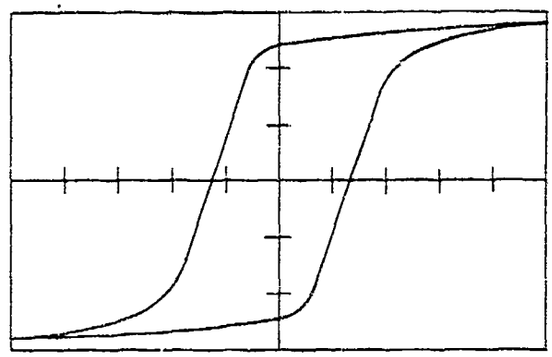

Lithium ferrite

B-H loop

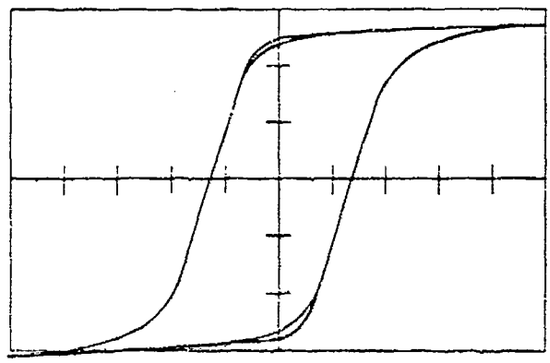

Transverse pressure

0 kg/cm²
112.4
196.6

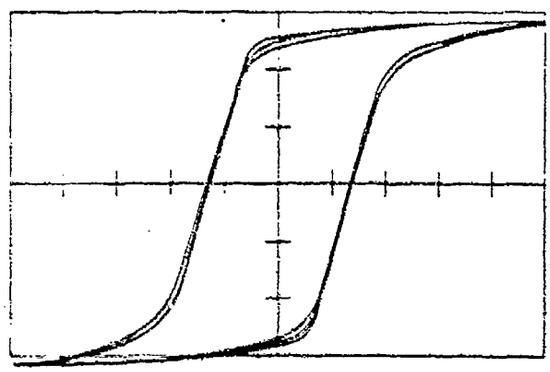

Longitudinal pressure

0 kg/cm²
112.4
196.6

Figure 7.11

B-H loop as a function of transverse and longitudinal pressure for lithium ferrite

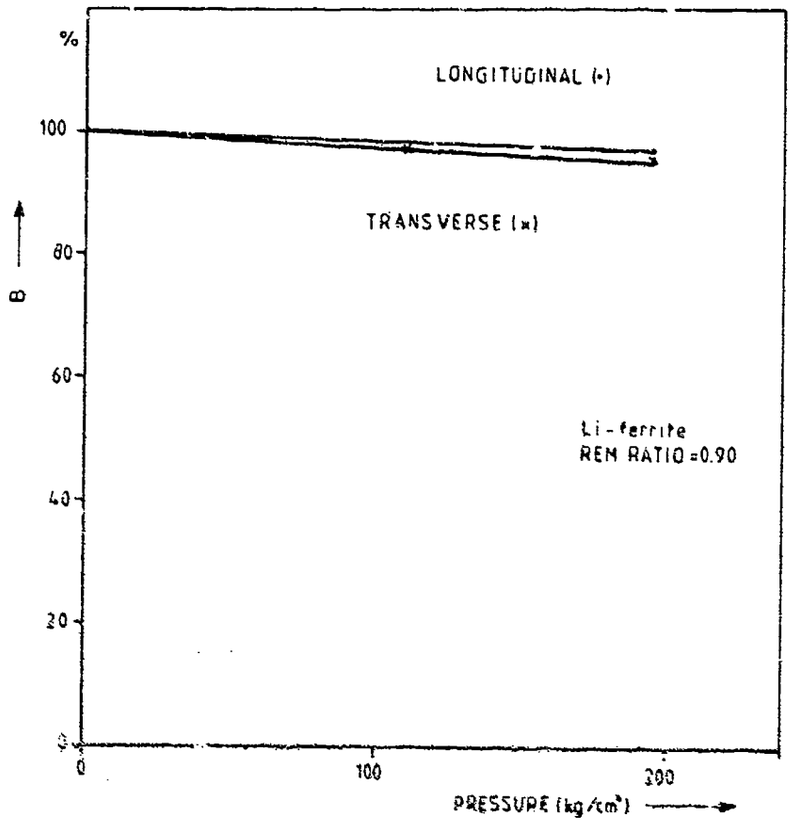

Figure 7.12

Magnetic induction B as a function of transverse and longitudinal pressure for lithium ferrite

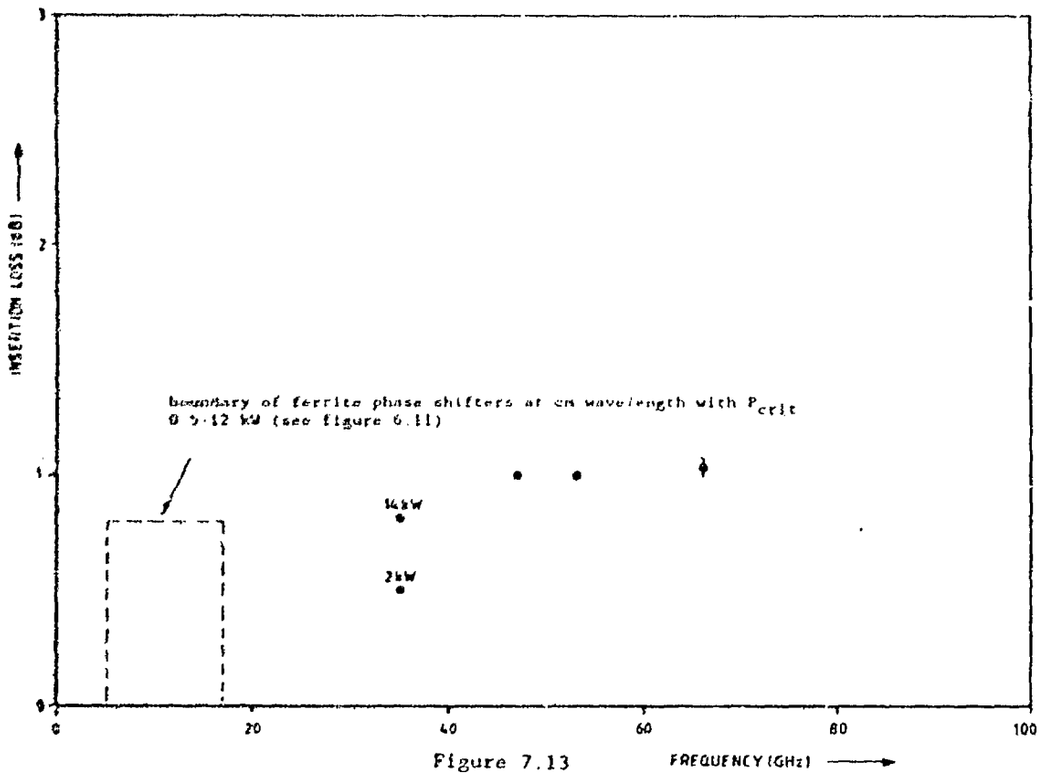

Figure 7.13

Insertion loss as a function of frequency for non-reciprocal latched ferrite phase shifters with indicated P_{crit} value

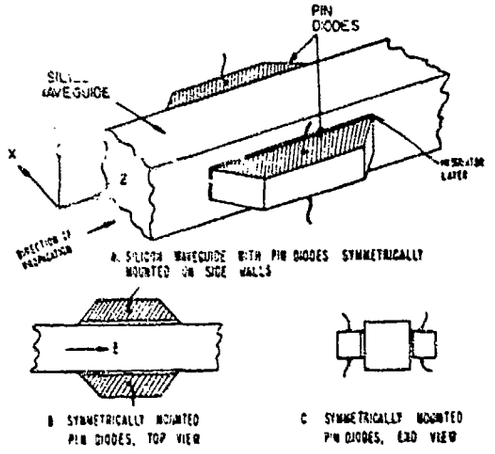

Figure 7.14

Arrangement of symmetrically mounted PIN diodes on the silicon waveguide

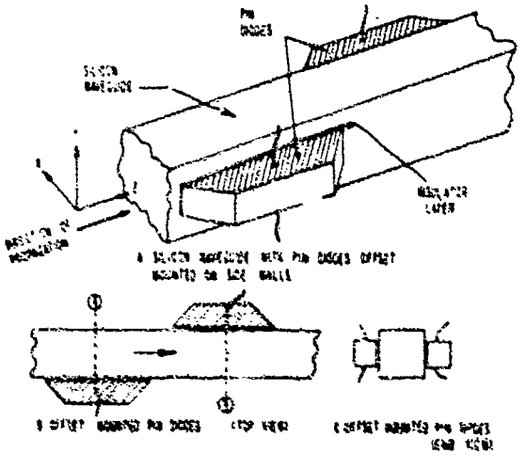

Figure 7.15

Arrangement of offset mounted PIN diodes on the silicon waveguide

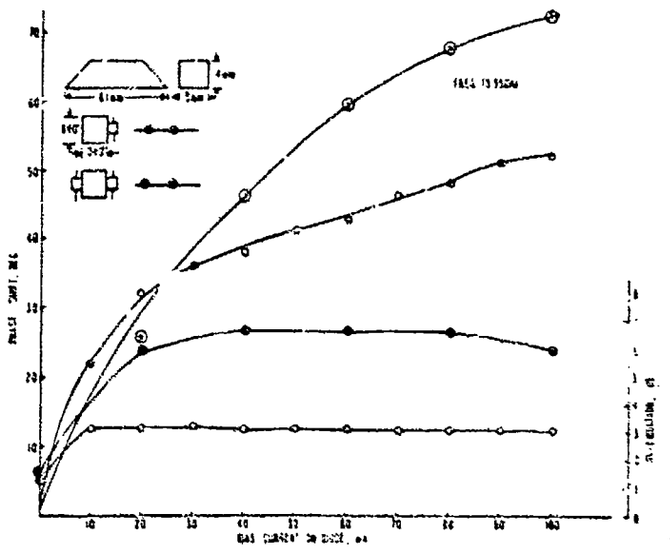

Figure 7.16

Phase shift and attenuation vs. bias current on p-i-n diodes

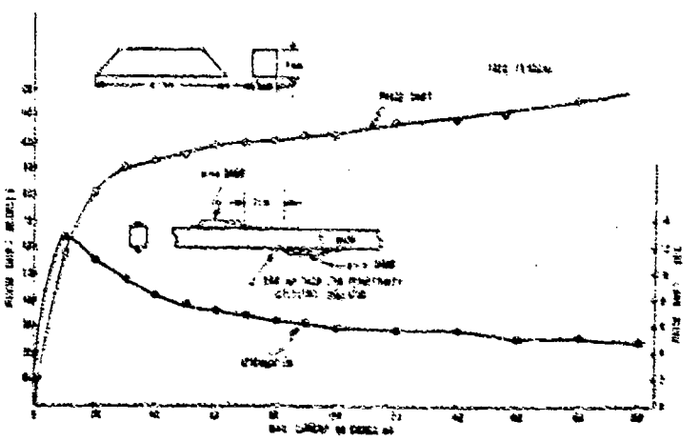

Figure 7.17

Phase shift and attenuation vs. bias current on p-i-n diodes

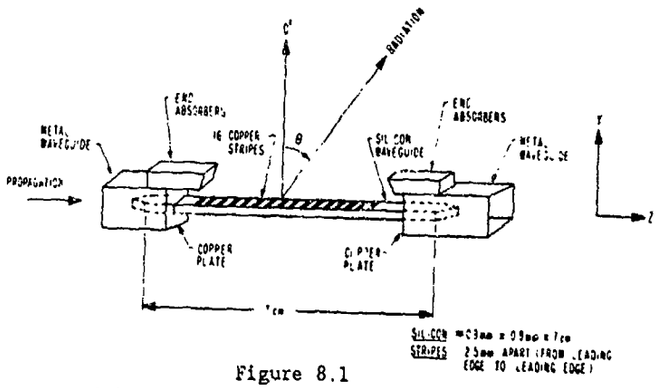

Figure 8.1
Silicon waveguide with perturbations

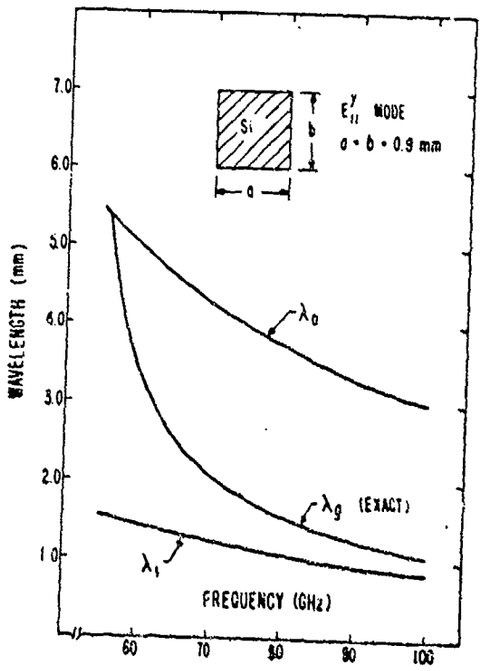

Figure 8.2
Variation of wavelength with frequency

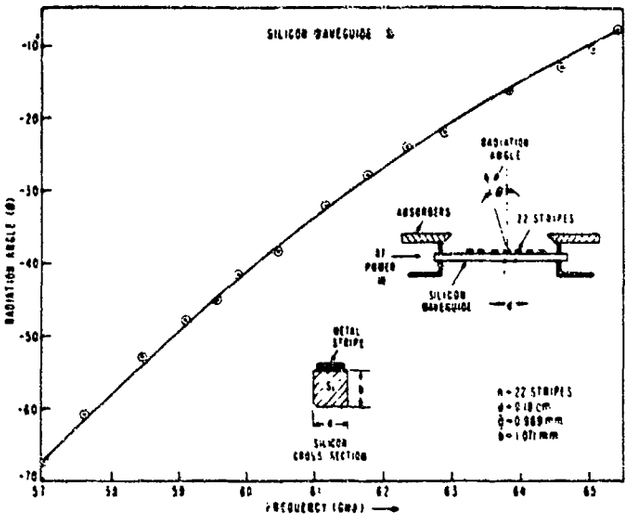

Figure 8.3
Experimental plot of radiation angle versus frequency

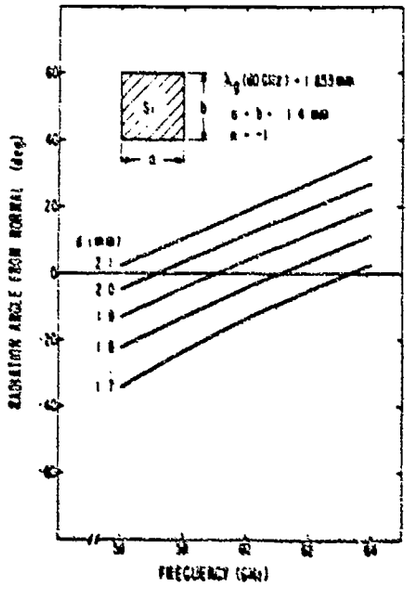

Figure 8.4
Effect of perturbation spacing d on radiation angle

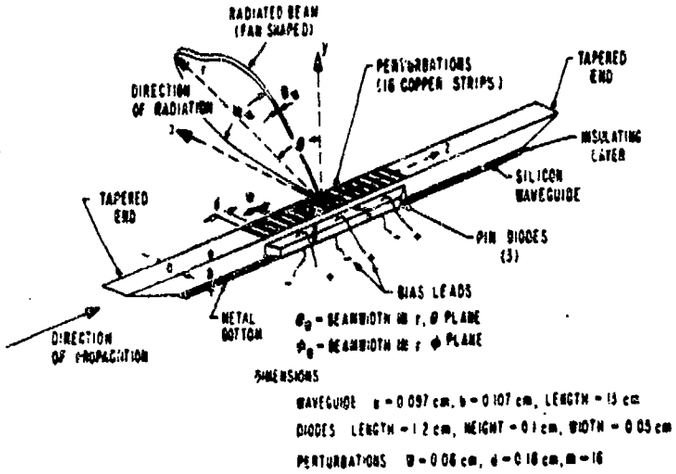

Figure 8.5
Line scanning antenna

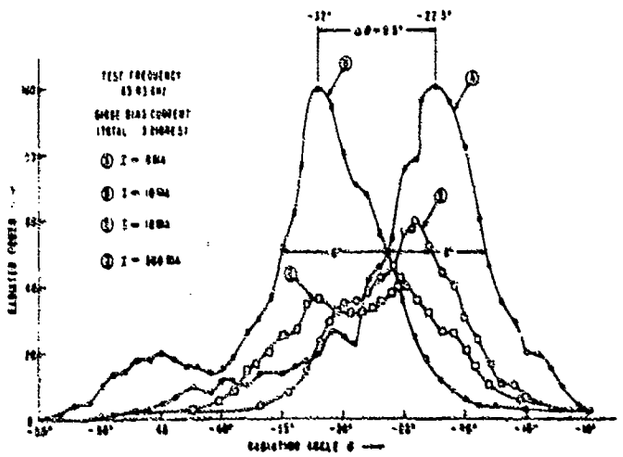

Figure 8.6
Radiated power versus angle as a function of bias current

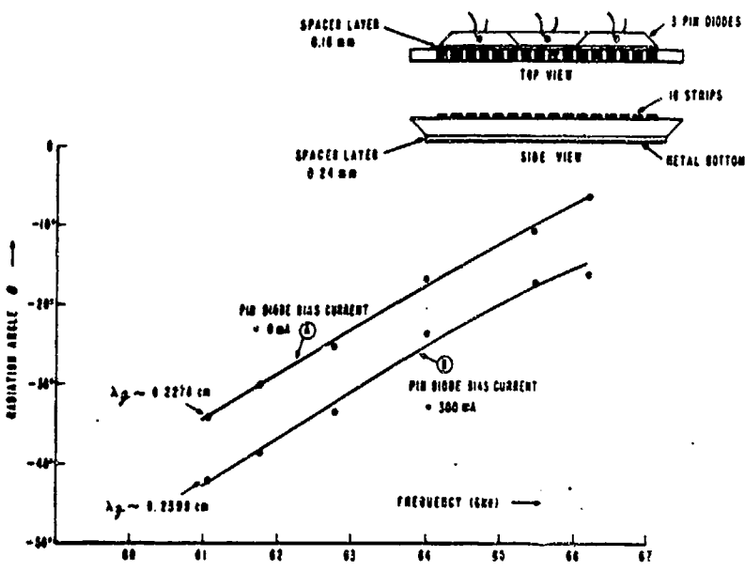

Figure 8.7

Radiation angle versus frequency, with and without p-i-n diode bias

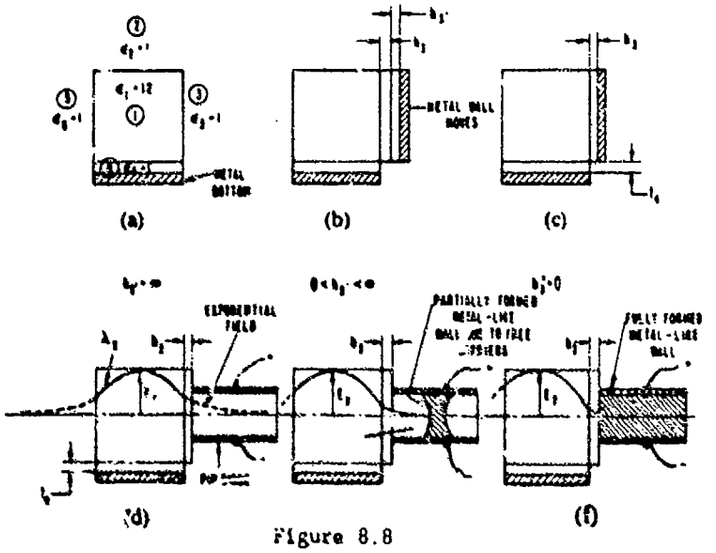

Figure 8.8

Silicon waveguide, cross section, and E-field distribution. (a) Diodes unbiased (ideal), (b) diodes partially biased (ideal), (c) diodes fully biased (ideal), (d) field distribution diodes unbiased, (e) E-field distribution diodes small bias, (f) E-field distribution diodes fully biased.

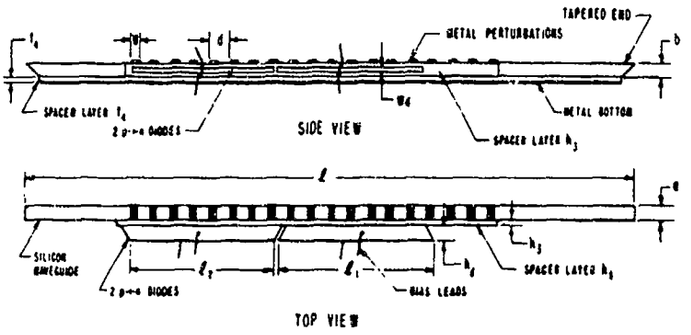

Figure 8.9

Line scanning antenna, design parameters. n = numbers of metal perturbations=19; a=dielectric waveguide width=0.991 mm; b=dielectric waveguide height=1.01 mm; d=perturbation spacing=1.88 mm; t_1=spacer layer thickness on bottom=0.24 mm; l=dielectric waveguide length=11.0 cm; h_3=spacer layer thickness between waveguide and diodes=0.24 mm. Diode length (l_1)=1.2 cm; diode length (l_2)=1.1 cm; diode height (h_d)=1.0 mm; diode width (W_d)=0.5 mm.

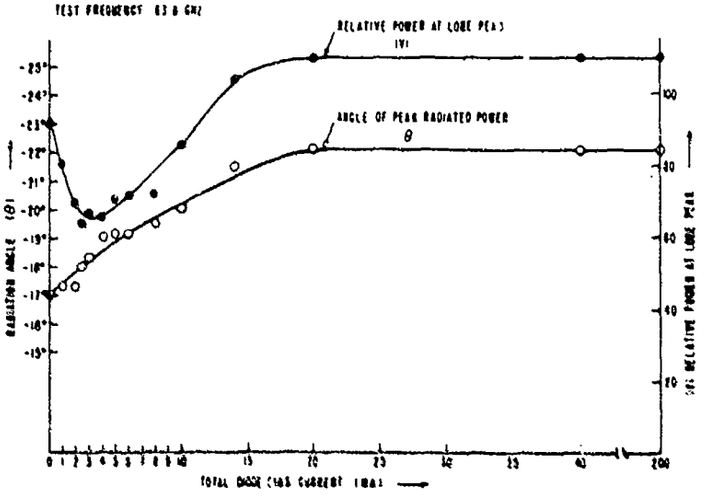

Figure 8.10

Peak radiation angle and relative peak power versus bias current

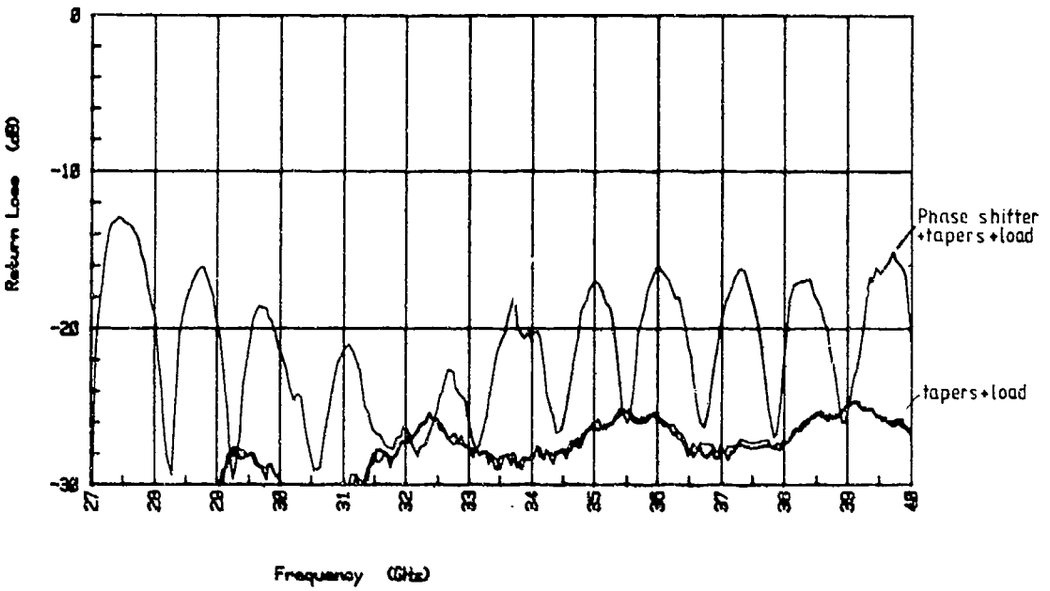

Figure 9.1

Return loss as a function of frequency of a phase shifter with tapers and load and of tapers and load

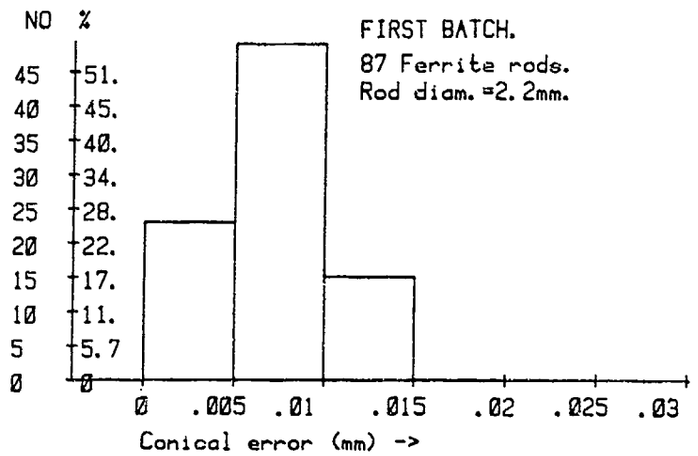

Figure 9.2

Number and percentage of ferrite rods as a function of conical error of first batch of 87 rods

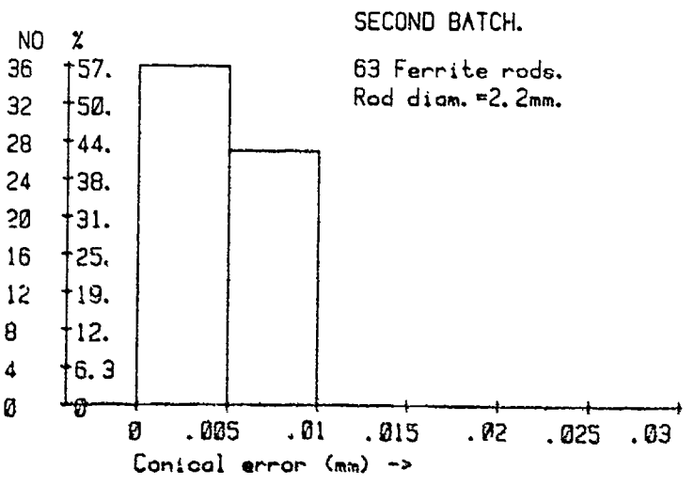

Figure 9.3

Number and percentage of ferrite rods as a function of conical error of second batch of 63 rods

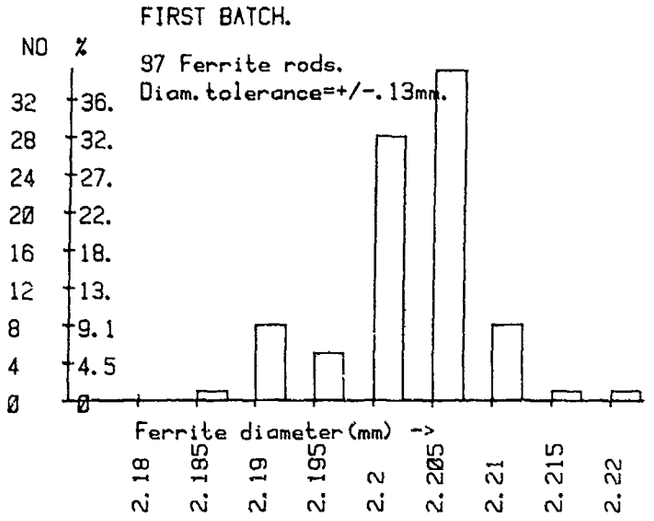

Figure 9.4

Number and percentage of ferrite rods as a function of diameter of first batch of 87 rods

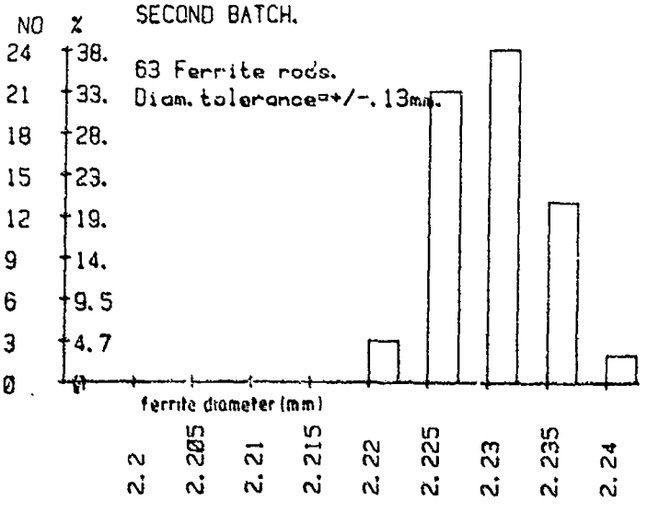

Figure 9.5

Number and percentage of ferrite rods as a function of diameter of second batch of 63 rods

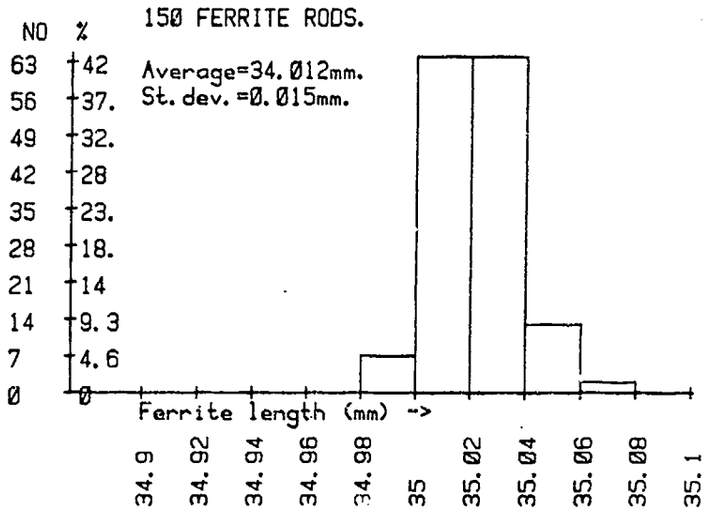

Figure 9.6
Number and percentage of ferrite rods as a function of length of 150 rods

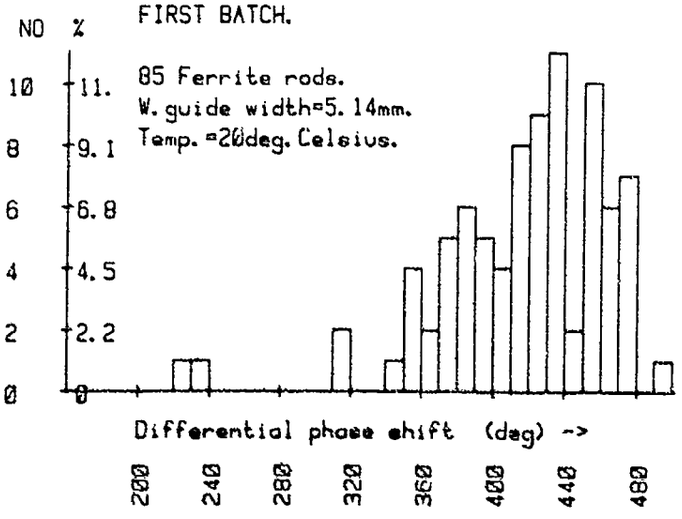

Figure 9.7
Number and percentage of ferrite rods as a function of differential phase shift of first batch of 85 rods

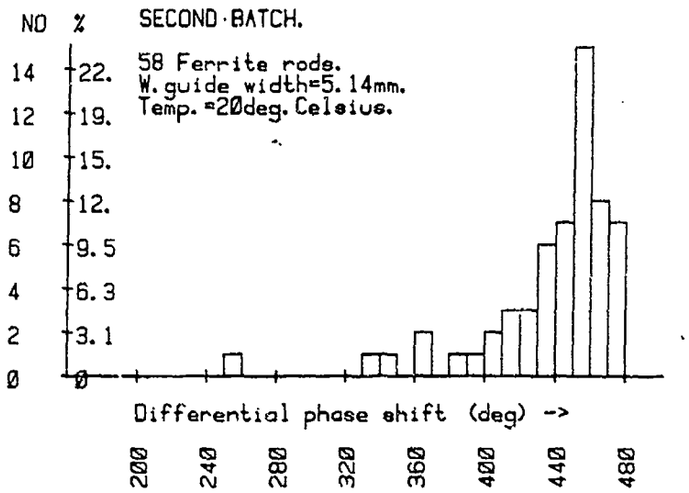

Figure 9.8

Number and percentage of ferrite rods as a function of differential phase shifts of second batch of 58 rods

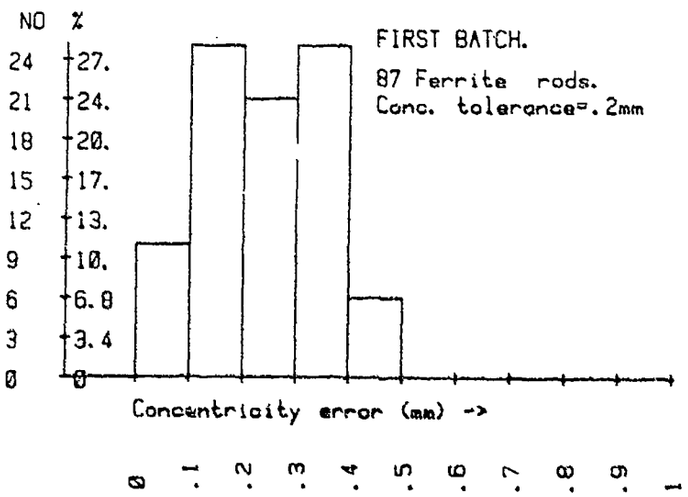

Figure 9.9

Number and percentge of ferrite rods as a function of concentricity of first batch of 87 rods

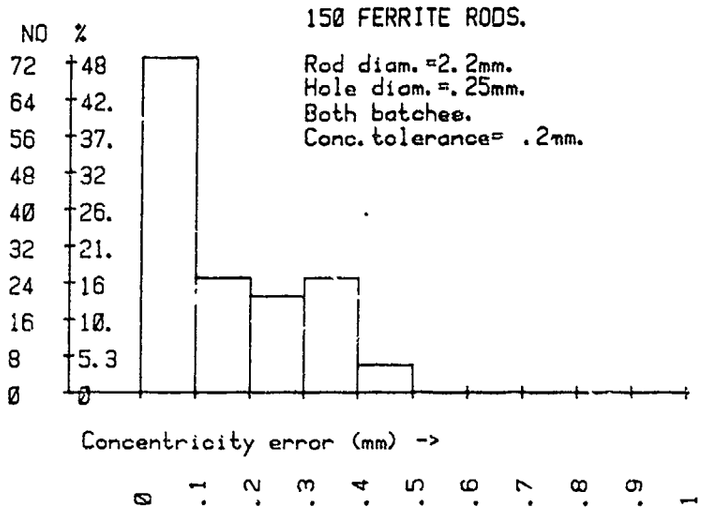

Figure 9.10

Number and percentage of ferrite rods as a function of concentricity of 150 rods

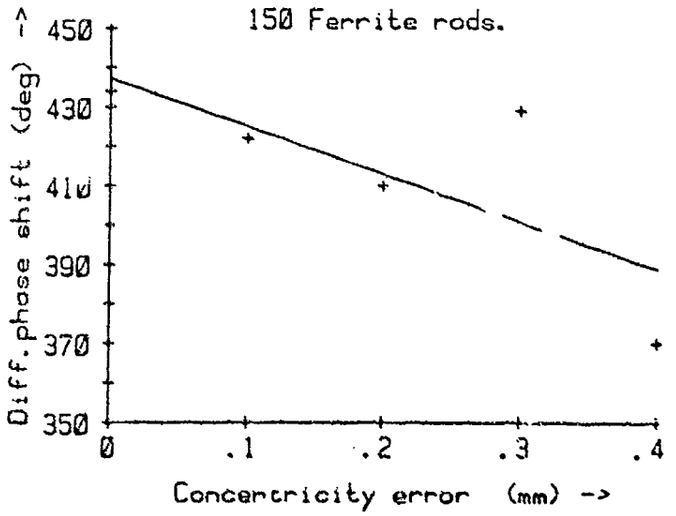

Figure 9.11

Differential phase shift as a function of concentricity of 150 ferrite rods

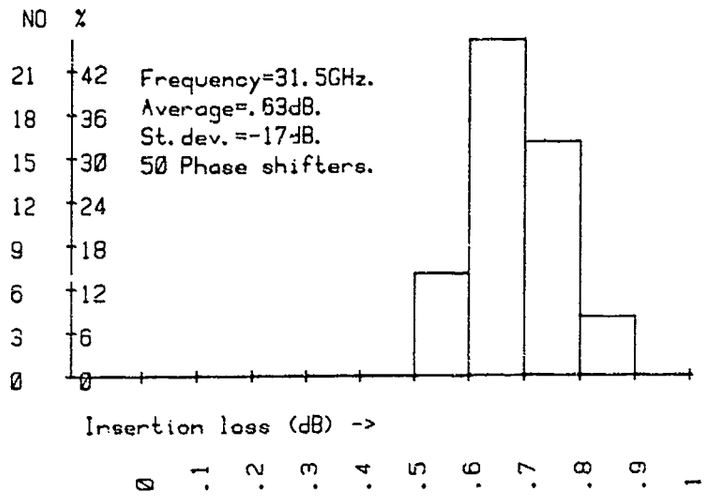

Figure 9.12

Number and percentage of 50 selected ferrite rods as a function of insertion loss measured at 31.5 GHz. Waveguide width 5.14 mm.

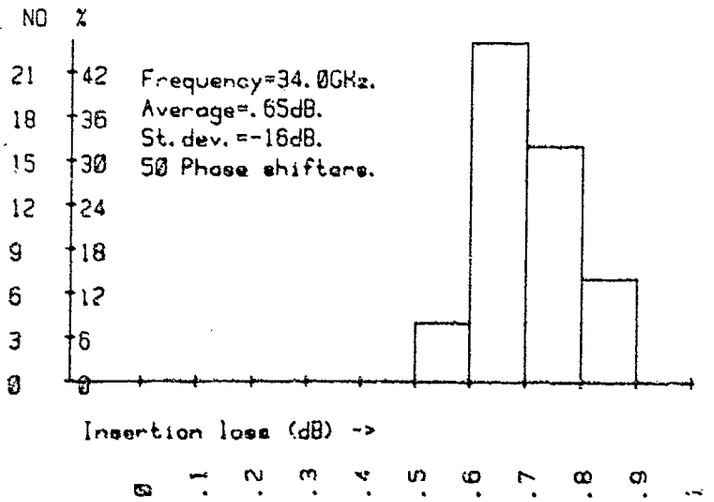

Figure 9.13

Same as figure 9.12, but now for 34 GHz

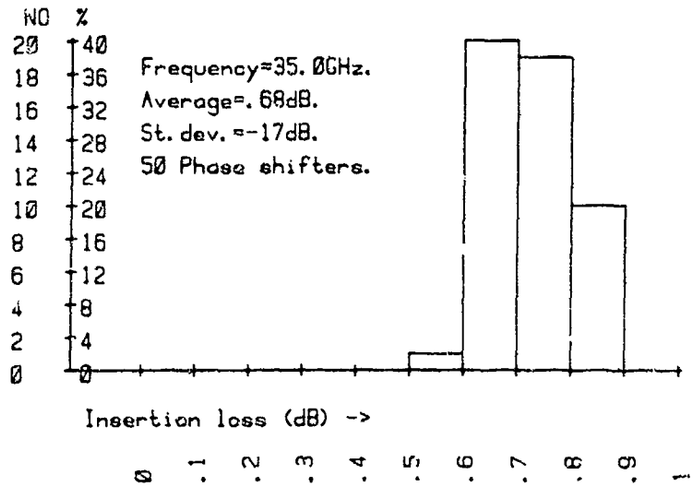

Figure 9.14

Same as figure 9.12, but now for 35 GHz

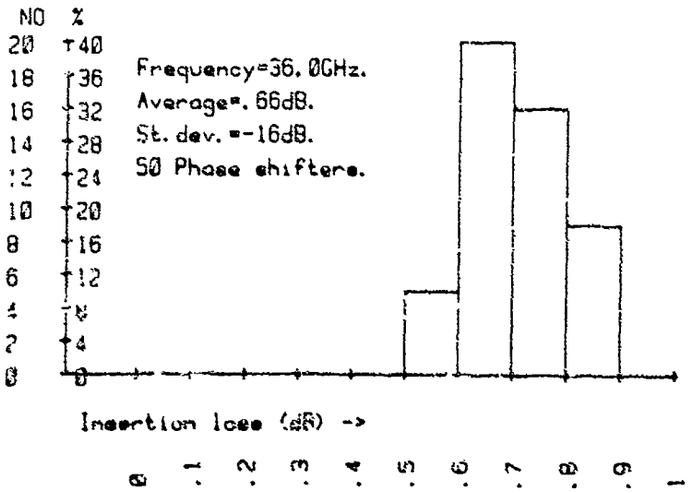

Figure 9.15

Same as figure 9.12, but now for 36 GHz

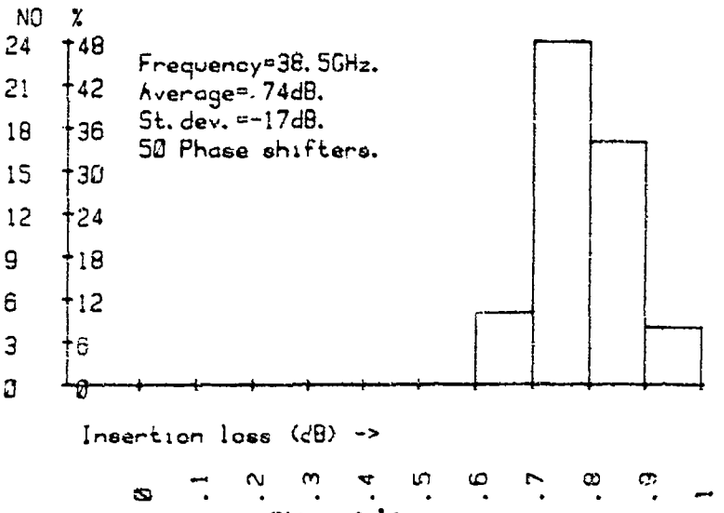

Figure 9.16

Same as figure 9.12, but now at 38.5 GHz

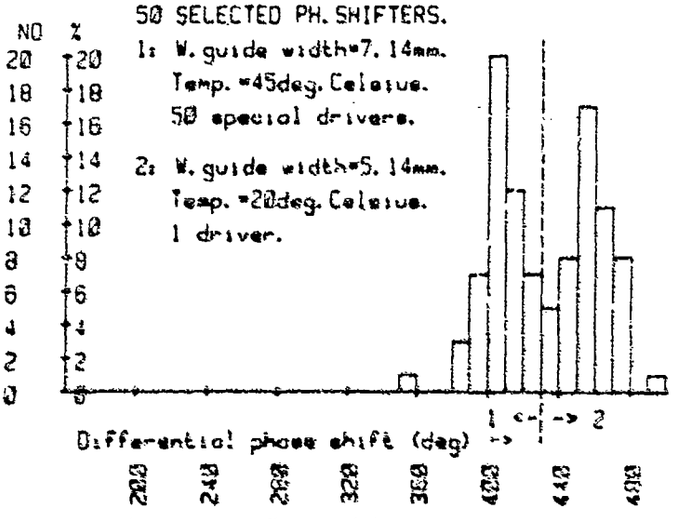

Figure 9.17

Number and percentage of 50 selected ferrite rods as a function of differential phase shift. At the left of dashed line each rod with its own not selected driver. At the right of the dashed line all rods measured with the same driver. Waveguide width 5.16 mm

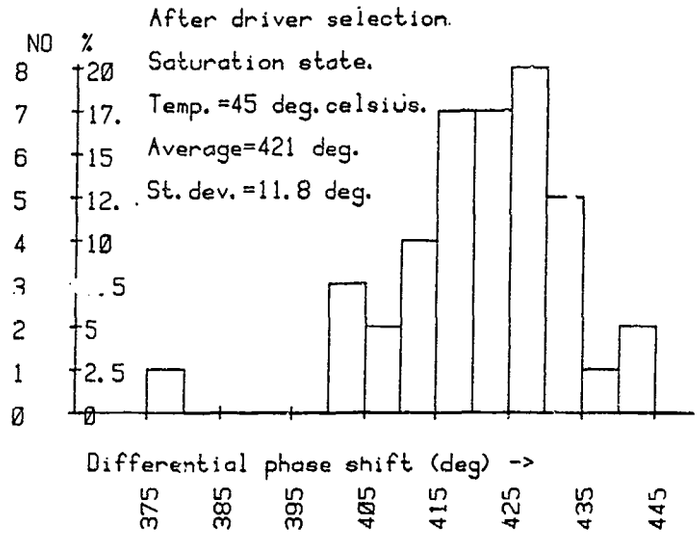

Figure 9.18
Number and percentage of 50 selected ferrite rods as a function of differential phase shifter.
Each rod with a selected driver. Waveguide width now 7.14 mm

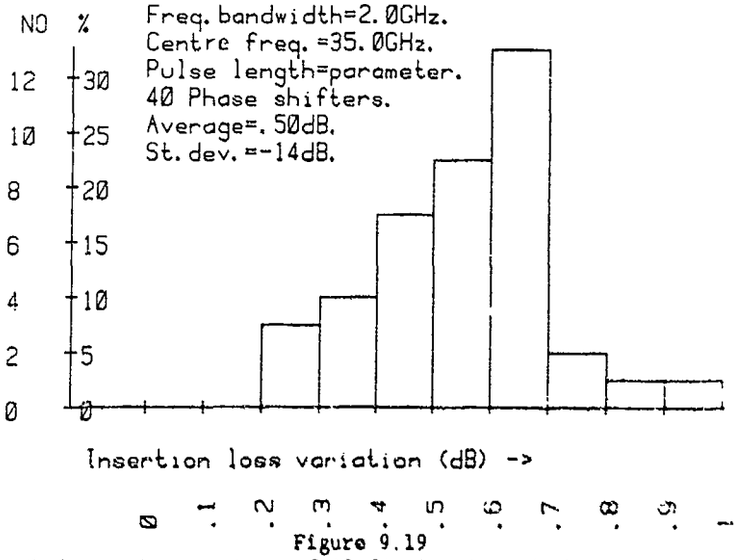

Figure 9.19
Number and percentage of 40 final selected phase shifters as a function of insertion loss for all phase shift values in a 2 GHz frequency bandwidth. Centre frequency 35 GHz.
An insertion loss of 0.2 dB due to the employed waveguide tapers for test purposes must be subtracted from these values

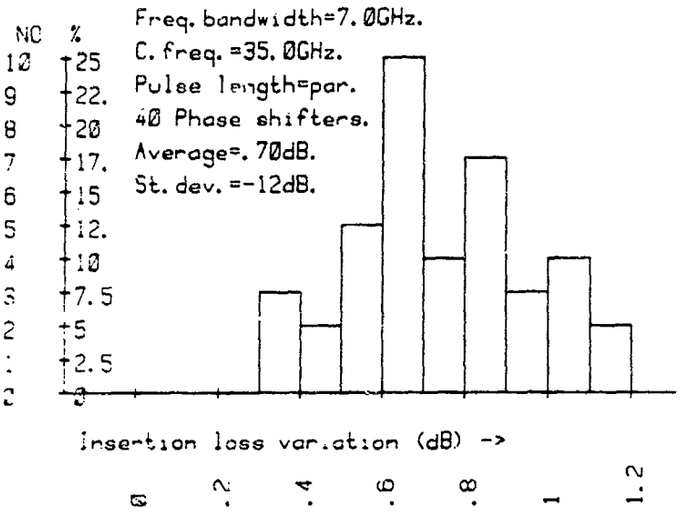

Figure 9 20

Same as figure 9.19 but now for a frequency bandwidth of 7 GHz

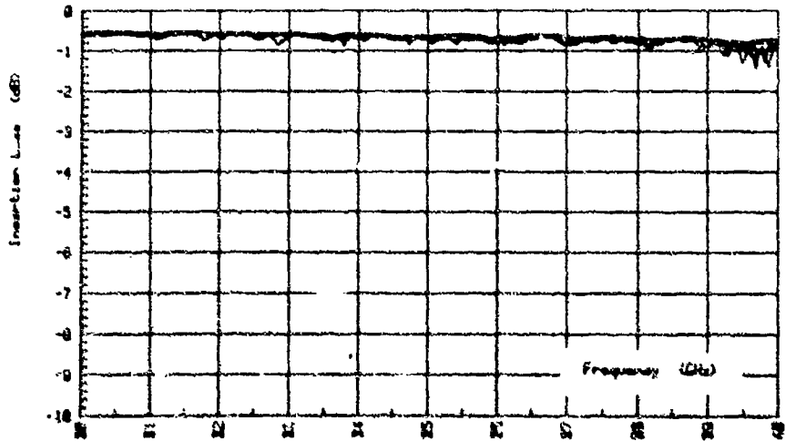

Figure 9.21

Insertion loss of phase shifter including two waveguide tapers of 0.2 dB loss as a function of frequency for various phase shift settings

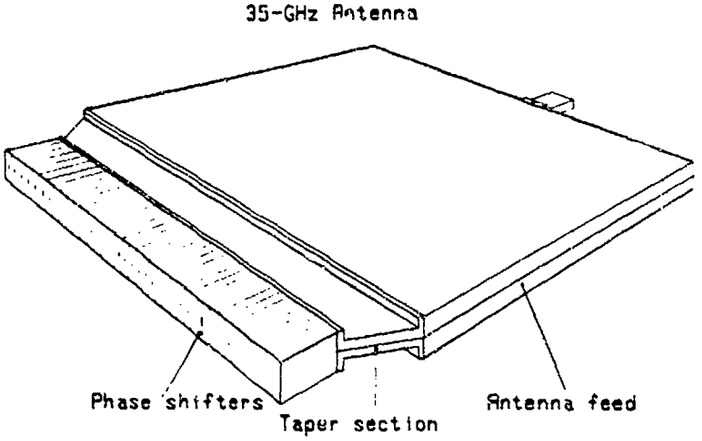

Figure 9.22

Sketch of constrained feed of 35 GHz linear phased array antenna

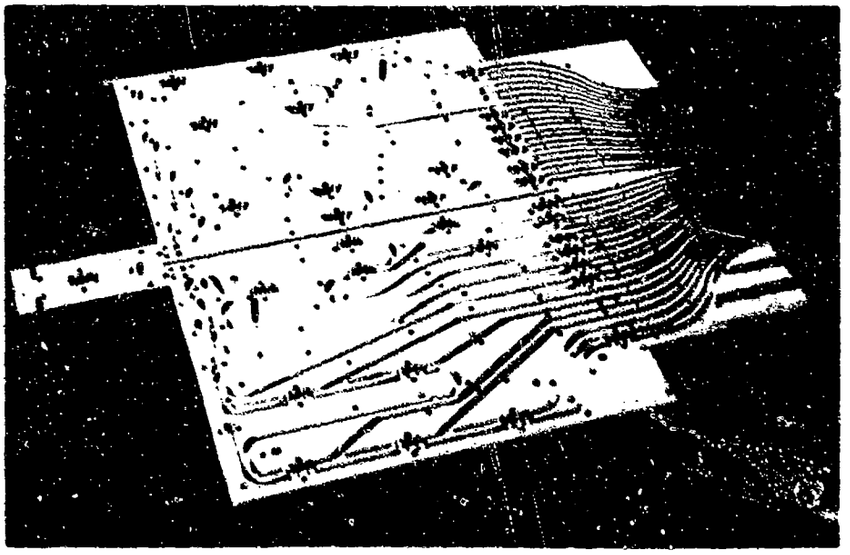

Figure 9.23

Photo of one half of 35 GHz constrained linear phased array antenna

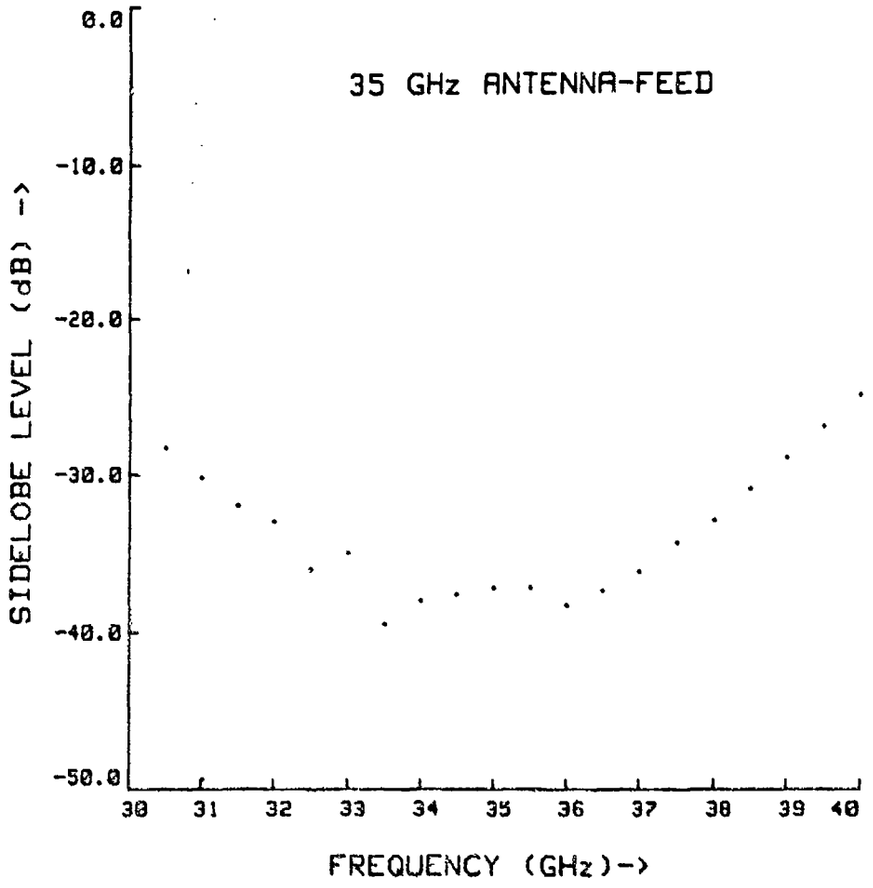

Figure 9.24

Worst side-lobe level as a function of frequency of first constructed 35 GHz constrained feed

UNCLASSIFIED

REPORT DOCUMENTATION PAGE (MOD-NL)

1. DEFENSE REPORT NUMBER (MOD-NL)	2. RECIPIENT'S ACCESSION NUMBER	3. PERFORMING ORGANIZATION REPORT NUMBER
TD89-3875		FEL-88-B258
4. PROJECT/TASK/WORK UNIT NO.	**5. CONTRACT NUMBER**	**6. REPORT DATE**
6145.70		JUNE 1990
7. NUMBER OF PAGES	**8. NUMBER OF REFERENCES**	**9. TYPE OF REPORT AND DATES COVERED**
126 (INCL. TITLEPAGE, EXCL. DISTR. LIST AND RDP)	21	FINAL REPORT

10. TITLE AND SUBTITLE
ELECTRONIC SCAN AT MILLIMETRE WAVE FREQUENCIES

11. AUTHOR(S)
DR. J. SNIEDER

12. PERFORMING ORGANIZATION NAME(S) AND ADDRESS(ES)
TNO PHYSICS AND ELECTRONICS LABORATORY, P.O. BOX 96864, 2509 JG THE HAGUE, THE NETHERLANDS

13. SPONSORING/MONITORING AGENCY NAME(S)

14. SUPPLEMENTARY NOTES

15. ABSTRACT (MAXIMUM 200 WORDS, 1044 POSITIONS)

THE POSSIBILITIES OF REALIZING PHASED ARRAY ANTENNAS IN THE MM-WAVE REGION IS REVIEWED IN A GENERAL WAY. THE USE OF DISCRETE COMPONENTS AND 'BULK' MATERIAL IS DISCUSSED. THE MMIC TECHNIQUES FOR THE REALIZATION OF PHASED ARRAY COMPONENTS ARE EXCLUDED FROM THIS REPORT. A SURVEY IS GIVEN OF THE DIFFERENT ELECTRONIC SCAN POSSIBILITIES. PIN DIODE PHASE SHIFTERS AND DIFFERENT TYPES OF FERRITE PHASE SHIFTERS ARE DISCUSSED, INCLUDING THE PRINCIPLE FUNCTIONING OF THESE COMPONENTS AS WELL AS THE ADVANTAGES AND DISAVANTAGES. THE AVAILABILITY OF VARIOUS FERRITE MATERIALS FOR PHASE SHIFTERS IS DISCUSSED. THE REQUIREMENTS FOR PHASED ARRAY ANTENNAS AND ITS PHASE SHIFTERS ARE GIVEN. THIS INCLUDES A DISCUSSION ON ARRAY ELEMENT SPACING, SIDE-LOBE LEVEL AND RELATED POWER LEVELS, EFFECT OF PULSE REPETITION FREQUENCY AND MUTUAL COUPLING. AN ATTEMPT IS MADE TO CORRELATE ALL THE AVAILABLE INFORMATION AT CM-WAVELENGTH (3-16 GHZ) AND TO EXTRAPOLATE IT TO MM-WAVELENGTH. ALL THE DETAILED PROPERTIES OF THE PHASE SHIFTERS ARE INCLUDED. THE EXPERIMENTAL RESULTS OF MM-WAVE PHASE SHIFTERS ARE GIVEN AND COMPARED WITH THE EXTRAPOLATED RESULTS GIVEN. THE DESIGN AND THE EXPERIMENTAL RESULTS OF THREE MILLIMETRIC PHASED ARRAY ANTENNA SYSTEMS ARE DISCUSSED. SOME ELEVEN CONCLUSIONS AND RECOMMENDATIONS ARE GIVEN.

16. DESCRIPTORS	IDENTIFIERS
PHASED ARRAY	FERRITE PHASE SHIFTER
ANTENNAS	MICRO WAVES
ELECTRONIC SCANNING	
PHASE SHIFTER	

17a. SECURITY CLASSIFICATION (OF REPORT)	17b. SECURITY CLASSIFICATION (OF PAGE)	17c. SECURITY CLASSIFICATION (OF ABSTRACT)
UNCLASSIFIED	UNCLASSIFIED	UNCLASSIFIED

18. DISTRIBUTION/AVAILABILITY STATEMENT	17d. SECURITY CLASSIFICATION (OF TITLES)
PUBLICLY AVAILABLE	UNCLASSIFIED

UNCLASSIFIED